

พอลิเมอไรเซชันสถานะของแข็งของ 2,5-ไดโบโรโม-3,4-เอทิลีนไดออกซีไทโอฟีนใน  
พอลิเมทิลเมทาคริเลตเมทริกซ์



นางสาวกชพร กิติกุลวรากร

ศูนย์วิทยพัทยากร

วิทยานิพนธ์นี้เป็นส่วนหนึ่งของการศึกษาตามหลักสูตรปริญญาวิทยาศาสตรมหาบัณฑิต

จุฬาลงกรณ์มหาวิทยาลัย

สาขาวิชาปิโตรเคมีและวิทยาศาสตร์พอลิเมอร์

คณะวิทยาศาสตร์ จุฬาลงกรณ์มหาวิทยาลัย

ปีการศึกษา 2552

ลิขสิทธิ์ของจุฬาลงกรณ์มหาวิทยาลัย

SOLID STATE POLYMERIZATION OF 2,5-DIBROMO-3,4-  
ETHYLENEDIOXYTHIOPHENE IN POLY(METHYL METHACRYLATE)  
MATRIX



Ms. Kodchaporn Kitikulvarakorn

ศูนย์วิทยทรัพยากร  
จุฬาลงกรณ์มหาวิทยาลัย

A Thesis Submitted in Partial Fulfillment of the Requirements  
for the Degree of Master of Science Program in Petrochemistry and Polymer Science

Faculty of Science

Chulalongkorn University


Academic Year 2009

Copyright of Chulalongkorn University


Thesis Title           SOLID STATE POLYMERIZATION OF 2,5-DIBROMO-3,4-ETHYLENEDIOXYTHIOPHENE IN POLY(METHYL METHACRYLATE) MATRIX  
By                        Ms. Kodchaporn Kitikulvarakorn  
Field of Study        Petrochemistry and Polymer Science  
Thesis Advisor       Assistant Professor Yongsak Sritana-anant, Ph.D.  
Thesis Co-advisor   Assistant Professor Voravee P. Hoven, Ph.D.

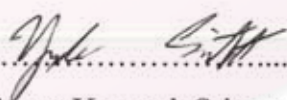
---

Accepted by the Faculty of Science, Chulalongkorn University in Partial Fulfillment of the Requirements for the Master's Degree


  
.....Dean of the Faculty of Science  
(Professor Supot Hannongbua, Dr.rer.nat.)

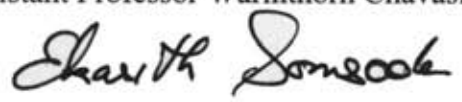
THESIS COMMITTEE

  
.....Chairman  
(Associate Professor Supawan Tantayanon, Ph.D.)

  
.....Thesis Advisor  
(Assistant Professor Yongsak Sritana-anant, Ph.D.)

  
.....Thesis Co-advisor  
(Assistant Professor Voravee P. Hoven, Ph.D.)

  
.....Examiner  
(Assistant Professor Warinthorn Chavasiri, Ph.D.)

  
.....External Examiner  
(Assistant Professor Ekasith Somsook, Ph.D.)

กขพร กิติกุลวรากร: พอลิเมอร์เรซินสถานะของแข็งของ 2,5-ไดโบรโม-3,4-เอทิลีนไดออกซีไทโอฟีนในพอลิเมทิลเมทาคริเลตเมทริกซ์ (SOLID STATE POLYMERIZATION OF 2,5-DIBROMO-3,4-ETHYLENEDIOXYTHIOPHENE IN POLY(METHYL METHACRYLATE) MATRIX) อ. ที่ปรึกษาวิทยานิพนธ์หลัก: ผศ.ดร. ยงศักดิ์ ศรีธนาอนันต์: อ. ที่ปรึกษาวิทยานิพนธ์ร่วม: ผศ.ดร. วรวิทย์ ไชยวัฒน์, 89 หน้า

ฟิล์มพอลิเมอร์คอมพอสิตนำไฟฟ้าที่มีองค์ประกอบของพอลิ(3,4-เอทิลีนไดออกซีไทโอฟีน) เตรียมได้โดยเริ่มจากวิธีอิเล็กโทรสปินนิงของสารละลายผสมระหว่าง 2,5-ไดโบรโม-3,4-เอทิลีนไดออกซีไทโอฟีน และ พอลิเมทิลเมทาคริเลต บนแผ่นกระจก หลังจากการกำจัดตัวทำละลายแล้วพอลิเมอร์เรซินในสถานะของแข็งของผลึก 2,5-ไดโบรโม-3,4-เอทิลีนไดออกซีไทโอฟีนที่ฝังตัวในพอลิเมอร์เมทริกซ์เกิดขึ้นได้โดยการให้ความร้อนที่ 70-80 องศาเซลเซียส ได้แผ่นฟิล์มคอมพอสิตสีน้ำเงินเข้มที่มีพอลิ(3,4-เอทิลีนไดออกซีไทโอฟีน)เกิดขึ้น จากการทดลองพบว่าการกดอัดระหว่างการให้ความร้อนจะทำให้ได้การกระจายตัวของพอลิเมอร์ที่ดีในแผ่นฟิล์ม จากการวัดค่าการนำไฟฟ้าพบว่าแผ่นฟิล์มคอมพอสิตมีค่าการนำไฟฟ้าสูงถึง 42.96 ซีเมนซ์/เซนติเมตร และพบว่าค่าการนำไฟฟ้าจะเพิ่มสูงขึ้นเมื่อเก็บแผ่นฟิล์มไว้ที่อุณหภูมิห้องซึ่งน่าจะเนื่องมาจากการเกิดปฏิกิริยาพอลิเมอร์เรซินอย่างช้าๆของมอนอเมอร์ที่ยังคงเหลืออยู่ ได้ทำการพิสูจน์เอกลักษณ์ของพอลิ(3,4-เอทิลีนไดออกซีไทโอฟีน) คอมพอสิตฟิล์ม ด้วย ฟลูเรียวทรานส์ฟอร์มสเปกโตรสโกปี, เอกซ์เรย์ดิฟแฟรกชัน, ดิฟเฟอเรนเชียลสแกนนิ่งแคลอริเมทรี และเทอร์โมกราวิเมทริกแอนาไลซิส

## ศูนย์วิทยทรัพยากร จุฬาลงกรณ์มหาวิทยาลัย

สาขาวิชา ปิโตรเคมีและวิทยาศาสตร์พอลิเมอร์.....ลายมือชื่อนิสิต.....วพ. กิติกุลวรากร.....

ปีการศึกษา.....2552.....ลายมือชื่อ อ.ที่ปรึกษาวิทยานิพนธ์หลัก.....

ลายมือชื่อ อ.ที่ปรึกษาวิทยานิพนธ์ร่วม.....

# # 5072545023: MAJOR PETROCHEMISTRY AND POLYMER SCIENCE  
 KEYWORDS: PEDOT PMMA COMPOSITE SOLID STATE POLYMERIZATION  
 CONDUCTING POLYMER

KODCHAPORN KITIKULVARAKORN: SOLID STATE POLYMERIZATION  
 OF 2,5-DIBROMO-3,4-ETHYLENEDIOXYTHIOPHENE IN POLY(METHYL  
 METHACRYLATE) MATRIX. THESIS ADVISOR: ASST. PROF. YONGSAK  
 SRITANA-ANANT, Ph.D., THESIS CO-ADVISOR: ASST. PROF. VORAVEE  
 P. HOVEN, Ph.D., 89 pp

The conductive polymer composite film containing poly (3,4-ethylenedioxy thiophene) (PEDOT) was prepared starting from electrospinning the solution mixture of 2,5-dibromo-3,4-ethylenedioxythiophene (DBEDOT) and poly(methyl methacrylate) (PMMA) matrix on glass slide. After the solvent was removed, the solid state polymerization (SSP) of the DBEDOT crystals embedded in the polymer matrix was then induced by heating at 70-80 °C. A dark blue composite film containing PEDOT was obtained. It was found that compression during heating produced better dispersed polymer in the film. The conductivity of the composite film reached as high as 42.96 S/cm and continued to increase upon storage at room temperature, which was possibly due to slow polymerization of the remaining monomers. The characteristics of the synthesized PEDOT composite film were determined by fourier-transform infrared spectroscopy, x-ray diffraction, differential scanning calorimetry, and thermogravimetric analysis.

Field of study: Petrochemistry and Polymer Science Student's signature: Kodchapor... Kitikulvarakorn

Academic year: 2009

Advisor's signature: *[Signature]*

Co-advisor's signature: *[Signature]*

## ACKNOWLEDGEMENTS

My utmost gratitude goes to my thesis advisors, Assist. Assist. Prof. Yongsak Sritana-anant and Prof. Voravee P. Hoven, for their expertise, kindness, support, and most of all, for their patience during the course of research including completing this thesis.

I am sincerely grateful to the members of the thesis committee, Assoc. Prof. Supawan Tantayanon, Assist. Prof. Warithorn Chavasiri, and Assist. Prof. Ekasit Somsuk for their valuable comments and suggestions.

I would like to thank the Center for Petroleum, Petrochemicals, and Advanced Materials from Chulalongkorn University for financial support.

I gratefully acknowledge the members of VP group and the research groups on the fourteenth floor, Mahamakut building for their companionship and friendship.

Finally, I am forever indebted to my parents and family members for their encouragement and understanding throughout the entire study.

ศูนย์วิทยทรัพยากร  
จุฬาลงกรณ์มหาวิทยาลัย

## CONTENTS

	Page
ABSTRACT IN THAI.....	iv
ABSTRACT IN ENGLISH.....	v
ACKNOWLEDGEMENTS.....	vi
CONTENTS.....	vii
LIST OF FIGURES.....	x
LIST OF TABLES.....	xiv
LIST OF SCHEMES.....	xv
LIST OF ABBREVIATION.....	xvi
CHAPTER I INTRODUCTION.....	1
1.1 Applications of organic conducting polymers.....	2
1.2 Conjugated polymers .....	2
1.3 Theoretical Aspects of charge transfer .....	7
1.4 Effect of doping .....	10
1.4.1 Chemical doping by charge transfer.....	11
1.4.2 Electrochemical doping .....	12
1.5 Effective conjugation length .....	13
1.6 Poly(3,4-ethylenedioxythiophene) (PEDOT) .....	14
1.7 Excellent characteristics of PEDOT .....	15
1.8 Synthesis of PEDOT Solid state polymerization.....	16
1.9 Processibility .....	18
1.10 Electrospinning process .....	22
1.11 Conductive measurement by four point probe technique .....	23
1.12 Objectives .....	26
1.13 Scope of the investigation .....	26

	Page
CHAPTER II EXPERIMENTAL.....	28
2.1 Materials.....	28
2.2 Equipments .....	28
2.2.1 Nuclear Magnetic Resonance (NMR) Spectrometer .....	28
2.2.2 Fourier-Transform Infrared Spectrometer (FT-IR) .....	28
2.2.3 UV-visible Spectrophotometer .....	29
2.2.4 Scanning Electron Microscopy (SEM) .....	29
2.2.5 X-ray Diffractometer (XRD) .....	29
2.2.6 Thermo Gravimetric Analysis (TGA) .....	29
2.2.7 Differential Scanning Calorimetry (DSC) .....	29
2.2.8 Surface Profile Measuring System .....	29
2.2.9 Four-Point Probe Conductometer (FPP) .....	29
2.3 Methods.....	30
2.3.1 Synthesis of 2,5-dibromo-3,4-ethylenedioxy thiophene (DBEDOT) .....	30
2.3.2 Preparation of PEDOT/polymer composite film ...	30
CHAPTER III RESULTS AND DISCUSSION .....	33
3.1 Synthesis of 2,5-dibromo-3,4-ethylenedioxythiophene (DBEDOT).	33
3.2 Preparation of DBEDOT/polymer composite fiber mats .....	36
3.3 Preparation of PEDOT/polymer composite .....	37
3.3.1 Effect of compression on the conductivity of the composite films .....	38
3.3.2 Effect of temperature and reaction time used for SSP .....	44



	Page
3.3.3 Effect of solvent and DBEDOT/polymer weight ratio .....	47
3.3.4 Effect of storage time .....	49
3.4 Physical characteristics of PEDOT-containing polymer composite films .....	50
CHAPTER IV CONCLUSION .....	55
REFERENCES.....	57
APPENDICES.....	64
APPENDIX A.....	65
APPENDIX B.....	77
VITAE.....	89



ศูนย์วิทยทรัพยากร  
 จุฬาลงกรณ์มหาวิทยาลัย

## LIST OF FIGURES

Figure	Page
1.1 Conductivity of different materials .....	1
1.2 Conjugated polymers.....	3
1.3 Energy band gaps in materials.....	3
1.4 The conductivity of conducting polymers decreases with falling temperature in contrast to that of metals .....	5
1.5 Chemical structures of few $\pi$ -conjugated polymers and their band gap Energy .....	6
1.6 Calculated (frontier) energy levels of oligothiophenes with $n = 1-4$ and polythiophene ( $E_g =$ band gap energy) .....	7
1.7 Depictions of a) neutral (undoped chain), b) polaron, and c) bipolaron..	8
1.8 UV-VIS absorption spectra of PEDOT film on ITO during the oxidation process in 0.1M TBAPF <sub>6</sub> -acetonitrile. The potential range is 1.0 $\pm$ 0.6V, scan rate 100 mV/s .....	10
1.9 A defect in polyacetylene and steric induced structural twisting in poly(3-alkylthiophene).....	13
1.10 Twisting of polythiophene .....	13
1.11 3,4-Ethylenedioxythiophene (EDOT) (a) and poly(3,4-ethylenedioxythiophene) (PEDOT) (b).....	14
1.12 Poly(3,4-ethylenedioxythiophene)/polystyrene sulfonic acid (PEDOT/PSS) .....	19
1.13 Schematic of electrospinning apparatus set up.....	23
1.14 Schematic representation of 4-point probe configuration .....	24
2.1 Schematic of electrospinning apparatus set-up .....	32
2.2 Schematic representation of the pressing of the DBEDOT/polymer fiber mats.....	32
3.1 <sup>1</sup> H-NMR spectra of EDOT and DBEDOT .....	35

Figure	Page
3.2 SEM image ( $\times 5000$ ) of as-spun PMMA fiber mat electrospun from 18% (w/v) PMMA in (a) DMF, (b) mixed 1:1 (v/v) THF/DMF, and as-spun DBEDOT/PMMA composite fiber mats electrospun from a mixture containing 3:1 (w/w) DBEDOT/PMMA in (c) DMF and (d) mixed 1:1 (v/v) THF/DMF .....	37
3.3 Resistance measured on the top and bottom side of the PEDOT/PMMA composite film prepared by SSP of the electrospun 3:1 (w/w) DBEDOT/ PMMA fiber mats by heating at 70 °C for 48 h with pressing as a function of reaction time.....	38
3.4 SEM micrographs (at 5000x) of the composite fiber mats electrospun from a mixture containing 3:1 (w/w) DBEDOT/PMMA in DMF before SSP (a), after SSP at 70 °C for 48 h without (b) and with pressing (c), SEM micrographs (at 5,000x) of PEDOT/PMMA composite film obtained after SSP at 70 °C for 48 h without (d), with pressing (e), PEDOT extracted from PEDOT/PMMA composite film prepared by SSP of the 3:1 (w/w) DBEDOT/PMMA fiber mats at 70 °C for 48 h without pressing (f) and with pressing (g).....	40
3.5 FT-IR spectra of PEDOT/PMMA composite film without pressing (a) 3:1, (b) 4:1, PEDOT/PMMA composite film pressing (c) 3:1 and (d) 4:1 .....	41
3.6 FT-IR spectra of (a) controlled PEDOT and (b) extracted PEDOT.....	42
3.7 TGA thermograms of (a) controlled PEDOT, (b) electrospun PMMA fiber mat, (c) PEDOT/PMMA (3:1) composite film non-pressing and (d) PEDOT/PMMA (3:1) composite film pressing .....	43
3.8 TGA thermograms of (a) manually mixed pure PEDOT and PMMA at 3 weight ratio and (b) extracted PEDOT .....	44

Figure	Page
3.9 SEM micrographs (at 500x) of PEDOT/PMMA composite film without pressing heat treatment at (a) 60 °C, (b) 70 °C and (c) 80 °C and (at 2000x) (d) PEDOT/PMMA composite film heat treatment at 60 °C.....	45
3.10 Resistance of the PEDOT/PMMA composite film prepared by SSP of the electrospun (a) 3:1 (w/w) DBEDOT/ PMMA fiber mats in DMF heated 80 °C, (b) at 70 °C, (c) 4:1 (w/w) DBEDOT/ PMMA fiber mats in DMF by heating at 80 °C and (d) at 70 °C .....	47
3.11 Percentage conversion of extracted PEDOT from PEDOT/PMMA and composite films as a function of DBEDOT/polymer weight ratio. The SSP was conducted at 70 °C for 48 h in 1:1 THF/DMF solvent .....	49
3.12 Conductivity of PEDOT/PMMA composite film prepared by SSP of the 3:1 (w/w) DBEDOT/PMMA fiber mat electrospun from 1:1 THF/DMF solution with pressing as a function of storage time at ambient temperature.....	50
3.13 UV-Visible spectra of (a) PEDOT/PMMA composite film in DMF, (b) controlled PEDOT, (c) extracted PEDOT and (d) PEDOT/PMMA composite film in DMF:THF (1:1) .....	51
3.14 XRD diffractograms of (a) electrospun PMMA fiber mat, (b) DBEDOT crystal, (c) electrospun 3:1 (w/w) DBEDOT/PMMA fiber mat, (d) electrospun 3:1 (w/w) PEDOT/PMMA fiber mat non-pressing, (e) electrospun 3:1 (w/w) PEDOT/PMMA fiber mat pressing and (f) controlled EDOT.....	52
3.15 DSC thermogram of (a) PMMA pellet, (b) electrospun PMMA fiber mat , (c) pure DBEDOT, (d) elctrospun 3:1 DBEDOT/PMMA fiber mat, (e) 3:1 PEDOT/PMMA composite film non-pressing, (f) 3:1 PEDOT/PMMA composite film pressing, (g) 4:1 PEDOT/PMMA composite film pressing .....	54

Figure	Page
A-1 A multiple reflection ATR system .....	66
A-2 FT-IR spectra of electrospun PMMA .....	66
A-3 FT-IR spectra of 3:1 PEDOT/PMMA composite film without pressing at 70 °C for 48 h .....	67
A-4 FT-IR spectra of 4:1 PEDOT/PMMA composite film without pressing at 70 °C for 48 h .....	67
A-5 FT-IR spectra of 3:1 PEDOT/PMMA composite film pressing at 70 °C for 48 h .....	68
A-6 FT-IR spectra of 4:1 PEDOT/PMMA composite film pressing at 70 °C for 48 h .....	68
A-7 Schematic representation of 4-point probe configuration .....	69
A-8 TGA thermograms of electrospun PMMA fiber mat .....	72
A-9 TGA thermograms of electrospun DBEDOT/PMMA fiber mat .....	72
A-10 TGA thermograms of PEDOT/PMMA (3:1) composite film without pressing .....	73
A-11 TGA thermograms of PEDOT/PMMA (4:1) composite film without pressing .....	73
A-12 TGA thermograms of PEDOT/PMMA (3:1) composite film with pressing .....	74
A-13 TGA thermograms of PEDOT/PMMA (4:1) composite film with pressing .....	74
A-14 TGA thermograms of controlled PEDOT .....	75
A-15 TGA thermograms of extracted PEDOT .....	75
A-16 TGA thermograms of manually mixed pure PEDOT powder and PMMA fiber mat at 3:1 weight ratio .....	76

## LIST OF TABLES

Table	Page
1.1 Conductivity data of PEDOT polymers.....	18
3.1 FT-IR C=O stretching signals of the PEDOT/PMMA composite film: prepared by SSP of the electrospun DBEDOT/PMMA fiber mats heated For 48h .....	41
3.2 Conductivity of the PEDOT/PMMA composite film prepared by SSP of the electrospun DBEDOT/PMMA fiber mat by heating for 48 h .....	46
3.3 Conductivity and thickness of the PEDOT/PMMA composite film prepared by SSP of the electrospun DBEDOT/PMMA fiber mat by heating for 48 h .....	48
A-1 Conductivity measured on the top side and the bottom side of the PEDOT/PMMA composite film (thickness of $55.8513 \pm 13.8211 \mu\text{m}$ ) prepared by SSP of the electrospun 3:1 (w/w) DBEDOT/ PMMA fiber mats by heating $70^\circ\text{C}$ with pressing as a function of reaction time .....	70
A-2 Resistance measured on the top side of the PEDOT/PMMA composite film (thickness of $55.8513 \pm 13.8211 \mu\text{m}$ ) prepared by SSP of the electrospun 3:1 (w/w) DBEDOT/ PMMA fiber mats by heating $70^\circ\text{C}$ and $80^\circ\text{C}$ with pressing as a function of reaction time .....	71

ศูนย์วิจัยทรัพยากร  
 จุฬาลงกรณ์มหาวิทยาลัย

## LIST OF SCHEMES

Scheme	Page
1.1 Solid state polymerization of DBEDOT.....	17
2.1 Bromination of EDOT.....	30
2.2 Solid state polymerization of DBEDOT .....	32
3.1 Synthesis of 2,5-dibromo-3,4-ethylenedioxythiophene .....	33
3.2 Bromination mechanism though electrophilic aromatic substitution .....	34
3.3 Bromination mechanism though radical-based single electron transfer followed by aromatic substitution .....	34
3.4 Mechanism of solid state polymerization of DBEDOT.....	38



ศูนย์วิทยทรัพยากร  
จุฬาลงกรณ์มหาวิทยาลัย

## LIST OF ABBREVIATION

Br <sub>2</sub>	: bromine
°C	: degree celsius
CDCl <sub>3</sub>	: deuterated chloroform
CH <sub>3</sub> COOH	: acetic acid
cm	: centimeter
conc.	: concentrated
CPs	: conjugated polymers
DBEDOT	: 2,5-dibromo-3,4-ethylenedioxythiophene
DMF	: <i>N, N</i> -dimethylformamide
DSC	: differential scanning calorimetry
EDOT	: 3,4-ethylenedioxythiophene
eq	: equivalent
FT-IR	: fourier-transform infrared spectrophotometer
g	: gram
HOMO	: highest occupied molecular orbital
I <sub>2</sub>	: iodine
kV	: kilovoltage
LUMO	: lowest unoccupied molecular orbital
min	: minute
mL	: milliliter
mm	: millimeter
M <sub>w</sub>	: weight average molecular weight
N/A	: not available
NaHCO <sub>3</sub>	: sodium hydrogen carbonate
NBS	: <i>N</i> -bromosuccinimide
nm	: nanometer
NMR	: nuclear magnetic resonance spectroscopy
PEDOT	: poly(3,4-ethylenedioxythiophene)
PMMA	: poly(methyl methacrylate)



S	: seimens
SEM	: scanning electron microscopy
SPS	: sulfonated polystyrene
SSP	: solid state polymerization
$T_g$	: glass transition temperature
$T_m$	: melting temperature
TGA	: thermogravimetric analysis
THF	: tetrahydrofuran
UV	: ultraviolet
w/v	: weight by volume
w/w	: weight by weight
XRD	: x-ray diffractometer
$2\theta$	: 2 theta
$\delta$	: chemical shift



ศูนย์วิทยทรัพยากร  
จุฬาลงกรณ์มหาวิทยาลัย

# CHAPTER I

## INTRODUCTION

During the last few decades, much attention has been paid to the field of organic electronics. Electrical devices made out of plastic materials provide great advantages due to their special chemical and electrical behavior as compared with standard semiconductors. Organic light emitting diodes (OLEDs), plastic solar cells or organic field effect transistors (OFETs) are some of the new devices in this area. Great progress has been made to investigate, understand, improve and utilize their unique physical features [1-2]. Commercial products are entering the consumer markets and show the potential of this new technology. The foundation of the field of organic electronics was established back in the seventies with the discovery that the conductivity of polyacetylene films can be changed over several orders of magnitude by chemical doping. For their groundbreaking work in this area, MacDiarmid, Heeger and Shirakawa were awarded the Nobel Prize in Chemistry 2000. Excellent introductions into the field of organic electronics are their Nobel lectures. Intrinsic conducting plastic materials and semiconductors, both electron (n-type) and hole transport (p-type) materials with band-like structures, could now be made. Since the early work, many innovative materials in pure form have been developed and characterized for the usage in electronic applications [3-4]. An overview of the conductivity of different materials from insulators to metals and the span organic materials cover is shown in Figure 1.1.

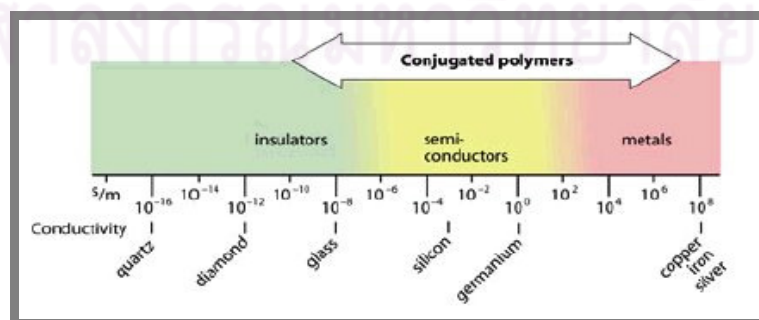


**Figure 1.1** Conductivity of different materials

## 1.1 Applications of organic conducting polymers

According to the attractive and tunable properties of organic conducting polymers, this facilitates the use of conducting polymers in many applications such as:

### 1) Applications utilizing the inherent conductivity of polymer

Antistatic coating (metal and polymer), microelectronic devices, stealth material for providing a minimum radar profile for military aircrafts and naval vessels

### 2) Electrochemical switching, energy storage and conversion

New rechargeable battery, redox supercapacitors

### 3) Polymer photovoltaics (light-induce charge separation)

### 4) Display technologies

Light emitting diode (LED), flat panel displays

### 5) Electromechanical actuators

Artificial muscles, windows wipers in spacecrafts, rehabilitation gloves electronic Braille screen, bionic ears for deaf patients.

### 6) Separation technologies

Novel smart-membrane, selective molecular recognition

### 7) Cellular communication

Growth and control of biological cell cultures

### 8) Controlled release devices

Ideal host for the controlled release of chemical substances

### 9) Corrosion protection

New-generation Corrosion protective coatings

## 1.2 Conjugated polymers [5-7]

Conjugated polymers (CPs) are organic semiconductors. These polymers consist of alternating single and double bonds, creating an extended p-network. Electron movement within this p-framework is the source of conductivity, with respect to electronic energy levels, hardly differs from inorganic semiconductors. Both have their electrons organized in bands rather than in discrete levels and their ground state energy bands are either completely filled or completely empty. The band

structure of a conjugated polymer originates from the interaction of the  $\pi$ -orbital of the repeating units throughout the chain. Figure 1.2 shows commonly known conjugated polymers that are conductive.

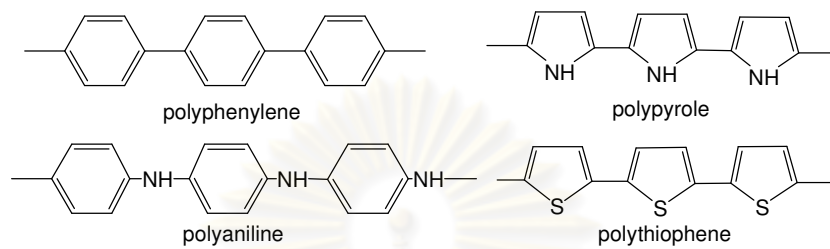


**Figure 1.2** Conjugated polymers

Analogous to semiconductors, the highest occupied band (originating from the HOMO of a single thiophene unit) is called the valence band, while the lowest unoccupied band (originating from the LUMO of a single thiophene unit) is called the conduction band. The difference in energy between these energy band levels is called the band gap energy or simply, band gap ( $E_g$ ). Generally speaking, because conducting polymers possess delocalized electrons in  $\pi$ -conjugated system along the whole polymeric chain, their conductivity is much higher than that of other polymers with no conjugated system. These latter non-conjugated polymers are usually known to be insulators.

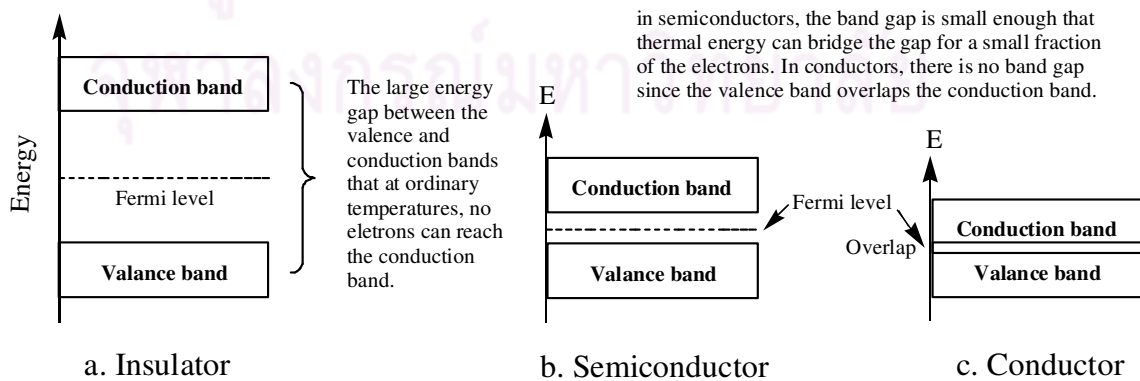


**Figure 1.3** Energy band gaps in materials [8]

The difference between  $\pi$ -conjugated polymers and metals is that in metals, the orbitals of the atoms overlap with the equivalent orbitals of their neighboring atoms in all directions to form molecular orbitals similar to those of isolated molecules. With  $N$  numbers of interacting atomic orbitals, there would be  $N$  molecular orbitals. In the metals or any continuous solid-state structures,  $N$  will be a very large number (typically  $10^{22}$  for  $1 \text{ cm}^3$  metal piece). With so many molecular orbitals spaced together in a given range of energies, they form an apparently continuous band of energies

In insulators, the electrons in the valence band are separated by a large gap from the conduction band. However, in conductors like metals, the valence band overlaps with the conduction band. And in semiconductors, there is a small enough gap between the valence and conduction bands that thermal or other excitations can bridge the gap. With such a small gap, the presence of a small percentage of a doping material can increase conductivity dramatically.

The conductivity of the metal is due either to partly-filled valence or conduction band, or to the band gap being near zero, so that with any weak electric field the electrons easily redistribute. Electrons are excited to the higher energy bands and leave unfilled bands or "holes" at lower energy. Metals and conducting polymers exhibit opposite directions of conducting behavior as a function of temperature as shown in Figure 1.4. Conductivity generally increases with decreasing temperature for metallic materials, (some of which become superconducting below certain critical temperature,  $T_c$ ) while it generally decreases with lowered temperature for polymeric semiconductors and insulators.

จุฬาลงกรณ์มหาวิทยาลัย

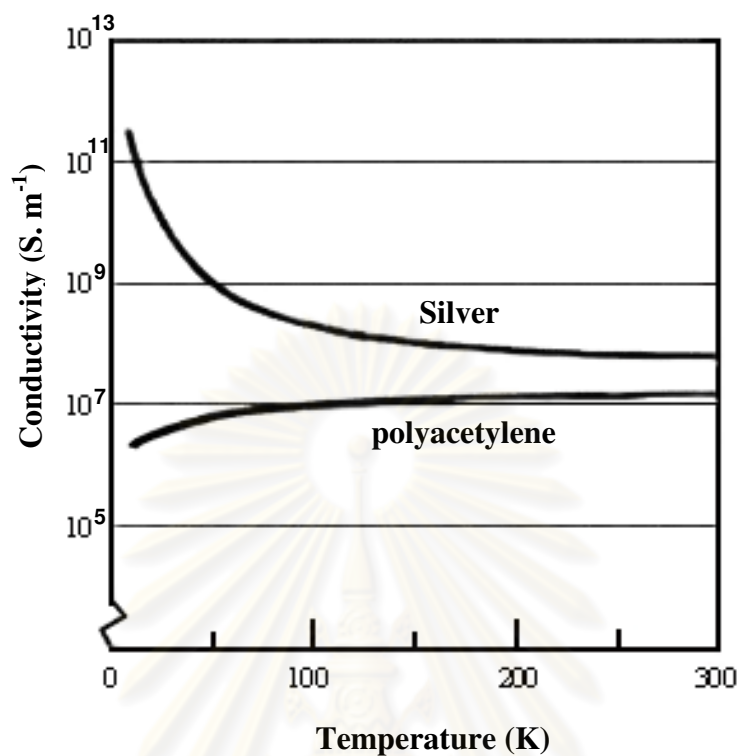


**Figure 1.4** The conductivity of conducting polymers decreases with falling temperature in contrast to that of metals [8]

Since  $\pi$ -conjugated polymers allow virtually endless manipulation of their chemical structures; the control of the band gap of these semiconductors is a research issue of ongoing interest. This “band gap engineering” may give the polymer to its desired electrical and optical properties. Reduction of the band gap to approximately zero is expected to afford an intrinsic conductor like metals. Example of them  $\pi$ -conjugated polymers being intensively studied are shown in Figure 1.5.

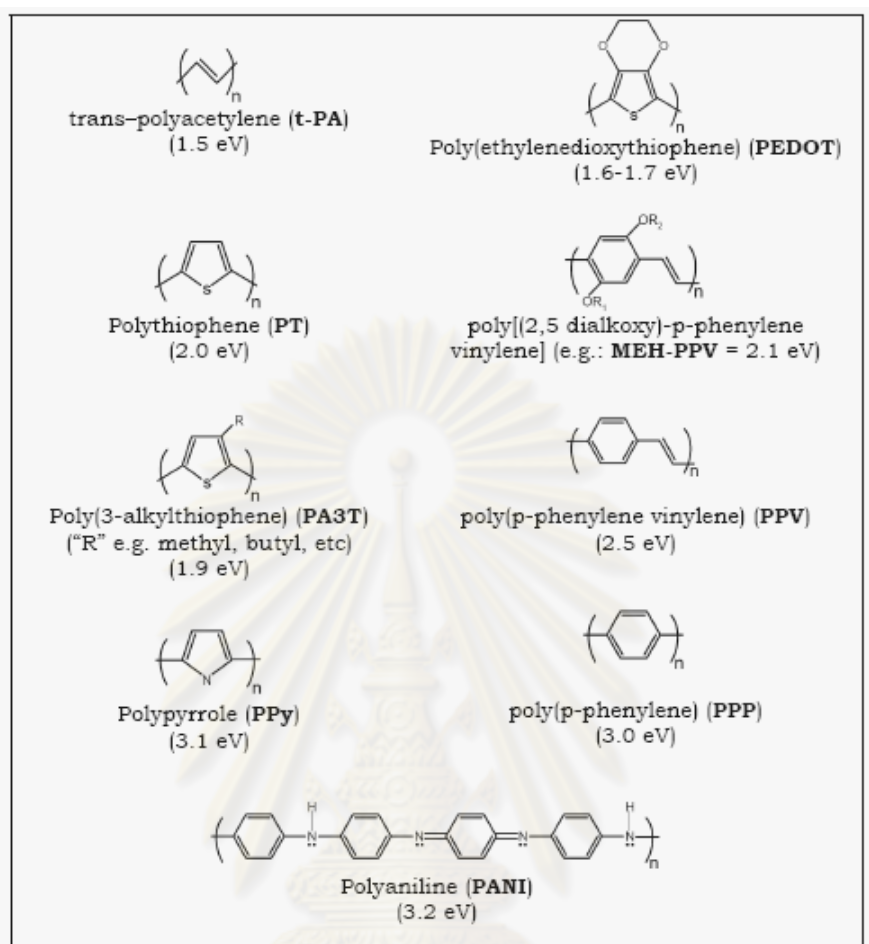


**Figure 1.5** Chemical structures of few  $\pi$ -conjugated polymers and their band gap Energy [9]

Both conjugated conducting polymers and inorganic semiconductor electronic structure are very similar in nature. They have their electrons organized in bands rather than in discrete levels and their ground state energy bands are either completely filled or completely empty. The band structure of a conjugated polymer originates from the interaction of the  $\pi$ -orbitals of the repeating units throughout the chain. This is illustrated in Figure 1.6 where the calculated energy levels of oligothiophenes with  $n = 1-4$  and polythiophene are shown as a function of oligomer length. Addition of each new thiophene unit causes rehybridization of the energy levels yielding more and more sublevels until a point reached at which there are bands rather than discrete levels. The interaction between the  $\pi$ -electrons of neighboring molecules lead to a three-dimensional band structure.

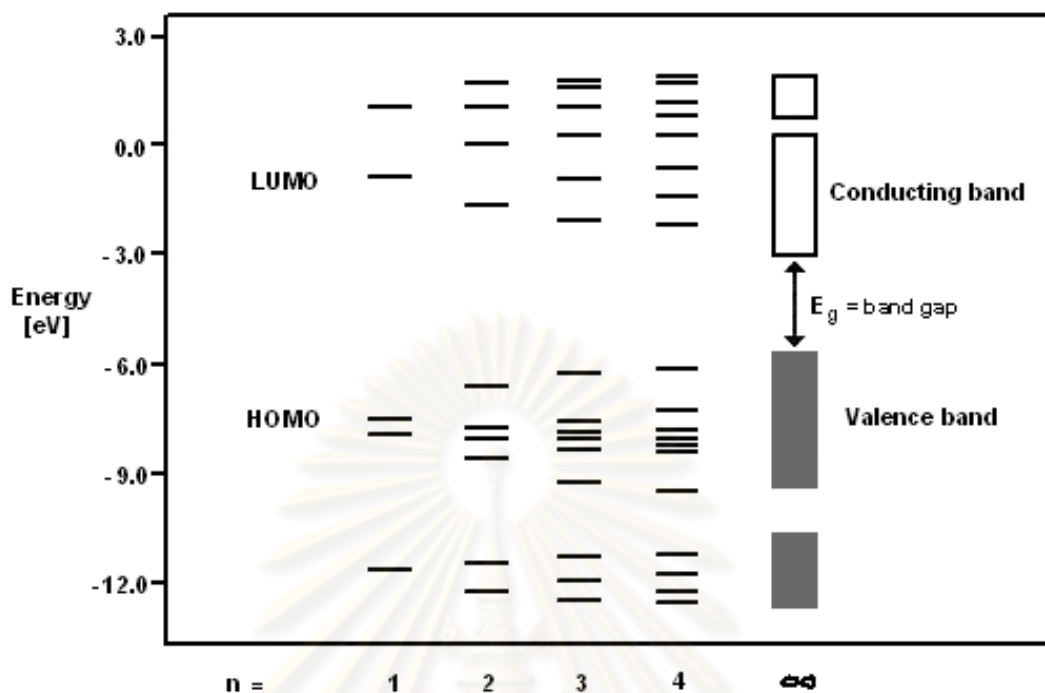


**Figure 1.6** Calculated (frontier) energy levels of oligothiophenes with  $n = 1-4$  and of polythiophene ( $E_g =$  band gap energy) [10]

### 1.3 Theoretical aspects of charge transfer [11]

Electron or charge transfer in conjugated polymers determines whether the polymer is conductive or insulating. How the charge is transported determines the performance of the devices fabricated from the polymer. Oxidation or reduction of a conjugated polymer leads to the introduction of positive or negative charges into the polymer chain, giving rise to an increased conductivity. The term *doping* can be misleading as what occurs is best viewed as a redox process. The insulating neutral polymer is converted into a salt consisting of a polycation (or polyanion) and counterions, which are the reduced forms of the oxidizing agent (or the oxidized forms of the reducing agent). From a chemical point of view, the “doped” polymers are actually new compounds – carbocations or carbanions of the original compound.

Using solid-state physics language, however, oxidation corresponds to *p*-type doping and reduction to *n*-type doping. *P*-doping occurs with a positive applied voltage, under which conditions the polymer chain is oxidized. Electrons move from the chain to the electrode giving rise to polarons (partially delocalized radical cations; see Figure 1.7) and bipolarons (polaron with a second electron removed) in the chain.



Polarons and bipolarons may be viewed as electron holes, which can move along the chain to produce an electrical current. Anions become incorporated into the polymer matrix to compensate the positively charged polymer backbone. *N*-doping occurs when a negative applied potential is applied to the polymer, under which conditions negative charges are created in the chain as electrons move from the electrode to the polymer. Consequently, cations from the solution become incorporated into the polymer structure to compensate for the negatively charged polymer backbone. Electrons serve as charge carriers in this case.

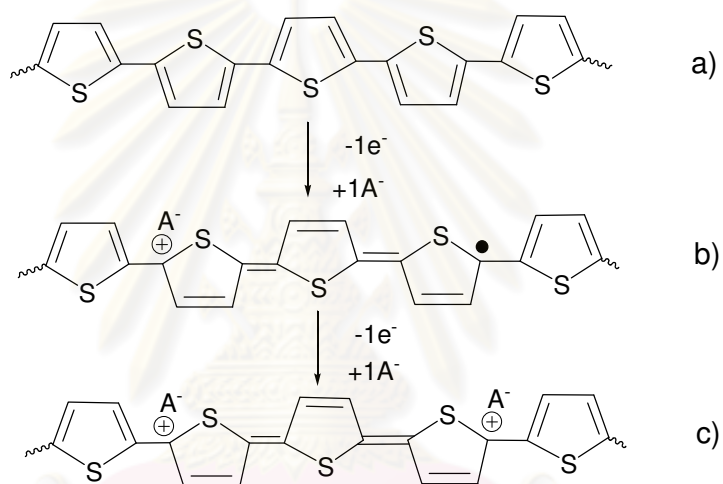


**Figure 1.7** Depictions of a) neutral (undoped chain), b) polaron, and c) bipolaron

Overall conductivity in a polymer is determined by both its intramolecular and intermolecular conductivities. Chain length plays the most important role in intramolecular conductivity. The longer the conjugated  $\pi$ -system, the greater the conductivity will be. Intermolecular conductivity returns us to the electron/hopping discussion which first arose when making a distinction between redox and conjugated polymers. Intermolecular conductivity is due to the same phenomenon as one finds in redox polymers (hopping). Because conjugated polymers are normally constructed of layered planar conjugated molecules, the attractive interactions between  $\pi$ -electron clouds enhance electron hopping between layers. This has been labeled  $\pi$ -dimerization.

The *doping level* is a measure of to what degree the polymer is oxidized or reduced. The electrically conducting form is obtained when the polymer is doped. For example, the polymer polyacetylene exhibits a conductivity of  $10^{-9} \Omega^{-1}\text{cm}^{-1}$  in its undoped form while achieving conductivities of  $10^3 \Omega^{-1}\text{cm}^{-1}$  and higher in the doped form. The electrical conductivity is strongly dependent upon the polymer's doping level. Polymers may be doped either chemically or electrochemically. The doping level is normally higher for electrochemically doped polymers than for chemically doped polymers. With chemical doping, electron acceptors (*p*-doping) or electron donors (*n*-doping) need to be added to the solution in order to make the doping reaction take place. Some examples are oxygen,  $\text{I}_2$  and arsenic pentafluoride. A polymer can be doped electrochemically by simply applying an appropriate potential across the film in the presence of counterions.

In Figure 1.8, UV-VIS spectroelectrochemical curves recorded for different electrode potential are shown for regioregular poly(3,4-ethylenedioxythiophene) prepared using the method of Kvarnstrom and coworkers [12]. Cyclic voltammograms of poly(3,4-ethylenedioxythiophene) unambiguously indicate that oxidative doping of this polymer is a two-step phenomenon since two overlapping redox couples are clearly seen. This two-step oxidation is also manifested in UV-vis spectroelectrochemical studies. The spectra recorded for increasing doping levels show gradual bleaching of the  $\pi$ - $\pi^*$  transition with simultaneous growth of two peaks at 580 nm and 700 nm, usually ascribed to the formation of bipolaron sub-gap states.

ศูนย์วิทยทรัพยากร  
จุฬาลงกรณ์มหาวิทยาลัย

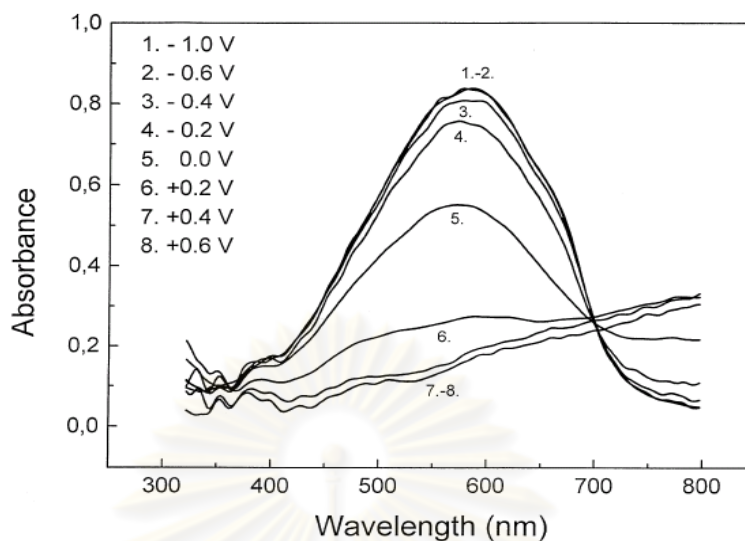


**Figure 1.8** UV-VIS absorption spectra of PEDOT film on ITO during the oxidation process in 0.1 M TBAPF<sub>6</sub>-acetonitrile. The potential range is -1.0–+0.6 V, scan rate 100 mV/s

#### 1.4 Effect of doping [13]

The doping process is an addition of a doping agent into the polymer expecting to enhance the conductivity of the polymer. The modification of electrical conductivity of conducting polymers from insulator to metal can be accomplished either by chemical doping or by electrochemical doping. Both *n-type* (electron donating) and *p-type* (electron accepting) dopants have been used to induce an insulator-to-conductor transition in electronic polymers. Familiar to inorganic semiconductors, these dopants remove or add charges to the polymers. However, unlike substitutional doping that occurs in conventional semiconductors, the dopant atomic or molecular ions are interstitially positioned between  $\pi$ -conjugated polymers chain, and donate charges to or accept charges from the polymer backbone. In this case, the counter ion is not covalently bound to the polymer, but only attracted to it by the Coulombic force. In self-doping cases, these dopants are covalently bound to the polymer backbone [14]. Initially added charges during doping process do not simply start to fill the conduction band to have metallic behavior immediately. The strong coupling between electrons and phonons near the doped charges causes distortions of the bond lengths. For degenerate ground state polymers such as trans-polyacetylene, doped charges at low doping levels are stored in charged solitons whereas nondegenerate systems they are

stored as charged polarons or bipolarons [15-18]. High doping for the non-degenerate polymers results in polarons interacting to form a polaron lattice or electrically conducting partially filled energy band [19-20]. Bipolarons or the pairs of polarons are formed in less ordered regions of doped polymers [21].

Simultaneous with the doping, the electrochemical potential (the Fermi level) (Figure 1.3) is moved either by a redox reaction or an acid-base reaction into a region of energy where there is a high density of electronic states; charge neutrality is maintained by the introduction of counter-ions. The electrical conductivity results from the existence of charge carriers through charge doping and from the ability of those charge carriers to move along the  $\pi$ -bonds; however, disorder restricts the carrier mobility and limits the electrical conductivity in the metallic state. Accordingly, electrical conductivity of doped conjugated polymers is improved due to two reasons:

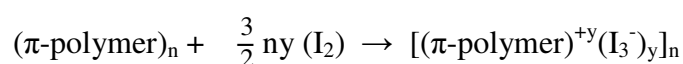
- 1) Doping process introduces carriers into the electronic structure. Since every repeating unit is a potential redox site, conjugated polymers can be doped *n*-type (reduced) or *p*-type (oxidized) to a relatively high density of charge carriers.
- 2) The attraction of an electron in one unit to the nuclei in the neighboring units leads to carrier delocalization along the polymer chain and to charge carrier mobility, which is extended into three dimensions through inter-chain electron transfer.

Charge injection or “doping” onto conjugated conducting polymers leads to the wide variety of interesting and important phenomena which define the field. The doping can be accomplished in a number of ways:

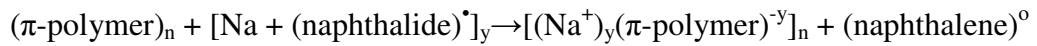
#### 1.4.1 Chemical doping by charge transfer

The first discovery of the ability to dope conjugated polymers involved charge transfer redox chemistry; oxidation (*p*-type doping) or reduction (*n*-type doping), as demonstrated with the following examples:

##### 1. *p*-type



## 2. *n*-type

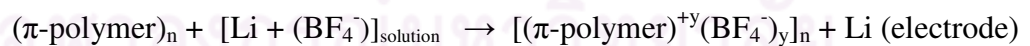


When the doping level is sufficiently high, the electronic structure of conjugated polymers approached to that of a metal.

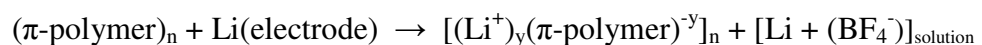
### 1.4.2 Electrochemical doping

Although chemical (charge transfer) doping is an efficient and straightforward process, it is normally difficult to control. Complete doping to the highest concentrations yields reasonably high quality materials; however, attempts to obtain intermediate doping levels often result in inhomogeneous doping. Electrochemical doping was originated to solve this problem. In electrochemical doping, the electrode supplies the redox charge to the conducting polymer, while ions diffuse into (or out of) the polymer structure from the nearby electrolyte to compensate the electronic charge. The doping level is determined by the voltage between the conducting polymer and the counter-electrode; at electrochemical equilibrium the doping level can be achieved by setting the electrochemical cell at a fixed applied voltage and simply waiting as long as necessary for the system to come to electrochemical equilibrium as indicated by the current through the cell going to Zero. Electrochemical doping is illustrated by the following examples:

#### 1. *p*-type



#### 2. *n*-type



### 1.5 Effective conjugation length (ECL)

Ideal conducting polymers should have its  $\pi$  electrons in the conjugated unsaturated bonds even by distributing throughout the whole chain. This requirement usually does not hold due to the following:

- i) Formation of defects in polymer
- ii) Twisting of planar structure out of conjugation in the polymer.

Examples of the two reasons above are exemplified in Figure 1.9. Formation of a defect in polyacetylene as a saturated  $sp^3$ -hybridized methylene caused the disruptive effect in the flow of electrons on polymer chain. In another case, the steric incumbent between adjacent R groups on HH thienyl units in irregular poly(3-alkylthiophene) brought about the twisting of the thienyl ring planes out of coplanarity, causing an increase in the energy needed to allow the flow of electrons through the polymer chain, hence making the polymer chain less conductive.

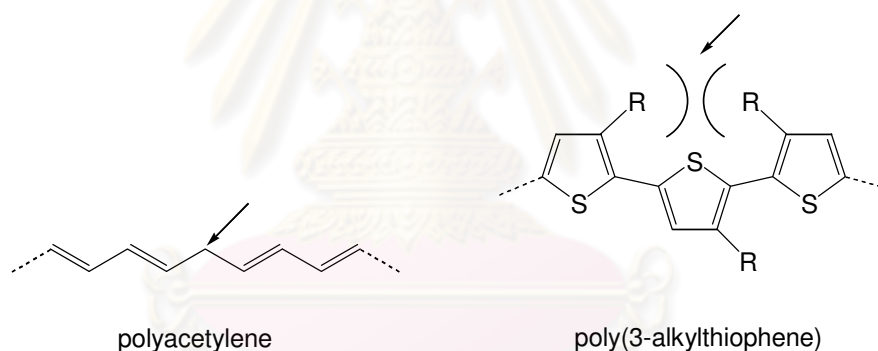


**Figure 1.9** A defect in polyacetylene and steric induced structural twisting in poly(3-alkylthiophene)

Another possible reason would be the twisting of polymer chain, which occurs randomly at the single bonds and divided the polymer into separated sections with their own coplanarity (Figure 1.10). Twisting of polymer chain would also cause the reduction of conjugation in the polymer.

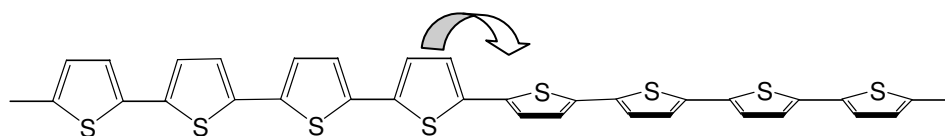


**Figure 1.10** Twisting of polythiophene

### 1.6 Poly(3,4-ethylenedioxythiophene) (PEDOT) [22-27]

Chemical modifications of polythiophene have been widely carried out in recent years to satisfy different application requirements. The most familiar and important one is regioregular poly(3,4-ethylenedioxythiophene) (PEDOT). PEDOT is also one of the few examples within the conjugated polymer family which is both p- and n-dopable. It is well known that upon electrochemical p-doping (n-doping) conducting polymers undergo oxidation (reduction) of the polymer backbone resulting not only in an increase of their electronic conductivity but also in structural transitions which give rise to spectral changes.

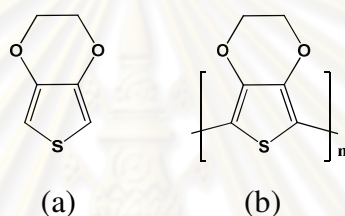


**Figure 1.11** 3,4-Ethylenedioxythiophene (EDOT) (a) and Poly(3,4-ethylenedioxythiophene) (PEDOT) (b)

PEDOT has been developed into one of the most successful materials from both fundamental and practical perspective. It possesses several advantageous properties as compared with other polythiophene derivatives: it combines a low oxidation potential and moderate band gap with good stability in the oxidized state. Also, by blocking the  $\beta$ -positions of the heterocyclic ring, the formation of  $\alpha$ - $\beta$  linkages during polymerization is prevented, resulting in a more regiochemically defined material. In addition to a high conductivity (550 S/cm in the electrochemical doped state), PEDOT is found to be highly transparent in thin, oxidized films. As a result, PEDOT derivatives are now utilized in several industrial applications including antistatic coatings for photographic films, electrode material in solid-state capacitors, substrates for electroless metal deposition in printed circuit boards, indium tin oxide (ITO) electrode-replacement material in inorganic electroluminescent lamps, and hole conducting material in organic/polymer-based light-emitting diodes (OLEDs/PLEDs).

3,4-Ethylenedioxythiophene (EDOT) is a commercially available, oxidatively polymerizable monomer which polymerizes at relatively low applied potentials (+1.0 V vs Ag/Ag<sup>+</sup>). Jonas and Heywang [24] first polymerized EDOT to poly(3,4-ethylenedioxythiophene), (PEDOT), and found the polymer to be useful for antistatic coatings. Ingnas and co-workers [26] showed the usefulness of PEDOT as a potential material for electrochromic devices due to its ability to cycle between an opaque blue-black in the reduced (undoped) state and a transmissive sky blue in the oxidized (doped) state. Conductivities reported for PEDOT prepared electrochemically range from 10 to 100 S/cm, and these conductivities have been found to be stable for up to 1000 h at 120 °C in a laboratory atmosphere.

### **1.7 Excellent characteristics of PEDOT [28-36]**

PEDOT is one of the most promising materials for practical applications due to its following characteristics:

- Reversible doping state

PEDOT can be repeatedly doped and undoped. PEDOT is almost transparent and light blue in the oxidized state and can be easily changed into opaque and dark blue appearance in the neutral state. Thus its color changes visibly when its doped state changes and may be suitable for optical applications, such as electrochromic displays [28].

- Excellent stability

PEDOT has improved chemical and thermal stability. Thermal studies show that a continuous degradation occurs above 150 °C and complete decomposition above 390 °C [29]. Electrical conducting properties appear to remain almost unaltered after aging in environmental conditions. Its high stability is attributed to favorable ring geometry and the electron-donating effect of the oxygen atoms at the 3,4-positions stabilizing the positive charge in the polymer backbone [30].

- Regular structure

Due to the structure of the monomer, competing polymerizations through 3- and 4- positions as in thiophene are avoided. Thus, only the 2,5-couplings of the 3,4-



ethylenedioxythiophene are expected. Therefore, PEDOT is expected to have fewer defects than the thiophene analogues.

- Low band-gap (High conductivity)

PEDOT has a low band gap of 1.5-1.6 eV [31]. The lower band-gap relative to polythiophene is thought to originate from the influence of the electron-donor ethylenedioxy groups on the energies of the frontier levels of the  $\pi$  system [32]. Experimental results show that after doping, PEDOT exhibits reduced absorption in the visible: the oscillator strength shifts from around 1.5 eV (lowest  $\pi$ - $\pi^*$  transition) to below 1 eV in the metallic state [33]. Thus it shows a high electrical conductivity (up to 550 S/cm) in the doped state.

- Electrochemical properties

Compared to other conducting polymers, electrochemically synthesized films of PEDOT have a low redox potential and excellent stability in their doped state [34]. Studied by cyclic voltammetry, it was found that the redox peaks at approximately 0 mV (oxidation) and -400 mV (reduction) remained almost unaffected during cycling. However, only under an applied negative potential of -700 mV were the neutral films found to be stable. Open circuit potential measurements showed that the neutral films were rapidly oxidized [35].

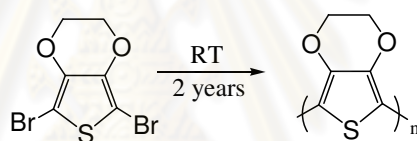
### **1.8 Synthesis of PEDOT Solid state polymerization [37-39]**

Polymerization of PEDOT by traditional oxidative polymerization with  $\text{FeCl}_3$  in organic solvents gives an insoluble blue-black polymer powder. The limitations of traditional polymerization methods can be a serious problem for PEDOT applications as well as for in-depth investigation of molecular order in this conducting polymer. It is generally not possible to obtain a well-defined polymer structure, unless the synthesis of conducting polymers is carried out via pure chemical polymerization routes, without adding any catalysts. A possible solution for this lies in a solid-state polymerization of a structurally pre-organized crystalline monomer.

The advantages of solid-state polymerization (SSP) include low operating temperatures, which restrain side reactions and thermal degradation of the product, while requiring inexpensive equipment, and uncomplicated and environmentally

sound procedures. Also by-products can be easily removed by application of vacuum or through convection caused by passing an inert gas.

In 2003, Meng et al. [38-39] reported that the solid-state polymerization (SSP) of DBEDOT was discovered by chance as a result of prolonged storage (2 years) of the monomer at room temperature. The colorless crystalline DBEDOT, with time, transformed into a black blue material without apparent change of morphology. Surprisingly, the conductivity of this decomposition product appeared to be very high (up to 80 S/cm) for an organic solid. Even though this type of non catalytic coupling was not known in organic chemistry, indeed, the most likely explanation for the observed transformation was polymerization with formation of bromine-doped PEDOT. The following characterizations unequivocally confirmed the proposed structure (see below).



**Scheme 1.1** Solid state polymerization of DBEDOT

The room-temperature conductivity of different SSP-PEDOT samples was measured by the four point probe method (Table 1.1). The highest conductivity belongs to the polymer prepared at lowest temperature and longest reaction time, which may reflect achievement of a higher degree of order. Indeed, heating above the monomer's melting point results in dramatically reduced conductivity (0.1 S/cm), which rises up to 5.8 S/cm after doping with iodine, approaching the value of an FeCl<sub>3</sub>-synthesized PEDOT (7.6 S/cm). Not very significant, but certain increase in conductivity of SSP-PEDOT (about 2 times) was found on exposing a sample to iodine vapor.

From the experiment, they concluded that heating DBEDOT in the solid state resulted in an unprecedented self-coupling reaction and gave highly conduction and relatively well-ordered bromine-doped PEDOT. Furthermore, heating DBEDOT above its melting point led to polymer with a lower conductivity.

**Table 1.1** Conductivity data of PEDOT polymers

	$\sigma_{rt}$ (SSP-PEDOT)/				$\sigma_{rt}$ (FeCl <sub>3</sub> -PEDOT)/
	Scm <sup>-1</sup>				Scm <sup>-1</sup>
Reaction Temperature (°C)	20	60	80	120	0-5
Reaction time	2 years	24 h	4 h	24 h	24 h
“crystals”/ “fibers”	80	33	20	NA	N/A
pellets as synthesized	30	18	16	0.1	N/A
pellets after I <sub>2</sub> doping	53	30	27	5.8	7.6
thin films	N/A	23	N/A	N/A	N/A
Thin films after I <sub>2</sub> doping	N/A	48	N/A	N/A	N/A

N/A = Not available

### 1.9 Processibility

Poly(3,4-ethylenedioxythiophene) (PEDOT) and other conductive polymer are convenient for oxidative polymerization by using oxidizing agents such as iodine and FeCl<sub>3</sub> and other way by electrochemical polymerization. These methods yielded non processible polymers product with hard, brittle, insoluble in most solvent and nonfusible even by heating up to their decomposition temperature.

Out of this thinking came the first exploratory polymerizations by Bayer and AGFA of PEDOT with the intent of applying it to the fields of antistatic coatings and photographic films. Chemical polymerization, aqueous dispersions of PEDOT: PSS, Baytron<sup>®</sup>, synthesized by Inganäs et al.[26], is successfully used and the fabrication volume of coated photographic film per year exceeds 108 m<sup>2</sup>. Poly(styrene sulfonate) (PSS) is used as a dopant for PEDOT. The doping process of the conjugated polymer is done by acid- rather than redox-doping. Thus, the PEDOT does not act as an electron donor but accepts a proton from the sulfonate group of the PSS dopant. A C=C  $\pi$ -bond of the EDOT opens up and the C bonds to an H<sup>+</sup> donated by the acid. As a result, there is a net positive charge on the PEDOT chain that will strongly attract the negative charge left on the acid. Since this happens at many points along the polymer, PEDOT and PSS become closely intertwined. An unpaired  $\pi$ - electron

remains on the PEDOT chain that is highly mobile along the conjugated backbone and leads to a high conductivity. Other dopants reported in literature include Tosylate and inorganic materials such as phosphomolybdate.

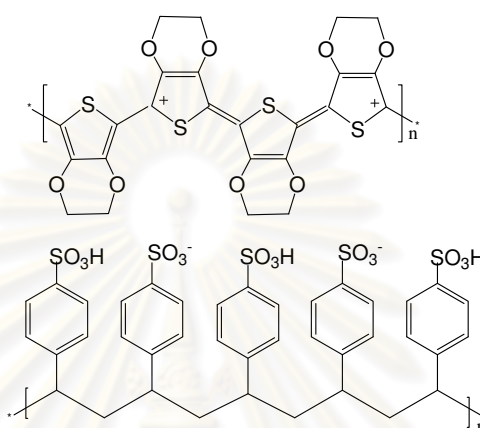


**Figure 1.12** Poly(3,4-ethylenedioxythiophene)/polystyrene sulfonic acid (PEDOT/PSS)

However, PEDOT:PSS also suffers from low conductivity of less than 1 S/cm, which is lower than that of some good conducting polymers by one to two orders of magnitude. Also, it is typically laid down in an acidic water-based solution whose corrosive properties cause other problems [40].

In this study, we have proposed a new way to overcome the mechanical properties of PEDOT is to blend it with another insulating polymer. Composites are formed by directly dispersing a soluble monomer, DBEDOT, into an insulating polymer matrix which can form solid film by electrospinning then transformed into PEDOT/polymer composite by solid state polymerization. Polymer matrix, poly(methyl methacrylate) are chosen as matrices because it is a polar matrix, and easy to be electrospun into desired forms while the mechanical integrity of the matrix is still maintained. Most of all, they can be easily mixed with DBEDOT in organic solvent. The following literatures describe the preparation of conducting polymer composites based on poly(methyl metharylate).

In 2000, Omastova and Simon [41] prepared conductive poly(methyl methacrylate)/polypyrrole composite by chemical modification of pyrrole in PMMA

latex matrix resulting in a network-like structure of polypyrrole embedded in the insulating polymer matrix. The electrical conductivity of compression-molded samples depends on the concentration of polypyrrole and reached values of between  $1 \times 10^{-9}$  S/cm to 0.1 S/cm.

In 2007, Veluru et al. [42] determined electrical properties of electrospun fibers of polyaniline- poly(methyl methacrylate) (PANI-PMMA) composites. The nanofibers of PANI dispersed in PMMA solution in chloroform. The conductivity of composite fibers is estimated as 0.289 S/cm. This value is about three orders less compared to that of the pure PANI sample (200-400 S/cm)

In 2008, M. Amrithesh et al. [43] have synthesized PANI-PMMA composites using bulk polymerized PMMA. The FTIR spectrum reveals that PANI has been dispersed as an interpenetrating network in the PMMA matrix. It is also observed that the photoluminescence (PL) intensity increases with increase in the PMMA content in the composite, possibly due to greater chances of exciton formation and subsequent radiative decay to the ground state. The enhancement of PL intensity of the composites with increase in the aniline to PMMA feed ratio is quite comparable with the enhancement in the DC electrical conductivity of these composites.

In 2008, Ji. S. et al. [44] prepared PMMA nanofibers by electrospinning and their composites with polyaniline (PANI) by *in situ* solution polymerization. The coaxial composite nanofibers so prepared were then transferred to the surface of a gold interdigitated electrode to construct a gas sensor. The electrical responses of the gas sensor based on the composite nanofibers towards triethylamine (TEA) vapors were investigated at room temperature. It was revealed that the sensor showed a sensing magnitude as high as 77 towards TEA vapor of 500 ppm. The responses were linear, reversible and reproducible towards TEA vapors of 20-500 ppm. In addition, it was found that the concentration of doping acids only led to changes in resistance of the sensor, but did not affect its sensing characteristics. The gas sensor with toluene sulfonic acid as the doping acid exhibited the highest sensing magnitude.

In 2007, Sun and Hagner [64] prepared PEDOT/poly(acrylic acid) (PAA) composites by oxidative polymerization of EDOT with  $\text{FeCl}_3$  in the presence of PAA. It was found that these composites were nanowires assembled by PAA chain acting as a template. They exhibited excellent conductivity (0.56 S/cm). It provided a new

water-dispersible and easily processable PEDOT dispersion. It also presented a simple self-assembly strategy for the morphology-controlled preparation of nanocomposites based on PEDOT and extended the use of polyelectrolyte as a template for designing interesting nanostructures.

In 2005, Sonmez and coworkers [65] found that PEDOT/poly(2-acrylamido-2-methyl-1-propane sulfonate) (PAMPS) composite films were electrochemically prepared from a mixture of water and DMF containing EDOT and polyelectrolyte, PAMPS. The conductivity of PEDOT/PAMPS free standing composite films reached the value of 80 S/cm. The PEDOT/PAMPS exhibited a band gap of 1.65 eV, identical to PEDOT doped with small ions that could be switched rapidly between the doped and neutral state with an excellent contrast ratio of 76%. Interesting cation-exchange properties have also been demonstrated with  $\text{Ru}(\text{NH}_3)_6\text{Cl}_3$ .

In 2006, Hansen and coworker [66] prepared a new method for integration of conducting polymer into PMMA substrates by chemical oxidative polymerization, e.g. using Fe (III) *p*-toluene sulfonate (ferri tosylate) followed by washing with a solvent which simultaneously removes residual and spent oxidant and at the same time dissolves the top layer of polymer substrate. It was found that the surface resistance of conducting polymer layer remains low while the surface layer at the same time adapts some of the mechanical properties of the substrate, resulting in a highly conducting surface with very good were resistance.

In 2007, Kusonsong [62] found that the highly conductive polymer composites of PEDOT/insulating polymer composites could be prepared by solid state polymerization (SSP) of 2,5-dibromo-3,4-ethylenedioxythiophene (DBEDOT) in the presence of either polystyrene (PS) or polybutadiene (PB) matrix. Nonetheless, the fabrication process based on solution casting yielded the composite films with non-uniform morphology and conductivity due to the inhomogeneous distribution of the PEDOT in the matrix caused by phase incompatibility between the polar PEDOT and the non-polar matrix.

In 2009, Keaw-on [63] prepared conducting polymer composite films containing PEDOT by solid state polymerization (SSP) of DBEDOT in the presence of polystyrene (PS) or sulfonated polystyrene (SPS) matrix. A thin fiber mat was first fabricated by electrospinning a solution mixture of polymer matrix (PS or SPS) and

DBEDOT on glass slides. After the solvent was removed, the solid state polymerization of the DBEDOT crystals embedded in the polymer matrix was then induced by heating at 60-80 °C, the temperature below the glass transition temperature of the polymer matrix and the melting temperature of DBEDOT. It was found that compression during heating was necessary to produce well dispersed sub-micron PEDOT in the polymer matrix. As measured by four-point probe conductometer, the conductivity of the composite film can reach as high as 15 S/cm, the value equivalent to the conductivity of the pure PEDOT also generated by SSP in the absence of polymer matrix.

### **1.10 Electrospinning process [45]**

A number of processing techniques such as drawing, template synthesis, phase separation, self-assembly, electrospinning have been used to prepare polymer nanofibers in recent years. The electrospinning process seems to be the only method which can be further developed for mass production of one-by-one continuous nanofibers from various polymers.

Figure 1.13 showed electrospinning process a high voltage is use to create and electrically charged jet of polymer solution or melt, which dries or solidifies to leave a polymer fiber. One electrode is placed into the spinning solution and other attached to a collector. Electric field is subjected to the end of a capillary tube that contains the polymer fluid held by its surface tension. This induces a charge on the surface of the liquid. Mutual charge repulsion causes a force directly opposite to the surface tension. As the intensity of the electric field is increased, the hemispherical surface of the fluid at the tip of the capillary tube elongates to form a conical shape known as the Taylor cone. With increasing field, a critical value is attained when the repulsive electrostatic force overcomes the surface tension and a charged jet of fluid is ejected from the tip of the Taylor cone. The discharged polymer solution jet undergoes a whipping process wherein the solvent evaporates, leaving behind a charged polymer fiber, which lays itself randomly on a grounded collecting metal screen. In the case of the melt the discharged jet solidifies when it travels in the air and is collected on the grounded metal screen.

The properties of fiber obtained from this process depend on two types of parameters, the first is system parameters including molecular weight, molecular weight distribution, architecture of the polymer (e.g. branched or linear chain) and solution properties (viscosity, conductivity and surface tension). The second one is processing parameters including electrical field strength, flow rate, solution concentration, distance between the capillary and the collector, and ambient parameters (temperature, humidity and air velocity in the chamber) [46].

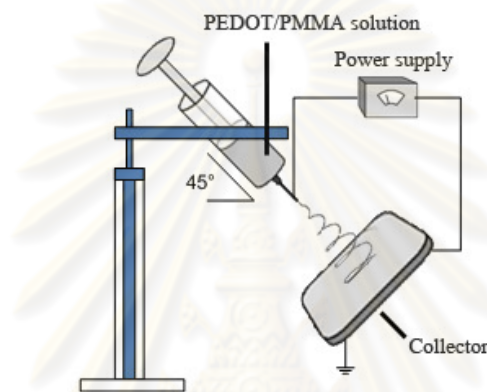


**Figure 1.13** Schematic of electrospinning apparatus set up

The advantages of electrospinning process are simple equipment, requiring a short time, cost effective and producing a very high orientated fiber with very small pore sizes. Therefore, electrospun fibers from electrospinning have regained more attention probably due in part to interest in many applications such as in the field of filtration systems [47], medical prosthesis mainly grafts and vessels, tissue template [48], electromagnet shielding, protective clothing [49], composite delamination.

### 1.11 Conductive measurement by four point probe technique [52]

The four point probe, as depicted schematically in Figure 1.14, contains four thin collinear tungsten wires which are made to contact the sample under test. Current  $I$  is made to flow between the outer probes, and voltage  $V$  is measured between the two inner probes, ideally without drawing any current. If the sample is of semi-infinite volume and if the interprobe spacings are  $s_1 = s_2 = s_3 = s$ , then it can be shown that the resistivity of the semi-infinite volume is given by



$$\rho_0 = 2\pi s \left( \frac{V}{I} \right) \quad (1.1)$$

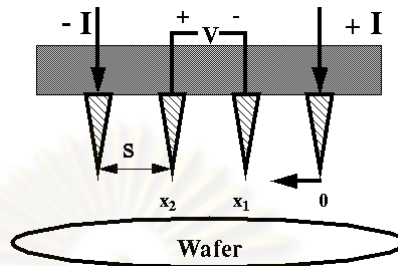


**Figure 1.14** Schematic representation of 4-point probe configuration

The subscript 0 in the preceding equation indicates the measured value of the resistivity and is equal to the actual value,  $\rho$ , only if the sample is of semi-infinite volume. Practical samples, of course, are of finite size. Hence, in general,  $\rho$  is *not equal to*  $\rho_0$ . Correction factors for six different boundary configurations have been derived by Valdes<sup>1</sup>. These show that in general if  $l$ , the distance from any probe to the nearest boundary, is at least  $5s$ , no correction is required. For the cases when the sample thickness is  $\leq 5s$ , we can compute the true resistivity from

$$\rho_0 = 2a\pi s \left( \frac{V}{I} \right) = a\rho_0 \quad (1.2)$$

where  $a$  is the thickness correction factor which is plotted on page GT-2. From an examination of the plot, we see that for values of  $t/s \geq 5$  the corresponding value of  $a$  is unity. Thus, for samples whose thickness is at least 5 times the probe spacing, no correction factor is needed. Typical probe spacings are 25-60 mils and the wafers used in most cases are only 10-20 mils thick, so unfortunately we cannot ignore the correction factor. Looking again at the plot, however, we see that the curve is a straight line for values of  $t/s \leq 0.5$ . Since it is a log-log plot the equation for the line must be of the form

$$a = K \left( \frac{t}{s} \right)^m \quad (1.3)$$

where K is the value of a at  $(t/s) = 1$ , and m is the slope. Inspection of the plot shows that in this case  $m = 1$ . K is determined to be 0.72 by extrapolating the linear region up to the value at  $(t/s) = 1$ . (The exact value can be shown to be  $1/(2\ln 2)$ .) Hence for slices equal to or less than one half the probe spacing

$$a = 0.72 \left( \frac{t}{s} \right) \quad (1.4)$$

When substituted into the basic equation we get:

$$\rho_0 = 2a\pi s \left( \frac{V}{I} \right) = 4.53 \left( \frac{V}{I} \right) \text{ for } \frac{t}{s} \leq 0.5 \quad (1.5)$$

All samples used in the lab satisfy the one-half relationship so the above formula can be used to determine  $\rho$ . Resistivity measurements will be performed on the starting material for each experiment. The value of  $\rho$  obtained will be referred to as the bulk resistivity, and the units are  $\Omega$ -cm. If both sides of Equation (1.5) are divided by t we get

$$R_s = \frac{\rho}{t} = 4.53 \left( \frac{V}{I} \right) \text{ for } \frac{t}{s} \leq 0.5 \quad (1.6)$$

which we refer to as sheet resistance. When the thickness t is very small, as would be the case for a diffused layer, this is the preferred measurement quantity. Note that  $R_s$  is independent of any geometrical dimension and is therefore a function of the material alone. The significance of the sheet resistance can be more easily seen if we refer to the end-to-end resistance of a rectangular sample.

Therefore,  $R_s$  may be interpreted as the resistance of a square sample, and for this reason the units of  $R_s$  are taken to be Ohms per square or  $\Omega/\text{sq}$ . Dimensionally,

this is the same as  $\Omega$ , but this notation serves as a convenient reminder of the geometrical significance of sheet resistance.

### 1.12 Objectives

- To prepare of conducting polymer composite film by electrospinning and solid state polymerization of 2,5-dibromo-3,4-ethylenedioxythiophene in PMMA matrix
- To determine effects of temperature, time and polymer matrix on conductivity of the composite.

### 1.13 Scope of the investigation

The stepwise investigation was carried out as follows:

1. Literature survey for related research work
2. To synthesize 2,5-dibromo-3,4-ethylenedioxythiophene (DBEDOT)
3. To prepare DBEDOT/polymer composite films by electrospinning of mixed solution between DBEDOT and PMMA. Parameters to be investigated in this step are as follow:
  - DBEDOT : PMMA weight ratio (1:1, 2:1, 3:1 and 4:1)
  - Solvent type (DMF and mixed solvent of DMF and THF (1:1))
4. To prepare PEDOT/PMMA composite films by heat-activated polymerization. Parameters to be investigated in this step are as follow:
  - Polymerization time (24, 36, 48, 60, and 72 h)
  - Polymerization temperature (70 and 80 °C)
  - Compression during in solid state polymerization
5. To determine the conductivity of the PEDOT/PMMA composite films
6. To characterize PEDOT/ polymer composite films by x-ray diffraction (XRD), FT-Raman spectroscopy, thermogravimetric analysis (TGA), and differential scanning calorimetry (DSC)
7. To characterize the PEDOT that has been extracted from the composite films by scanning electron microscope (SEM), XRD, and FT-IR spectroscopy

8. To investigate the effect of storage time on the conductivity of the PEDOT/ polymer composite films.



ศูนย์วิทยทรัพยากร  
จุฬาลงกรณ์มหาวิทยาลัย

# CHAPTER II

## EXPERIMENTAL

### 2.1 Materials

All the chemicals and reagents used were of analytical grade.

- |   |                     |
|---|---------------------|
| 1. Acetone  | : Merck             |
| 2. Acetic acid, glacial                                   | : Merck             |
| 3. Chloroform   | : Lab-scan          |
| 4. Dichloromethane  | : Fluka             |
| 5. Ethanol  | : Merck             |
| 6. Hexane   | : Fluka             |
| 7. <i>N</i> -bromosuccinimide                             | : Merck             |
| 8. <i>N,N</i> -Dimethylformamide                          | : Carlo Erba        |
| 9. Methanol   | : Merck             |
| 10. Poly(methyl methacrylate) ( $M_w = 1.2 \times 10^5$ ) | : Aldrich           |
| 11. Sodium hydrogen carbonate                             | : Labscan           |
| 12. Tetrahydrofuran                                       | : Fisher Scientific |

### 2.2 Equipments

#### 2.2.1 Nuclear Magnetic Resonance (NMR) Spectrometer

All spectra were collected by NMR, model Varian Mercury plus 400. Samples were dissolved in  $CDCl_3$  and operated at 400 MHz for  $^1H$  and 100.54 MHz for  $^{13}C$  nuclei.

#### 2.2.2 Fourier-Transform Infrared Spectrophotometer (FT-IR)

IR spectra of a standard PEDOT and PEDOT extracted from the PEDOT/polymer composite film were analyzed by FT-IR model Nicolet Impact 410. All samples were prepared as KBr pellets.

### **2.2.3 UV-visible spectrophotometer**

UV-visible spectrophotometer model UV-2550 SHIMADZU was used to investigate surface absorption spectrum of PEDOT/polymer composite film and extracted PEDOT powder.

### **2.2.4 Scanning electron microscope (SEM)**

The morphology of the electrospun fiber mats before and after SSP as well as the extracted PEDOT were observed with a scanning electron microscope (SEM) model JSM-6480LV. The scanning electron images were obtained by using an acceleration voltage of 15 kv with a magnification of 500x and 5000x.

### **2.2.5 X-ray diffractometer (XRD)**

Diffractograms of standard PEDOT and extracted from the PEDOT/polymer composite film by XRD model Rigaku D5000 using a scan range of 5.00-50.00 degree, a scan speed of 5.00 deg min<sup>-1</sup> and a sample width of 0.020 degree.

### **2.2.6 Thermogravimetric analysis (TGA)**

The combustion stage and melting point were investigated by TA instruments thermogravimetric analyser model TGA 2950. PEDOT/polymer composite film was analyzed by heating from 30 to 600 °C using 20 °C.min<sup>-1</sup> heating rate under ambient atmosphere.

### **2.2.7 Differential Scanning Calorimetry (DSC)**

Thermal properties, glass transition temperature (T<sub>g</sub>) and melting temperature (T<sub>m</sub>) of PEDOT/polymer composite films were investigated by a Du pont Differential Scanning Calorimeter model DSC 2910 by heating the samples sealed in an aluminum pan from 30 °C to 300 °C using 10 °C.min<sup>-1</sup> heating rate under nitrogen atmosphere.

### **2.2.8 Surface Profile Measuring System**

The thickness of PEDOT/polymer composite films was determined by a Surface Profile Measuring System model Veeco Dektak<sup>3</sup> ST using by force 1 mg and a scanning rate of 0.625 μm.s<sup>-1</sup> for 3000 μm.

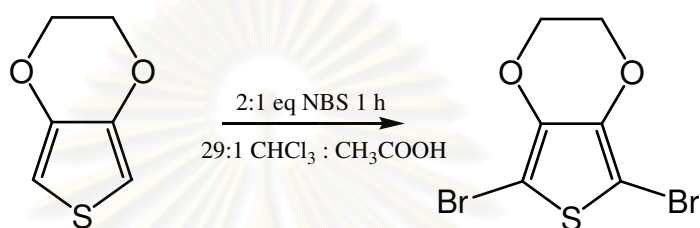
### **2.2.9 Four-Point Probe Conductometer**

The conductivity values of PEDOT/polymer composite films were determined by a four-point probe conductometer model KEITHLEY Semiconductor Characterization System 4200. The reported conductivity is an average value

measured from four different areas when 100 measurements for each area were performed.

## 2.3 Methods

### 2.3.1 Synthesis of 2,5-dibromo-3,4-ethylenedioxythiophene (DBEDOT)



**Scheme 2.1** Bromination of EDOT

To stirred a solution of 3,4-ethylenedioxythiophene (EDOT) (0.57 g, 4 mmol) dissolved in a 2:1 (v/v) mixture of chloroform (29 mL) and glacial acetic acid (1 mL) was added slowly 2.1 eq *N*-bromosuccinimide (NBS) (1.50 g, 8.4 mmol). The reaction was carried out at 0-5 °C under nitrogen atmosphere for 1 h. Then the mixture was quenched and washed with saturated sodium hydrogen carbonate solution (50 mL × 3 times). The organic layer was separated and the aqueous layer was extracted with chloroform. The crude mixture was purified by passing through a silica gel column, and elute with 3:2 mixtures of hexane and dichloromethane. When approximately 2 mL of the solution mixture was left after the solvent removal by rotary evaporator, 3 mL of methanol was added to the evaporating flask in order to induce crystallization of DBEDOT which appeared as white needle-like crystals in 85 %yield.

### 2.3.2 Preparation of PEDOT/polymer composite film

A mixed solution of DBEDOT and poly(methyl methacrylate) was prepared by dissolving 0.36 g poly(methyl methacrylate) matrix in 2.0 mL of dimethylformamide (DMF) and 1:1 (v/v) of dimethylformamide (DMF), tetrahydrofuran (THF) overnight followed by an addition of 1.08 g DBEDOT and

then stirred for 30 min. Each of the prepared solutions was then placed in a 5-mL syringe blunt 20-gauge stainless steel hypodermic needle (i.e. outside diameter = 0.91 mm.) a nozzle was connected with the positive electrode. The tilt angle of the syringe was set at 45° from a horizontal baseline. Fiber mats were fabricated by electrospinning using a driving voltage of 20 kV (high voltage power supply model Gamma High Voltage Research DES30PN/M692). A grounded metal screen covered by a glass slide was used as the counter electrode and the distance between the needle and the grounded metal target was 10 cm. The schematic of the set-up is shown in Figure 3.1. After spinning for 1.30 hours, the polymer matrix/DBEDOT fiber mats was dried in desiccators at ambient temperature overnight. The fiber mat containing DBEDOT deposited was pressed against a glass slide coated with Teflon tape and clamped with paper clips then heated in an oven at 70 and 80 °C for a certain period of time to induce polymerization of DBEDOT (Scheme 3.2)

The PEDOT/polymer composite film was first dissolved in chloroform. The insoluble PEDOT were removed by centrifugational wash at 4,000 rpm for 40 min with chloroform (5x). All fractions of supernatant collected after each washing were combined under reduced pressure by a rotary evaporator. The solution containing the matrix and the unreacted DBEDOT was purified by passing through a silica gel column using 3:2 (v/v) of hexane and dichloromethane as an eluent. The purity of the extracted DBEDOT which appeared as transparent-white crystal was verified by TLC. The percentage of DBEDOT conversion was calculated based on using the following equation, assuming that all DBEDOT consumed was converted to PEDOT.

$$\% \text{ DBEDOT conversion} = \frac{(\text{initial weight of DBEDOT} - \text{weight of extracted DBEDOT}) \times 100\%}{(\text{initial weight of DBEDOT})} \dots (3.1)$$



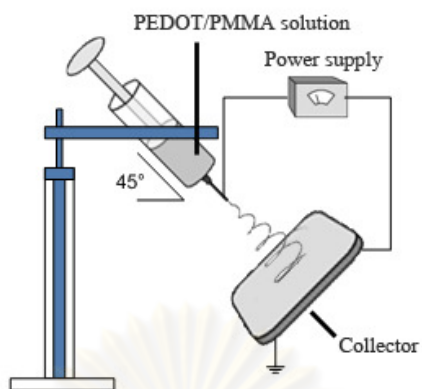


**Figure 2.1** Schematic of electrospinning apparatus set-up.

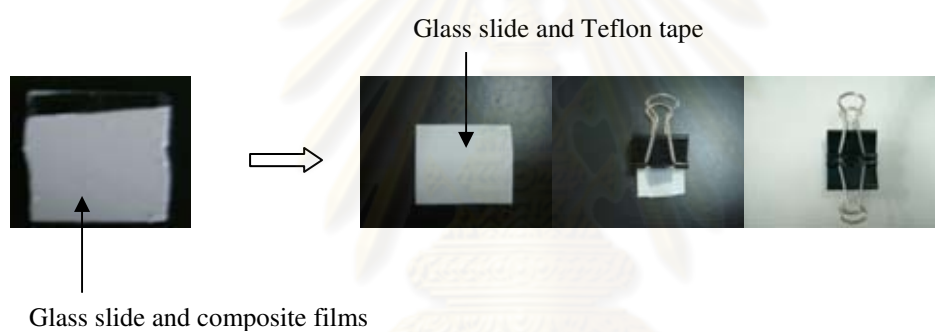
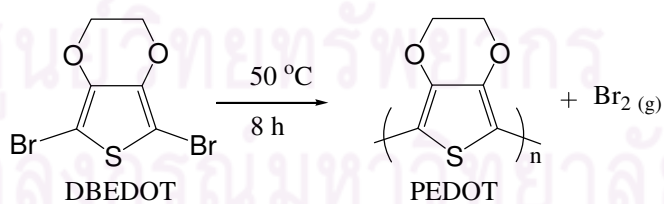


**Figure 2.2** Schematic representation of the pressing of the DBEDOT/polymer fiber mats



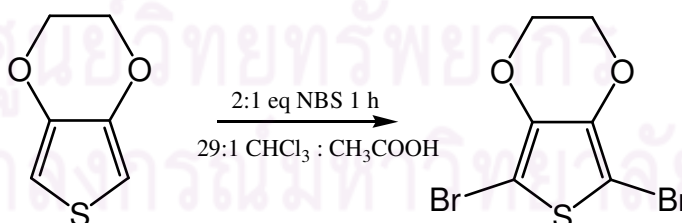
**Scheme 2.2** Solid state polymerization of DBEDOT

## CHAPTER III

### RESULTS AND DISCUSSION

The aim of this work is to prepare polymer composites containing 3,4-polyethylenedioxythiophene (PEDOT) by solid state polymerization of 2,5-dibromo-3,4-ethylenedioxythiophene (DBEDOT) and electrospinning in the matrix of commercial polymers i.e. the relatively polar poly(methyl methacrylate) (PMMA). This chapter is divided into 3 parts. The first part involves the synthesis of DBEDOT by bromination of ethylenedioxythiophene (EDOT). The second part is dedicated to the preparation of PEDOT/polymer composite films by electrospinning. Several parameters that can affect physical properties and conductivity of the composite films, DBEDOT:polymer matrix weight ratio, solvent (DMF and mixed solvent (THF:DMF)). The last part investigates the effect of polymer matrix, time, temperature and compression during solid state polymerization on the conductivity of the composite film.

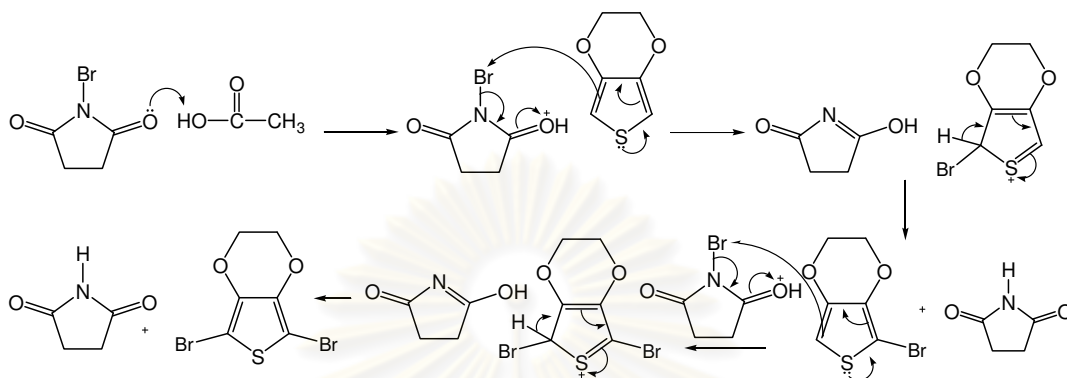
#### 3.1 Synthesis of 2,5-dibromo-3,4-ethylenedioxythiophene (DBEDOT)



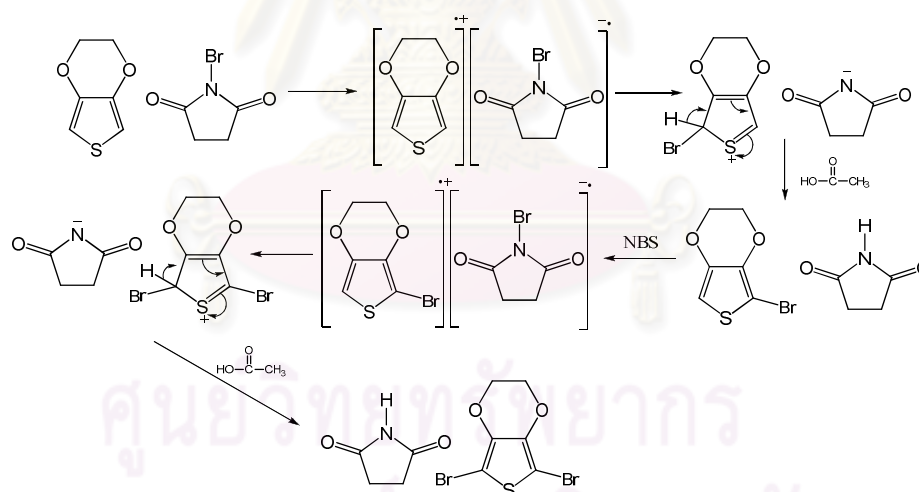
**Scheme 3.1** Synthesis of 2,5-dibromo-3,4-ethylenedioxythiophene

DBEDOT is the monomer to be used for solid state polymerization to form PEDOT. DBEDOT can be synthesized by bromination of EDOT as shown in Scheme 3.1. The mechanism of bromination of EDOT has been proposed into 2 possible

pathways, the electrophilic aromatic substitution and radical based single electron transfer (scheme 3.2-3.3) [53,54].



**Scheme 3.2** Bromination mechanism through electrophilic aromatic substitution



**Scheme 3.3** Bromination mechanism through radical-based single electron transfer followed by aromatic substitution

Unlike the method described by Meng and coworkers [39], the bromination of EDOT using *N*-bromosuccinimide (NBS) in this work is a one step process. The quenching and neutralization were done simultaneously by washing the chloroform layer with saturated sodium hydrogen carbonate solution (50 mL  $\times$  3 times). The

crystallization of DBEDOT product was then induced by an addition of a small amount of ethanol (3 mL) to the concentrated chloroform solution (containing ~ 2 mL of chloroform). After most of chloroform was removed under reduced pressure using a rotary evaporator, white needle-like crystals (84% yield) were recovered after purification by column chromatography. The product was characterized by  $^1\text{H-NMR}$ . It was highly soluble in common organic solvent and has the melting temperature at 94 °C.

$^1\text{H-NMR}$  spectra of the synthesized DBEDOT and EDOT are shown in Figure 3.1. The absence of the signal at 6.4 ppm suggested that the protons of EDOT at  $\alpha$  positions of the thiophene ring were substituted by bromine atoms after bromination by NBS while the proton signals of ethylene bridge at 4.27 ppm remained. [39]

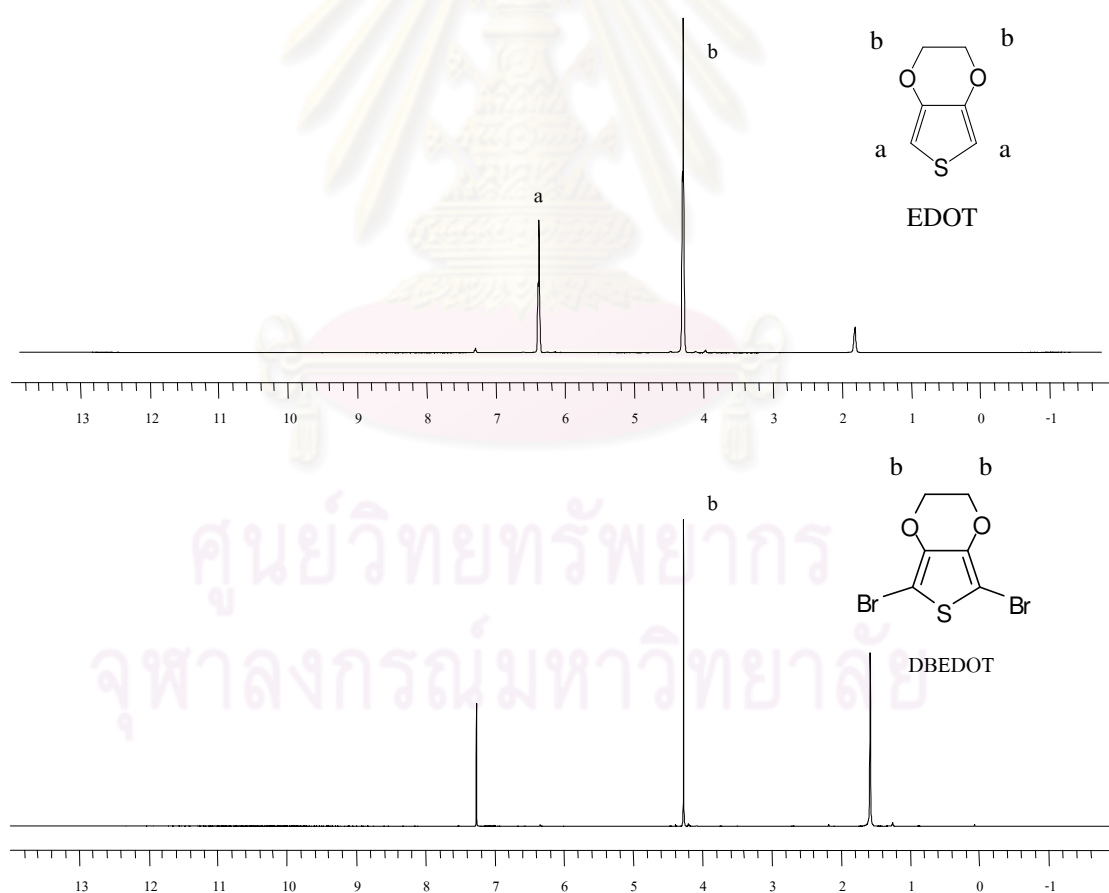


**Figure 3.1**  $^1\text{H-NMR}$  spectra of EDOT (upper) and DBEDOT (lower)

### 3.2 Preparation of DBEDOT/polymer composite fiber mats

The highly conductive polymer composites containing PEDOT were proposed to be prepared by solid state polymerization (SSP) of DBEDOT embedded in an insulating polymer matrix film. To improve the possible inhomogeneous distribution of PEDOT caused by phase separation between the polar PEDOT and non-polar matrix in the previous report, [61] more polar matrix together with electrospinning method were used.

In this research, PMMA was selected as the polar matrix having a glass transition temperature ( $T_g = 100\text{ }^\circ\text{C}$ ) above the melting temperature of DBEDOT ( $T_m = 94\text{ }^\circ\text{C}$ ). The condition of PMMA electrospinning fiber preparations have been investigated in various solvent. We selected DMF as the solvent due to its sufficiently high viscosity and made the solution easy to be electrospun. The polymer DMF solution of PMMA with lowest concentration at 18 % (w/v) of polyaniline (PANI) has been prepared by Ji and coworkers. [44] The concentration of polymer and type of solvent has been shown to have a significant impact on the morphology of the electrospun fiber. The polymer solution at low concentration generally leads to the formation of droplets or electrospray. [55]

Figure 3.2 (a-b) shows the SEM images of pure PMMA fiber mat electrospun from DMF and 1:1 (v/v) THF:DMF solution. It was found that the mixed solvent system seemed to give fibers with more homogeneity in the morphological distribution. This observation was also found in the case of the mixed solution between PMMA and DBEDOT that had also been electrospun into fibers (Figure 3.2 c-d).

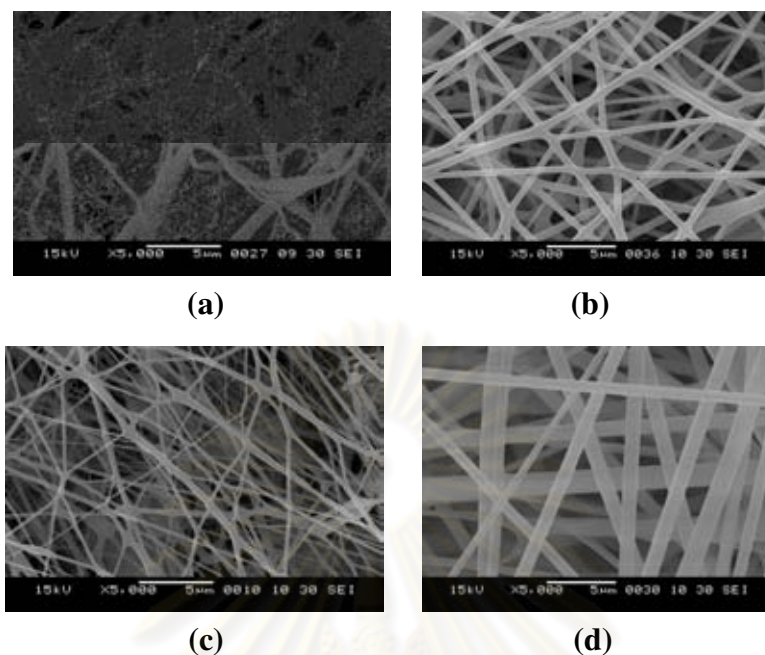
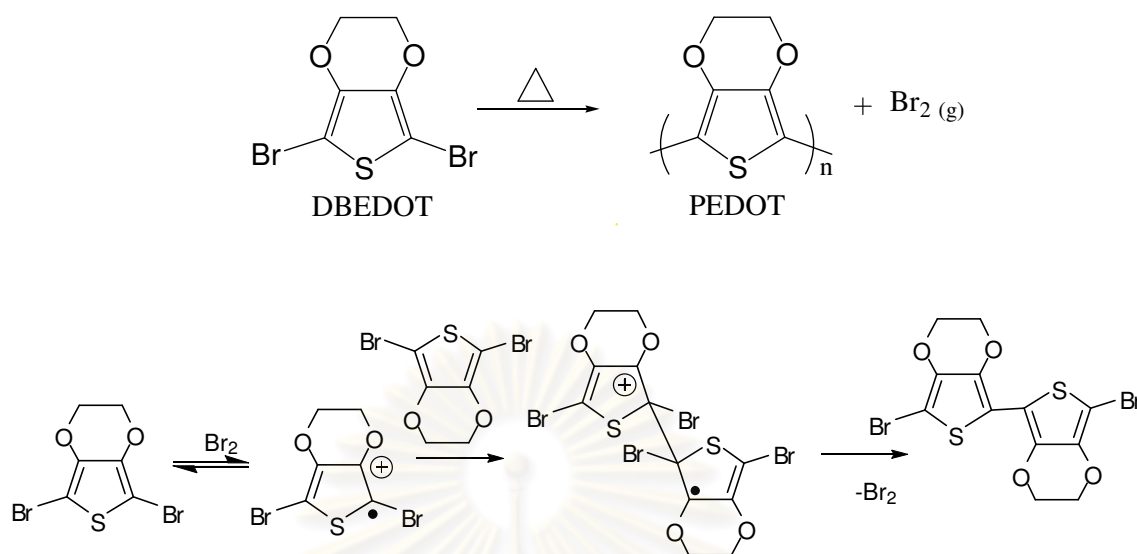


**Figure 3.2** SEM images ( $\times 5000$ ) of as-spun PMMA fiber mat electrospun from 18% (w/v) PMMA in (a) DMF, (b) 1:1 (v/v) THF/DMF, and as-spun DBEDOT/PMMA composite fiber mats electrospun from a mixture containing 3:1 (w/w) DBEDOT/PMMA in (c) DMF and (d) 1:1 (v/v) THF/DMF

### 3.3 Preparation of PEDOT/polymer composite

The mechanism of SSP of DBEDOT has been proposed by Meng and co-workers (Scheme 3.4). [38,39] DBEDOT molecules in the form of crystal pack closely in parallel fashion which facilitates polymerization process in solid state. It is likely that the polymerization occurs along the stacks of the monomer and must be accompanied by significant rotation and some movement of the molecules. DBEDOT can transform to PEDOT by condensation during heat treatment. The initiation involves oxidation of DBEDOT by bromine ( $\text{Br}_2$ ) and generates DBEDOT radical carbocation. In the propagation step, this radical carbocation first reacts with another DBEDOT to form DBEDOT dimer, also in the form of radical carbocation. The elimination of bromine then yields DBEDOT dimer which will go through another propagation step and eventually forms PEDOT. The presence of bromine in the reaction, in fact, facilitates polymerization in the initiation step and redopes the resulting polymer at the end.



**Scheme 3.4** Mechanism of solid state polymerization of DBEDOT

### 3.3.1 Effect of compression on the conductivity of the composite films

The resistance of the PEDOT/PMMA composite film shown in Figure 3.3 did not significantly decrease as the heating time was extended beyond 24 h. The fact that the conductivity values measured on the bottom side could almost align to those measured on the top side, implied that the PEDOT was distributed evenly throughout the matrix of the composite film.

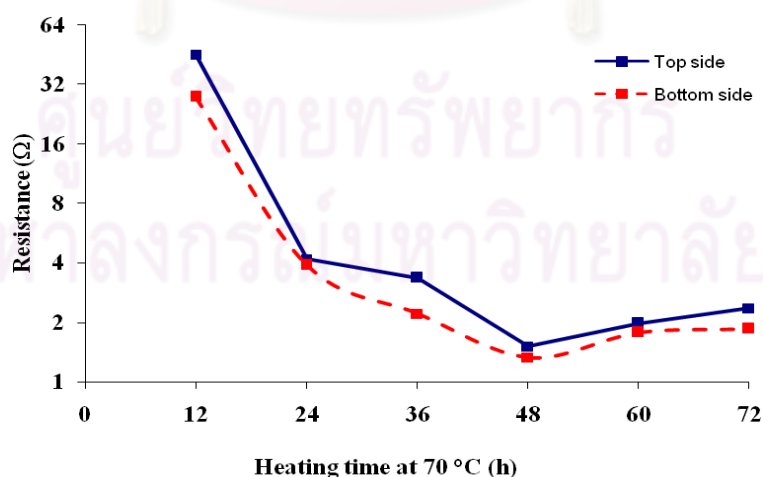


**Figure 3.3** Resistance measured on the top and bottom sides of the PEDOT/PMMA composite film prepared by SSP of the electrospun 3:1 (w/w) DBEDOT/ PMMA fiber mats heating at 70 °C for 48 h with pressing as a function of reaction time

The color of the DBEDOT/PMMA fiber mats pressed on a glass substrate changed from white to dark blue and turned black within 24 h by heat treatment at 70 °C. Without pressing, the heated sample only turned to gray because it was not completely polymerized (Figure 3.4b). The heat treatment of the DBEDOT/PMMA fiber mats completely destroyed their fibrous feature as visualized from SEM images shown in Figure 3.3d and e. The blue color could primarily be used as an indication of the SSP and the formation of PEDOT. The compression of the DBEDOT/PMMA fiber mats during the heat treatment was found to be critical to the effectiveness of SSP process. If the compression was applied during the heat treatment, the resulting PEDOT/PMMA composite film (Figure 3.4e) became smoother and more homogeneous than that obtained without the compression (Figure 3.4d). The PEDOT could be well dispersed in the compression case. The morphology of the extracted PEDOT from PEDOT/PMMA composite film shown in Figure 3.4 (f and g) could indicate possible interactions between PEDOT and PMMA matrix. The conductivity as high as 40.33 S/cm was found from the compressed PEDOT/PMMA composite film at 4:1 weight ratio, while without compression, the weight ratio 4:1 composite film gave the conductivity at only 0.46 S/cm. The difference of these values was supported by the fact that the compression raised the percentage of the conversion of PEDOT in the matrix from 38 % to 71 %.



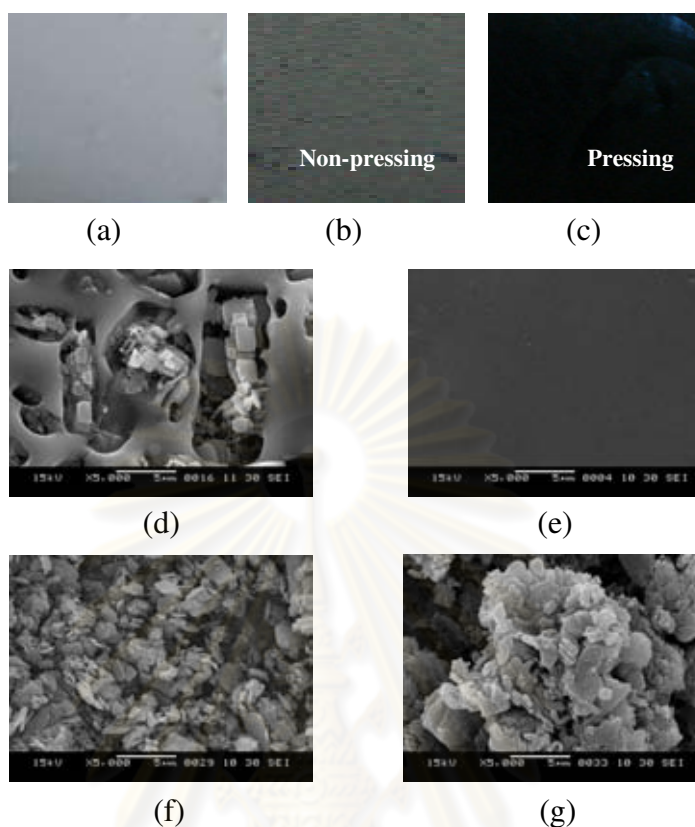


**Figure 3.4** SEM micrographs (at 5000x) of the composite fiber mats electrospun from a mixture containing 3:1 (w/w) DBEDOT/PMMA in DMF before SSP (a), after SSP at 70 °C for 48 h without (b) and with pressing (c), SEM micrographs (at 5,000x) of PEDOT/PMMA composite film obtained after SSP at 70 °C for 48 h without (d), with pressing (e), PEDOT extracted from PEDOT/PMMA composite film prepared by SSP of the 3:1 (w/w) DBEDOT/PMMA fiber mats at 70 °C for 48 h without pressing (f) and with pressing (g).

FT-IR spectra of PMMA and PEDOT/PMMA composite film fiber mats are shown in Figure A-2 (Appendix A). The peak at  $1726\text{ cm}^{-1}$  was assigned to C=O stretching of the carbonyl group of PMMA. The decrease of the intensity of the peak at  $1726\text{ cm}^{-1}$  indicated the degradation of PMMA moiety in the blend [59]. The signal of C=O stretching was also found in the PEDOT/PMMA composite film prepared by SSP of the electrospun DBEDOT/PMMA fiber mat heated for 48 h as shown in Figure 3.5. Full spectra of these samples are illustrated in Figure A-3 to A-6

(Appendix A). Data outlined in Table 3.1 indicate that the signals of the composite films prepared from 3:1 and 4:1 weight ratio appeared at higher frequency when the films were pressed. The slight shift of the signal might indicate some type of interactions between the polymer chains of PEDOT and PMMA.

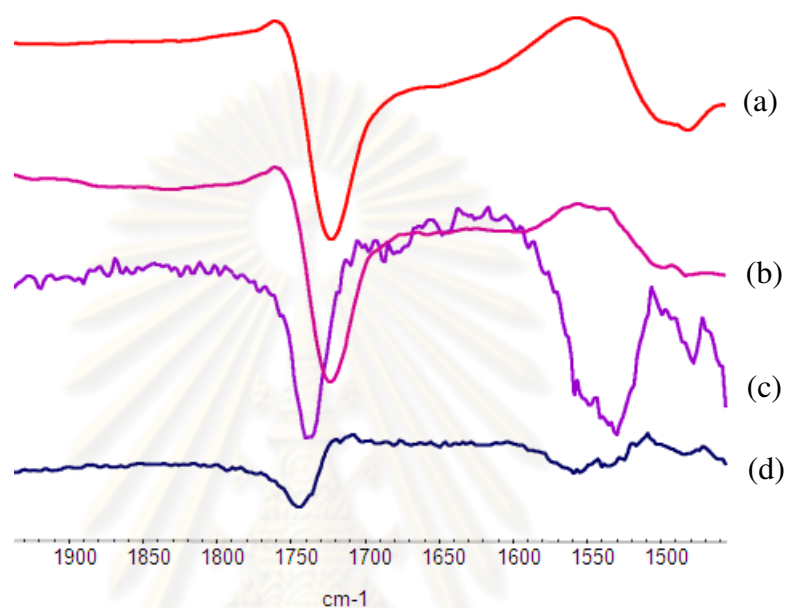


**Figure 3.5** FT-IR spectra of PEDOT/PMMA composite film prepared without pressing of (a) 3:1 and (b) 4:1 (w/w) DBEDOT/PMMA fiber mats, PEDOT/PMMA composite film prepared with pressing of (c) 3:1 and (d) 4:1 (w/w) DBEDOT/PMMA fiber mats

**Table 3.1** FT-IR C=O stretching signals of the PEDOT/PMMA composite films prepared by SSP of the electrospun DBEDOT/PMMA fiber mats heated for 48 h

DBEDOT:PMMA weight ratio of composite film	C= O stretching signals (cm <sup>-1</sup> )	
	Non-pressing	Pressing
3:1	1724	1744
4:1	1722	1737

Plain PEDOT was prepared by SSP of DBEDOT in the absence of the polymer matrix, which is called “controlled PEDOT”. Its IR spectrum (Figure 3.6) was compared to that of PEDOT extracted from PEDOT/polymer composite film, which is called “extracted PEDOT”. Both spectra exhibited the relatively similar fingerprints which confirmed the success of SSP in the PMMA matrix. The peak assignments of PEDOT corresponded well to that from the literature [60]. The peaks at 1510.9 and 1410.0  $\text{cm}^{-1}$  originated from the asymmetric stretching of C=C and symmetric stretching of C=C, respectively. The peak at 1355.7  $\text{cm}^{-1}$  was assigned to C–C inter-ring stretching. The peak from C–C antisymmetric stretching could be seen at 978.6  $\text{cm}^{-1}$ . The peak at 901.1  $\text{cm}^{-1}$  corresponded to the ethylenedioxy ring deformation. The peaks at 1079.3 and 746.1  $\text{cm}^{-1}$  were assigned to the =C–O stretching and C–S–C bending, respectively.

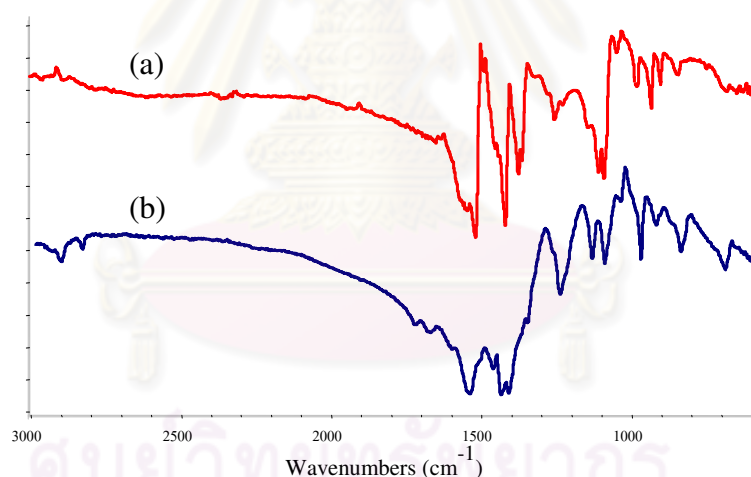


**Figure 3.6** FT-IR spectra of (a) controlled PEDOT and (b) extracted PEDOT

It was found that the major weight loss of PMMA appeared at the temperature range of 350-400 °C which corresponded to the degradation of PMMA (Figure 3.7 (b)). The weight loss at 150-180 °C and ~370 °C were found in the controlled PEDOT (Figure 3.7 (a)). PEDOT/PMMA composite film at weight ratio 3:1 and 4:1 without pressing (Figure A-9 and A-10 Appendix A) showed weight loss in both regions indicating the coexistence of PEDOT and PMMA in the composites regardless of the compression. However, the lower peak area in the region of 150-180 °C (belonging to

the degradation of PEDOT) of the composite film prepared without pressing indicated that there was smaller content of the PEDOT in the composite in comparison with those prepared with pressing. This fact coincides with the evidence from the percentage of DBEDOT conversion. An additional peak in a temperature range of 500-560 °C suggested that there was a portion of composites that possessed greater thermal decomposition. This result also supported the idea that there were some interactions between PEDOT and PMMA chains. This speculation can be verified by the fact that such thermal transition is absent in the manually mixed pure PEDOT and PMMA shown in Figure 3.8(a) indicating that this additional signal only appeared in the PEDOT/PMMA composites prepared by SSP

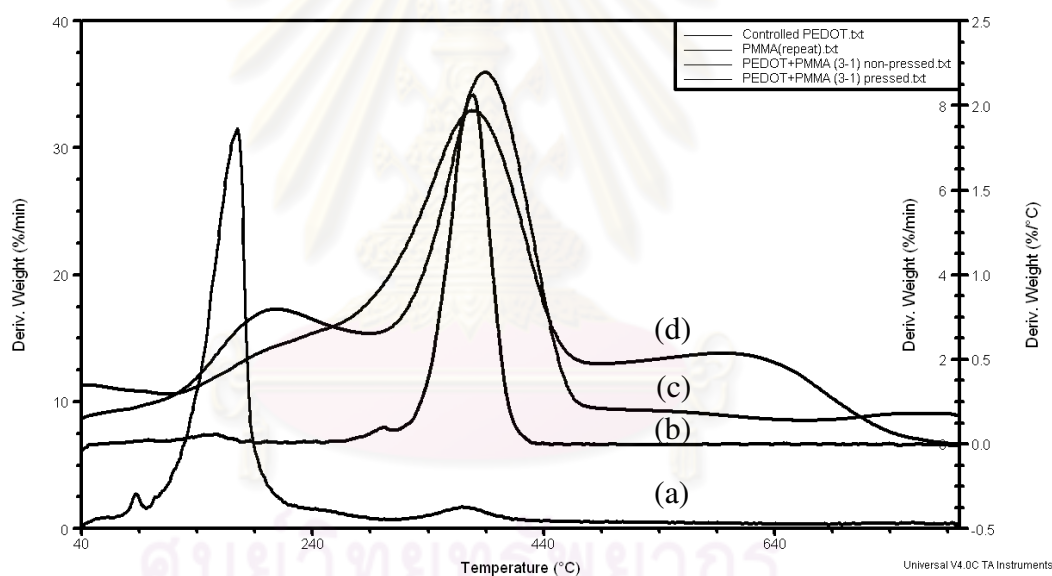


**Figure 3.7** TGA thermograms of (a) controlled PEDOT, (b) electrospun PMMA fiber mat, (c) PEDOT/PMMA (3:1) composite film, non-pressing and (d) PEDOT/PMMA (3:1) composite film, pressing

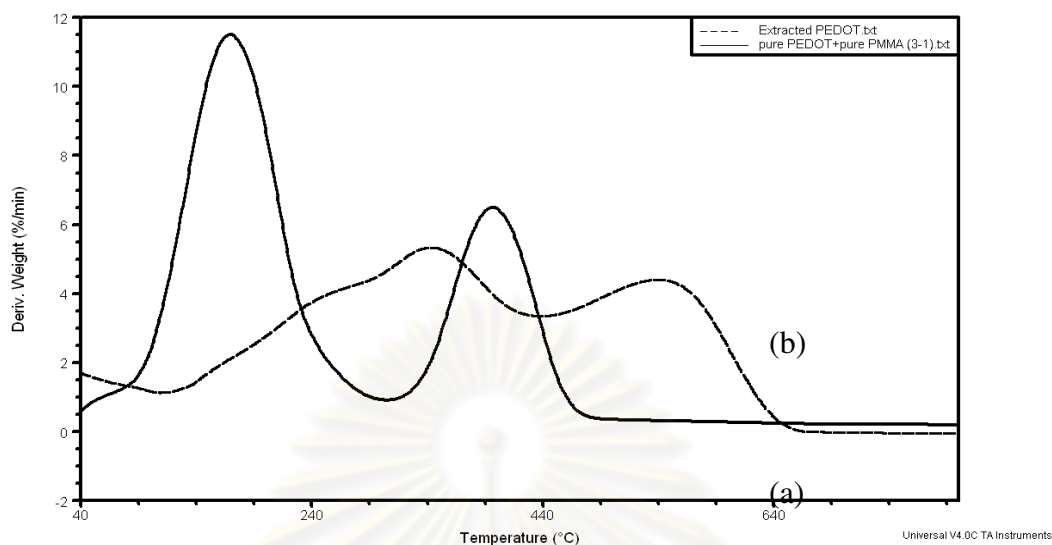


**Figure 3.8** TGA thermograms of (a) manually mixed pure PEDOT and PMMA at 3:1 weight ratio and (b) extracted PEDOT

### 3.3.2 Effect of temperature and reaction time used for SSP

Figure 3.9 shows the morphology of PEDOT/PMMA film heated without pressing at 60-80 °C. It was found that only at the temperature 60 °C, the composite could still retain its texture, indicating little progress in polymerization. (Figure 3.9 a,b)

The temperature range of 70-80 °C was chosen to be used for inducing SSP mainly because it is below the melting temperatures of the composite ( $T_m$  of PMMA >140 °C [57]) and DBEDOT ( $T_m = 94$  °C). It should be emphasized that heating above 80 °C was found to cause the composite film to turn transparent and melt during the heat treatment whereas the temperature below 70 °C was found to be ineffective to induce SSP. The observation on color change of the film from white to dark blue which led to the extent of SSP as a function of temperature could be quantitatively correlated to the conductivity values as outlined in Table 3.2. Using the same heating time of 48 h, the 70 °C seemed to be the suitable temperature for heat treatment as indicated by the highest conductivity obtained. The temperature at 80 °C gave the lower value might be due to the fact that it is too close to  $T_g$  of PMMA and  $T_m$  of

DBEDOT. The softening DBEDOT/PMMA composite was no longer in the solid state and caused disorder within the film and obstructed the SSP. When comparing between two compositions, the composite film became more highly conductive upon increasing the DBEDOT:PMMA weight ratio from 3:1 to 4:1 but at weight ratio of 4:1, the resulting composite film was rather brittle and seemed to be quite difficult to be further processed or used.

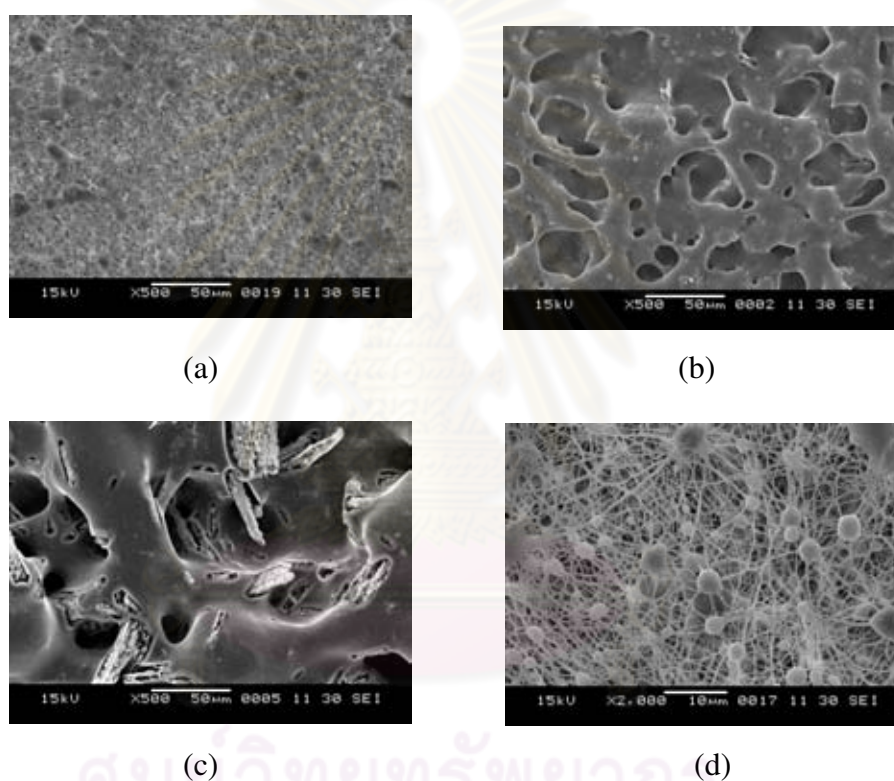


**Figure 3.9** SEM micrographs (at 500x) and (at 2000x) of PEDOT/PMMA composite film heated without pressing at (a) 60 °C, (b) 70 °C (c) 80 °C and (d) 60 °C

**Table 3.2** Conductivity of the PEDOT/PMMA composite film prepared by SSP of the electrospun DBEDOT/PMMA fiber mat heated for 48 h

DBEDOT:PMMA (% w/w)	Heating temperature (°C)	Thickness (μm)	Resistance (Ω)	Conductivity (S/cm)
3:1	70	45.0198±5.0774	4.57	10.73
	80	43.1725±4.3373	20.43	2.50
4:1	70	55.8513±13.8211	0.98	40.33
	80	48.9574±1.4174	2.26	19.95

The resistance data [Table A-2 Appendix A] shown in Figure 3.10 suggested the lowest resistance could be obtained at the reaction time of 48 h. After 48 h, the higher resistance might be because of the loss of doped bromine during such too long time of heat treatment.

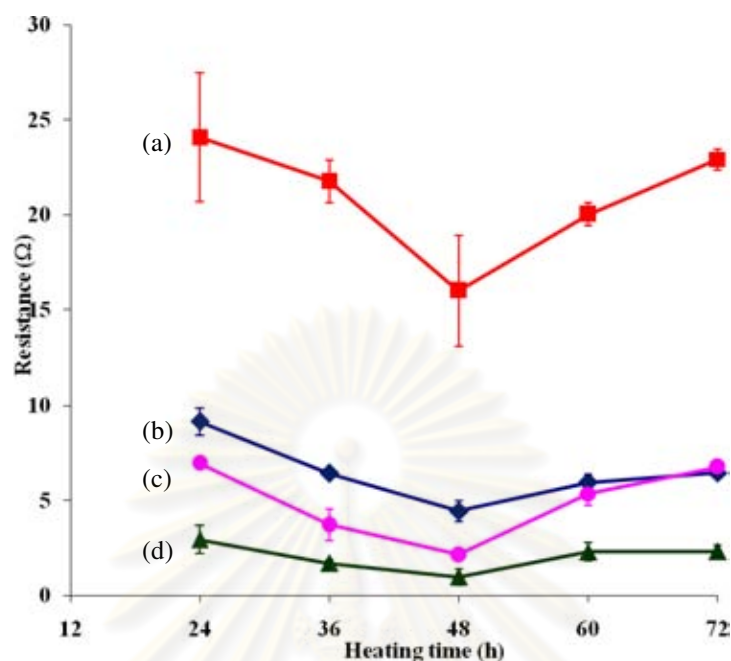


**Figure 3.10** Resistance of the PEDOT/PMMA composite film prepared by SSP of the electrospun (a) 3:1 (w/w) DBEDOT/ PMMA fiber mats in DMF heated at 80 °C, (b) at 70 °C, (c) 4:1 (w/w) DBEDOT/ PMMA fiber mats in DMF by heating at 80 °C and (d) at 70 °C

### 3.3.3 Effect of solvent and DBEDOT/polymer weight ratio

The greatest conductivity of the PEDOT/PMMA composite film was obtained when 1:1 THF/DMF was used as the solvent for sample preparation before electrospinning. THF helped smoothen and reduce the thickness of the PEDOT/PMMA composite film. (Table 3.3) The conductivity values of PEDOT/PMMA composite film prepared in 1:1 THF/DMF at 1:1, 2:1, 3:1, 4:1 DBEDOT/PMMA weight ratio were shown in Table 3.3. It was found that the conductivity of the PEDOT/PMMA film increased with higher ratio of DBEDOT when comparing the sample from electrospinning of DBEDOT/PMMA at 3:1 weight ratio, using 1:1 THF/DMF solvent yielded the sample with much higher conductivity using DMF. The lower boiling point of THF (66 °C) comparing to that of DMF (153 °C) might have induced better distribution of the DBEDOT monomer within the composite film.



**Table 3.3** Conductivity and thickness of the PEDOT/PMMA composite film prepared by SSP of the electrospun DBEDOT/PMMA fiber mat by heating for 48 h

<b>DBEDOT:PMMA (% w/w)</b>	<b>solvent</b>	<b>Thickness (<math>\mu\text{m}</math>)</b>	<b>Conductivity (S/cm)</b>	<b>% Conversion</b>
1:1	1:1 THF/DMF	25.0418 $\pm$ 2.6162	0.018	31.24
2:1	1:1 THF/DMF	38.7647 $\pm$ 3.6520	17.20	63.86
3:1	DMF	45.0198 $\pm$ 5.0774	10.73	70.64
	1:1 THF/DMF	35.1791 $\pm$ 10.7332	31.69	80.76
4:1	1:1 THF/DMF	55.8513 $\pm$ 13.8211	42.96	83.11

Figure 3.11 displays the percentage conversion of PEDOT extracted from the PEDOT/polymer composite film as a function of DBEDOT/polymer weight ratio. In the case of low DBEDOT/polymer weight ratio, especially at 1:1 of which DBEDOT quantity is the lowest, the DBEDOT crystals were presumably so far apart that they could not lead to efficient SSP. The ratio of 1:1 gave rather heterogeneous distribution of PEDOT throughout the composite films which could be easily observed. In contrary, the weight ratio of 4:1 yielded the highest % conversion which was probably due to more concentrated DBEDOT crystals close to each other and induced efficient SSP. Another effect from residual polar solvent was also believed to possess a screening effect between the dopant (counter ions) and charged carriers of the PEDOT main chain, which suppressed the coulomb interactions between the positively charged PEDOT and the bromine dopant which usually promoted the charge transport within the PEDOT/PMMA composites.

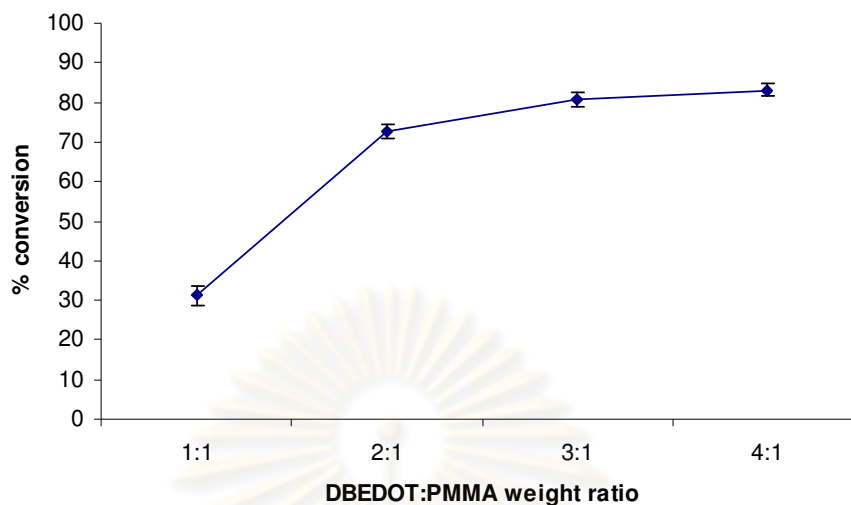


**Figure 3.11** Percentage conversion of extracted PEDOT from PEDOT/PMMA and composite films as a function of DBEDOT/polymer weight ratio. The SSP was conducted at 70 °C for 48 h in 1:1 THF/DMF solvent.

### 3.3.4 Effect of storage time

As demonstrated in Figure 3.12, it was found that the conductivity of the SSP kept going up upon storage. The conductivity of the stored PEDOT/PMMA composite film was two times higher than the freshly prepared PEDOT/PMMA composite film. This feature implied that although the SSP could be accelerated by heat treatment, the polymerization did not come to completion within a limited amount of time. This evidence agreed with what has been described by Meng et al. that the most efficient SSP occurred spontaneously and very slowly at ambient temperature [38,39].

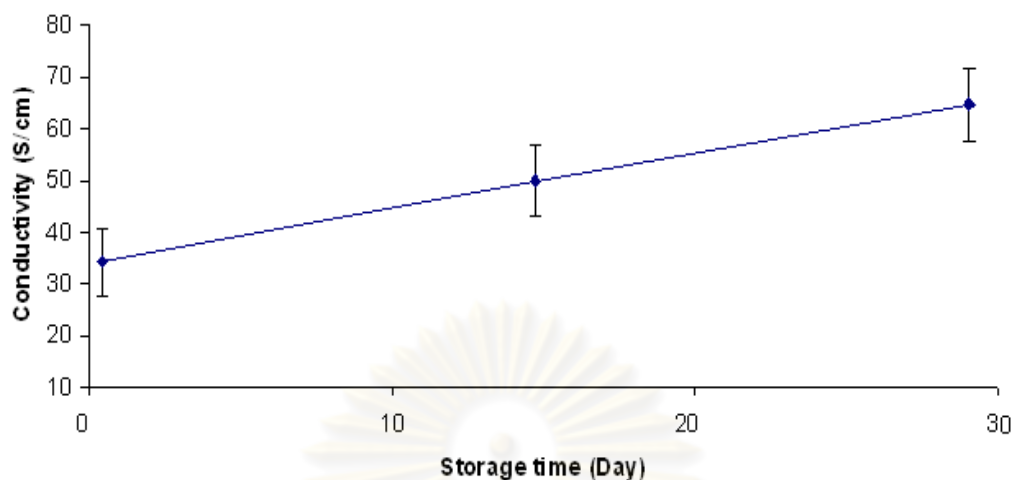


**Figure 3.12** Conductivity of PEDOT/PMMA composite film prepared by SSP of the 3:1 (w/w) DBEDOT/PMMA fiber mat electrospun from 1:1 THF/DMF solution with pressing as a function of storage time at ambient temperature.

### 3.4 Physical characteristics of PEDOT-containing polymer composite films

UV–Vis spectra of the PEDOT/PMMA composite films and the pellets of PEDOT sample were shown in Figure 3.13. All spectra exhibited one very broad absorption band with a maximum at ~550 nm, corresponding to the  $\pi$ - $\pi^*$  transition of the conjugated main chain with inter-chain interaction and  $\pi$ -stacking. The band usually appeared during the doping process of conjugated polymers and was ascribed to polaron type carriers [39]. The appearance of the absorption band from the neutral state below 400 nm suggested that parts of the PEDOT in the extracted PEDOT and the PEDOT/PMMA composite film were undoped. This could be resulted from the loss of doping bromine during the extraction process in the case of the extracted PEDOT.

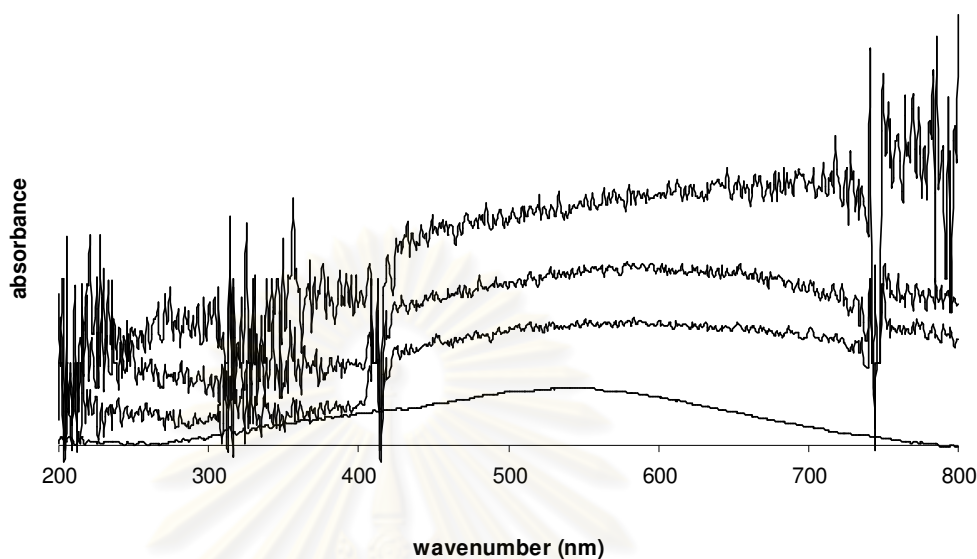


**Figure 3.13** UV-Visible spectra of (a) PEDOT/PMMA composite film obtained from monomer preparation in DMF, (b) controlled PEDOT, (c) extracted PEDOT and (d) PEDOT/PMMA composite film obtained from monomer preparation in DMF:THF (1:1)

X-ray diffraction patterns shown in Figure 3.14 revealed the crystalline structure of the DBEDOT, PEDOT, PMMA and PEDOT/PMMA composite film in comparison with the controlled PEDOT directly obtained from heating of DBEDOT in the absence of polymer matrix. Similar to the XRD pattern of PEDOT previously reported [39,56], a broad peak was found in the range of  $2\theta = 20-30^\circ$  for both the controlled PEDOT (Figure 3.14(f)) and PEDOT in the composite film (Figure 3.14(e)), indicating the disordered structure. The crystalline structure of DBEDOT (Figure 3.14(b)) exhibited strong and quite sharp diffraction peaks were observed at  $2\theta \sim 6.1^\circ$ ,  $13.1^\circ$  and  $25.6^\circ$  corresponding to the (100), (200), and (020) of the orthorhombic crystal structure. The fact that the characteristic pattern of the DBEDOT in DBEDOT/PMMA composite film (Figure 3.14(c)) closely resembled that of the plain DBEDOT (Figure 3.14(b)) strongly suggested that the electrospinning process did not alter the structure of the DBEDOT. The XRD pattern of the PEDOT/PMMA composite film obtained after SSP without pressing (Figure 3.14(d)) was similar to

that of DBEDOT/PMMA fiber mats, which evidently indicated that most of the DBEDOT still remained unpolymerized. This is in good agreement with the conductivity result.

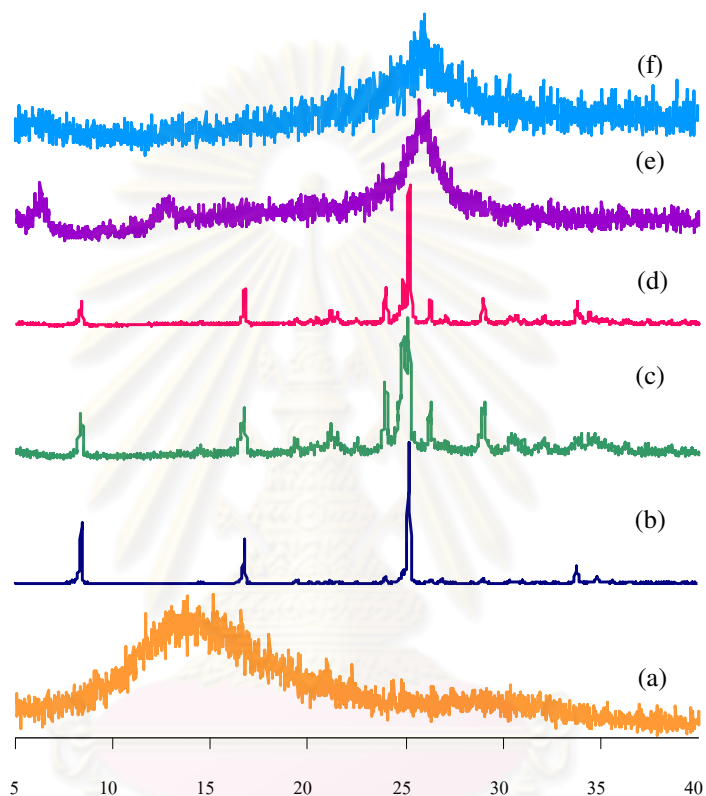


**Figure 3.14** XRD diffractograms of (a) electrospun PMMA fiber mat, (b) DBEDOT crystal, (c) electrospun 3:1 (w/w) DBEDOT/PMMA fiber mat, (d) electrospun 3:1 (w/w) PEDOT/PMMA fiber mat without pressing, (e) electrospun 3:1 (w/w) PEDOT/PMMA fiber mat with pressing and (f) controlled PEDOT.

Thermal properties of the PEDOT/polymer composite film and electrospun DBEDOT/polymer fiber mat in comparison to the controlled PEDOT as well as the starting materials including PMMA pellets, electrospun PMMA fibers, were characterized using DSC and TGA techniques. The DBEDOT/PMMA fiber mats were electrospun from the solution of 3:1 (w/w) DBEDOT/PMMA in DMF. The

condition used for SSP was heating the sample at 70 °C for 48 h with or without pressing. (Figure 3.15)

The exothermic peaks appeared at ~ 90 °C in the thermogram of the pure DBEDOT and DBEDOT/PMMA fiber mats (Figure 3.15(c,d)) signified the thermal transitions of the DBEDOT which was in agreement with the value reported by Meng and coworkers [39]. This also indicated that the thermal characteristic of the DBEDOT was not affected by the electrospinning process.

The incomplete polymerization of the DBEDOT in electrospun fiber mats (Figure 3.15(d)) when subjected to heat treatment without pressing could be verified by the unchanged thermogram of the PEDOT/PMMA film (Figure 3.15(e)), compared to that of the DBEDOT/PMMA fiber mats before heat treatment (Figure 3.15(d)). When pressing was applied, the SSP of the DBEDOT into the PEDOT was much more efficient and showed no characteristic feature of the DBEDOT in the thermogram (Figure 3.15(f)). The weight ratio of the starting DBEDOT/PMMA appeared to have little or no effect on the resulting thermograms of the polymer composites. (Figure 3.15 (f, g))

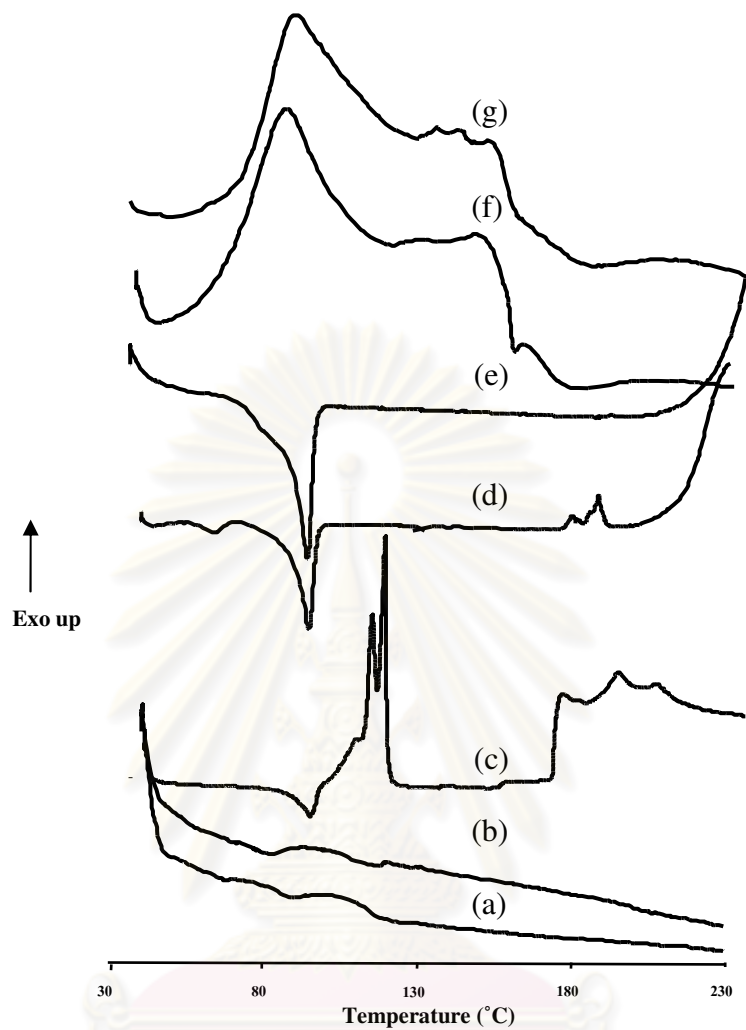


**Figure 3.15** DSC thermogram of (a) PMMA pellet, (b) electrospun PMMA fiber mat, (c) controlled DBEDOT, (d) electrospun 3:1 DBEDOT/PMMA fiber mat, (e) 3:1 PEDOT/PMMA composite film non-pressing, (f) 3:1 PEDOT/PMMA composite film pressing, (g) 4:1 PEDOT/PMMA composite film pressing.

จุฬาลงกรณ์มหาวิทยาลัย

## CHAPTER IV

### CONCLUSION

2,5-Dibromo-3,4-ethylenedioxythiophene (DBEDOT) was synthesized by a bromination of 3,4-ethylenedioxythiophene (EDOT) using a method modified from the published procedure. The polymer concentration that resulted in reasonably uniform fibers and good surface coverage was 18% (w/v). DMF and 1:1 THF/DMF were found to be the most suitable solvents for electrospinning DBEDOT/PMMA. In mixed solvent 1:1 THF and DMF gave more fibrous polymer film than in DMF solution.

The DBEDOT/PMMA fiber mat obtained after electrospinning could be transformed into the conductive PEDOT/PMMA composite film by heat activated solid state polymerization (SSP). The optimal condition for SSP of the DBEDOT was to heat at 70 °C for at least 24 h. The compression or pressing of the electrospun DBEDOT/PMMA fiber mats during the heat treatment was found necessary to efficiently induce SSP. If the compression was applied, the resulting dark blue PEDOT/PMMA composite film was smoother and more homogeneous than that obtained without the compression, suggesting that the PEDOT could be well dispersed in the former case. The conductivity of the composite film could reach as high as 42.96 S/cm. The fact that the conductivity values measured on the bottom side were comparable to those measured on the top side implied that the PEDOT distributed evenly throughout the composite film. Without pressing during heat treatment, the majority of the DBEDOT was left unpolymerized as identified by XRD, DSC and TGA analyses. The conductivity value increased when the weight ratio of PEDOT/PMMA increased. The conductivity value that kept going up upon storage implied that although the SSP could be accelerated by heat treatment, the polymerization did not go to completion within a limited amount of time. The highest conductivity of 64.95 S/cm could be obtained when the PEDOT/PMMA composite film prepared by SSP of the 3:1 (w/w) DBEDOT/PMMA fiber mat electrospun from 1:1 THF/DMF solution with pressing was kept at room temperature for 1 month.



FT-IR spectrum of the extracted PEDOT exhibited quite similar fingerprint of the controlled PEDOT confirmed the success of SSP. The wavenumbers at  $1724\text{ cm}^{-1}$  (carbonyl group) were shift after SSP of the PEDOT/PMMA composite could be due to some interactions of PEDOT and PMMA which conformed with TGA data. The percentage conversion into PEDOT in the composite prepared with compression is 71 % then without pressing at 38 %.



ศูนย์วิทยทรัพยากร  
จุฬาลงกรณ์มหาวิทยาลัย

## REFERENCES

- [1]. Chaing, C. K.; Fincher, C. R. Jr., Park, Y. W., Heeger, A. J., Shirakawa, H., Louise, E. J., Gau, S. C., McDiarmid, A. G. Electrical conductivity in doped polyacetylene. Phys. Rev. Lett. 39(1977): 1098–1101.
- [2]. McDiarmid, A. G. Synthetic metals: A novel role for organic polymers (Nobel lecture). Angew. Chem. Int. Ed. 40(2001): 2581–2590.
- [3]. Tourillon, G.; Garnier, F. New electrochemically generated organic conducting polymers. J. Electroanal. Chem. 135 (1982): 173-178.
- [4]. Patil, O.; Heeger, A. J.; Wudl F. Optical properties of conducting polymers. Chem. Rev. 88 (1988): 183-200.
- [5]. Roncali, J. Conjugated poly(thiophene): synthesis, functionalization, and applications. Chem. Rev. 92(1992): 711.
- [6]. Sirakul, T. *Synthesis of Processible Poly(3,4-Diakoxy Thiophene)*. Master's Thesis, Program of Petrochemistry and Polymer Science, Faculty of Science, Chulalongkorn University, 2006
- [7]. Mullekom, H. A. M. *The Chemistry of High and Low Band Gap Conjugated Polymers*. Ph.D. Dissertation, Eindhoven University of Technology, the Netherlands, 2000.
- [8]. Heeger, A. J. Semiconducting and Metallic Polymers: The Fourth Generation of Polymeric Materials. Synth. Met. 125 (2002): 23-42.
- [9]. Forrest, S. R. The Path to Ubiquitous and Low Cost Organic Electronic Appliances on Plastic. Nature 428 (2004): 911-918.
- [10]. Heeger, A. J. Nobel Lecture: Semiconducting and metallic polymers: The Fourth Generation of Polymeric Materials. Rev. Mod. Phys. 73 (2001): 681-700.

- [11]. Schimmel, T.; Schworer, M; Naarmann, H. Mechanisms limiting the d.c. conductivity of high-conductivity polyacetylene. Synth. Met. 37(1990): 1-6.
- [12]. Kvarnstrom, C.; Neugebauer, H.; Blomquist, S.; Ahonen, H. J.; Kankare, J.; Ivaska, A. In situ spectroelectrochemical characterization of poly(3,4-ethylenedioxythiophene). Electrochim. Acta. 44(1999): 2739-2750.
- [13]. Heeger, A. J. Semiconducting and metallic polymers: the fourth generation of polymeric materials. Synth. Met. 125(2002): 23-42.
- [14]. Greenham, N. C.; Friend, R. H. Semiconductor Device Physics of Conjugated Polymers, in Solid State Physics, Advances in Research and Application. Academic Press: New York, 1995.
- [15]. Su, W. P.; Schrieffer, J. R.; Heeger, A. J. Solitons in Polyacetylene. Phys. Rev. Lett. 42 (1979): 11698-1701.
- [16]. Brazovskii, S. A. Fröhlich Conductivity at Temperatures Excitations in the Peierls-Fröhlich State. Sov. Phys. JETP Lett. 28 (1978) : 606.
- [17]. Rice, M. J. Charged  $\pi$ -Phase Kinks in Lightly Doped Polyacetylene. Phys. Lett. A 71 (1979): 152-154.
- [18]. Campbell, D. K.; Bishop, A. R. Soliton Excitations in Polyacetylene and Relativistic Field Theory Models. Phys. Rev. B 24 (1981): 4859-4862.
- [19]. Epstein, A. J.; Ginder, J. M.; Zuo, F.; Bigelow, R. W.; Woo, H.-S.; Tanner, D. B.; Richter, A. F.; Huang, W.-S.; MacDiarmid, A. G. Very Low Temperature Nuclear Spin Diffusion in Trans-Polyacetylene. Synth. Met. 18 (1987) : 303-309.
- [20]. Strafstrom, S.; Brédas, J. L.; Epstein, A. J.; Woo, H. S.; Tanner, D. B.; Huang, W. S.; MacDiarmid, A. G. Correlation Functions for Hubbard-type Models: The Exact Results for the Gutzwiller Wave Function in One Dimension. Phys. Rev. Lett. 59 (1987) : 1472-1475.

- [21]. Pinto, N. J.; Shah, P. D.; Kahol, P. K.; McCormick, B. J. Conducting State of Polyaniline Films: Dependence on Moisture. Phys. Rev. B 53 (1996): 10690-10694.
- [22]. Groenendaal, L.; Zotti, G.; Aubert, P.-H.; Waybright, S. M.; Reynolds, J. R. Electrochemistry of poly(3,4-alkylenedioxythiophene) derivatives. Adv. Mater. 15(2003): 855– 879.
- [23]. Kwon, C. W.; Campet, G.; Kale, B. B. Structure of thin films of poly(3,4-ethylenedioxythiophene). Act. Pass. Electr. Comp. 26(2003): 81–86.
- [24]. Jonas, F.; Schrader, L. Conductive modifications of polymers with polypyrroles and polythiophenes. Synth. Met. 41(1991): 831.
- [25]. Jonas, F.; Heywang, G. Technical applications for conductive polymers. Electrochim. Acta. 39(1994): 1345-1347.
- [26]. Inganas, O.; Salaneck, W. R.; Österholm, J. E.; Laakso, J. Thermochromic and solvatochromic effects in poly(3-hexylthiophene). Synth. Met. 22(1988): 395–406.
- [27]. Groenendaal, L.; Jonas, F.; Freitag, D.; Pielartzik, H.; Reynolds, J. Poly(3,4-ethylenedioxythiophene) and its derivatives: Past, Present, and Future. Adv. Mater. 12(2000): 481.
- [28]. Reynolds, J. R.; Kumar, A.; Reddinger, J. L.; Sankaran, B.; Sapp, S. A.; Sotzing, G. A. Unique variable-gap polyheterocycles for high-contrast dual polymer electrochromic devices. Synth. Met. 85 (1997): 1295-1298.
- [29]. Kiebooms, R.; Aleshin, A.; Hutchison, K.; Wudl, F. Thermal and electromagnetic behavior of doped poly(3,4-ethylenedioxythiophene) films. J. Phys. Chem. B. 101 (1997): 11037-11039.
- [30]. Ahonen, H. J.; Lukkari, J.; Kankare, J. n- and p-Doped Poly(3,4-ethylenedioxythiophene): Two electronically conducting states of the polymer Macromolecules. 33 (2000): 6787-6793.

- [31]. Pei, Q.; Zuccarello, G.; Ahskog, M.; Inganäs, O. Electrochromic and highly stable poly(3,4-ethylenedioxythiophene) switches between opaque blue-black and transparent sky blue. *Polymer*. 35 (1994): 1347-1351.
- [32]. Cornil, J.; Dos Santos, D. A.; Beljonne, D.; Bredas, J. L.; Electronic Structure of Phenylene Vinylene Oligomers: Influence of Donor/Acceptor Substitutions. *J. Phys. Chem.* 99 (1995): 5604-5611.
- [33]. Heywang, G.; Jonas, F. Poly(alkylenedioxythiophene)s - new, very stable conducting polymers. *Adv. Mater.* 4 (1992): 116-118.
- [34]. Dietrich, M.; Heinze, J.; Heywang, G.; Jonas, F. Electrochemical and spectroscopic characterization of polyalkylenedioxythiophenes. *J. Electroanal. Chem.* 369 (1994): 87-92.
- [35]. Kvarnstrom, C.; Neugebauer, H.; Blomquist, S.; Ahonen, H. J.; Kankare, J.; Ivaska, A.; Sariciftci, N. S. In situ FTIR spectroelectrochemical characterization of poly(3,4-ethylenedioxythiophene) films. *Synth. Met.* 101 (1999): 66.
- [36]. Wang, Y. Research progress on a novel conductive polymer - poly(3,4-ethylenedioxythiophene) (PEDOT). *J. Phys. Conf. Ser.* 152 (2009): 012023.
- [37]. Vouyiouka, S. N.; Karakatsani, E. K.; Papaspyrides, C. D. Solide state polymerization. *Prog. Polym. Sci.* 30(2005): 10-37.
- [38]. Meng, H.; Perepichaka, D. F.; Wudl, F. Facial solid-state synthesis of highly conducting poly(ethylenedioxythiophene). *Angew. Chem. Int. Ed.* 42(2003): 658-661.
- [39]. Meng, H.; Perepichaka, D. F.; Bendikov, M.; Wudl, F.; Pan, G. Z.; Yu, W.; Dong, W.; Brown, S. Solid-state synthesis of conducting polythiophene via an unprecedented heterocyclic coupling reaction. *J. Am. Chem. Soc.* 125(2003): 15151-15162.

- [40]. Ouyang, J.; Chu, C.; Chen, F.; Chen, F.; Xu, Q.; Yang, Y. High-Conductivity Poly(3,4-Ethylenedioxythiophene): Poly(styrenesulfonate) film and its application in polymer optoelectronic devices. Adv. Funct. Mater. 15(2005): 203-208).
- [41]. Omastova, M.; Simon, F. Surface characterizations of conductive poly(methyl methacrylate)/polypyrrole composites. Journal of materials science. 35(2000): 1743-1749.
- [42]. Veluru, B. J.; Satheesh K. K.; Trivedi D. C.; Murthy V. R.; Natarajan Y. S. Electrical properties of electrospun fiber of PANI-PMMA composites. Journal of Engineered Fibers and Fabrics. 2(2007): 25-30
- [43]. Amrithesh, M.; Aravind, S.; Jayalekshmi, S.; Jayasree, R. S. Enhanced luminescence observed in polyaniline-polymethylmethacrylate composites. J. Alloys Compd. 449(2008): 176.
- [44]. Ji, S.; Li, Y.; Yang, M. Gas sensing properties of a composite composed of electrospun poly(methyl methacrylate) nanofibers and in situ polymerized polyaniline. Sensor and actuators B. 133(2008): 644
- [45]. Huang, Z. M.; Zhang, Y. Z.; Kotaki, M.; Ramakrishna, S. A review on polymer nanofibers by electrospinning and their applications in nanocomposites. Compos. Sci. Technol. 63 (2003): 2223-2253.
- [46]. Doshi, J.; Reneker, D, H. Electrospinning process and applications of electrospinning. Polymer 40 (1995): 4585-4592.
- [47]. Sai, P. P.; Schreuder-Gibson, H.; Gibson, P. Different electrostatic method for making electret filters. J. Electrostat. 54 (2002): 333-341
- [48]. Hafemann, B.; Ensslen, S.; Erdmann, C.; Niedballa, R.; Zühlke, A.; Ghofrani, K.; Kirkpatrick, C. J. Use of collagen/elastin-membrane for the tissue engineering of dermis. Burns 25 (1999): 373-384

- [49]. Gibson, P. W.; Schreuder-Gibson, H. L.; Rivin, D. Electrospun fiber mats: Transport properties. Am. Inst. Chem. Eng. 45 (1999): 90-195.
- [50]. Saikrasun, S.; Amornsakchai, T.; Sirisinha, C.; Meesiri, W.; Bualeklimcharoen, S. Kevlar reinforcement of polyolefin-based thermoplastic lastomer. Polymer 40 (1999): 6437-6442.
- [51]. Gouma, P. I. Nanostructured polymorphic oxides for advanced chemo-sensors. Rev. Adv. Mater. Sci. 5 (2003): 147-154.
- [52]. "Keithley instruments inc." Information available online under <http://www.keithley.com>
- [53]. Kellog, R. M.; Schaap, A. P.; Harper E. T.; Wynberg, H. Acid-Catalyzed Brominations, Deuterations, Rearrangements, and Debrominations of Thiophenes under Mild Conditions. J. Org. Chem. 32 (1968) : 2902-2909.
- [54]. Thirasart, N. *Synthesis of  $\beta$ -Substituted 2,5-Dibromothiophene and their S,S-Dioxides*. Master's thesis, Program of Petrochemistry and Polymer Science, Faculty of Science, Chulalongkorn University, 2004.
- [55]. Pantano, C.; Gañá-Calvo, A. M.; Barero, A. Zeroth-order, Electrohydrostatic solution for electrospraying in Cone-jet mode. J. Aerosol Sci 25 (1994): 1065-1077.
- [56]. Aasmundtveit, K. E.; Samuelsen, E. J.; Inganas, O.; Pettersson, L. A. A.; Johansson, T. B.; Ferrer, S. Structural aspects of electrochemical doping and dedoping of poly (3,4-ethylenedioxythiophene). Synth. Met. 113 (2000): 93-97.
- [57]. Information available online under <http://www.plasticballs.com/acetate>
- [58]. Kim, J. Y.; Jung, J. H.; Lee, D. E.; Joo, J. Enhancement of electrical conductivity of poly(3,4-ethylenedioxythiophene)/poly(4-styrenesulfonate) by a change of solvents. Synth. Met. 126 (2002): 311-316.

- [59]. Rajulu, A. V.; Reddy, R. L.; Avasthi, D. K.; Asokan, K. Infrared spectroscopic investigation of some polymer and polymer blend films irradiated by  $^{28}\text{Si}$  ion beam. Radiation effect & defects in solid. 152 (1999) : 57-66.
- [60]. Wanga, X. J.; Wong, K. Y. Effects of a base coating used for electropolymerization of poly(3,4-ethylenedioxythiophene) on indium tin oxide electrode. Thin Solid Film 515(2006): 1573-1578.
- [61]. Damlin, P.; Kvarnström, C.; Ivaska, A. Electrochemical synthesis and in situ spectroelectrochemical characterization of poly(3,4-ethylenedioxythiophene) (PEDOT) in room temperature ionic liquids. J. Electroanal. Chem. 570(2004): 113-122.
- [62]. Kusonsong, S., Preparation of conducting polymer composites by solid state polymerization of 2,5- dibromo-3,4-ethylenedioxythiophene. Master's Thesis, Program of Petrochemistry and Polymer Science, Faculty of Science, Chulalongkron University, 2007.
- [63]. Keaw-on N., S.; Conducting polymer composites of polystyrene and poly(3,4-ethylenedioxythiophene) prepared by electrospinning and heat-activated polymerization. Master's Thesis, Program of Petrochemistry and Polymer Science, Faculty of Science, Chulalongkron University, 2009.
- [64]. Sun, X.; Hagner, M. Novel Poly(acrylic acid)-mediated formation of composited poly(3,4-ethylenedioxythiophene)-based conducting polymer nanowires. Macromolecules 40 (2007): 8537-8539.
- [65]. Sonmez, G.; Scgottland, P.; Reynolds, J. R. PEDOT/PAMPS: An electrically conductive polymer composite with electrochromic and cation exchange properties. Synth. Met. 155 (2005): 130-137.





**APPENDICES**

ศูนย์วิทยทรัพยากร  
จุฬาลงกรณ์มหาวิทยาลัย

## APPENDIX A

### Characterization Techniques

#### FT-IR Spectroscopy (ATR)

IR spectroscopy is its ability as an analytical technique to obtain spectra from a very wide range of solids, liquids and gases. The technique of Attenuated Total Reflectance (ATR) has in recent years revolutionized solid and liquid sample analyses because it combats the most challenging aspects of infrared analyses, namely sample preparation and spectral reproducibility.

An attenuated total reflection accessory operates by measuring the changes that occur in a totally internally reflected infrared beam when the beam comes into contact with a sample (indicated in Figure A-1). An infrared beam is directed onto an optically dense crystal with a high refractive index at a certain angle. This internal reflectance creates an evanescent wave that extends beyond the surface of the crystal into the sample held in contact with the crystal. It can be easier to think of this evanescent wave as a bubble of infrared that sits on the surface of the crystal. This evanescent wave protrudes only a few microns ( $0.5\ \mu$ -  $5\ \mu$ ) beyond the crystal surface and into the sample. Consequently, there must be good contact between the sample and the crystal surface. In regions of the infrared spectrum where the sample absorbs energy, the evanescent wave will be attenuated or altered. The attenuated energy from each evanescent wave is passed back to the IR beam, which then exits the opposite end of the crystal and is passed to the detector in the IR spectrometer. The system then generates an infrared spectrum.

As with all FT-IR measurements, an infrared background is collected, in this case, from the clean ATR crystal. The crystals are usually cleaned by using a solvent soaked piece of tissue. Typically water, methanol or isopropanol are used to clean ATR crystals. The ATR crystal must be checked for contamination and carry over before sample presentation, this is true for all liquids and solids. [54]

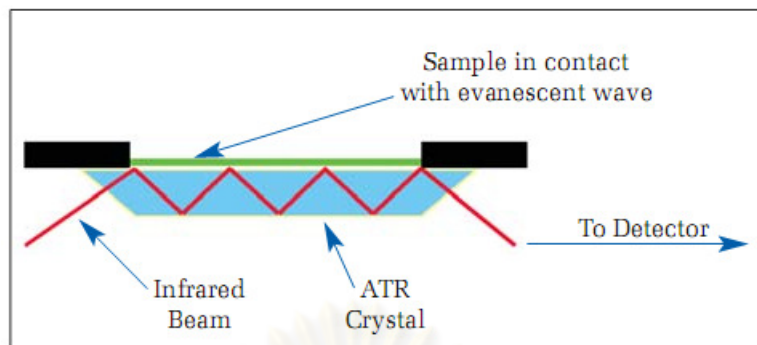


**Figure A-1** A multiple reflection ATR system.

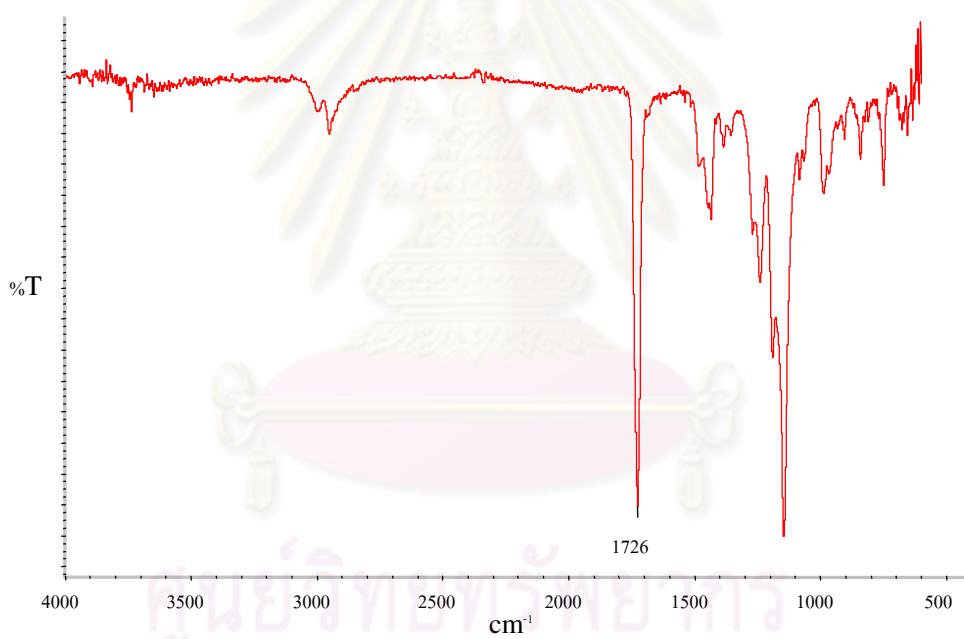


**Figure A-2** FT-IR spectra of electrospun PMMA

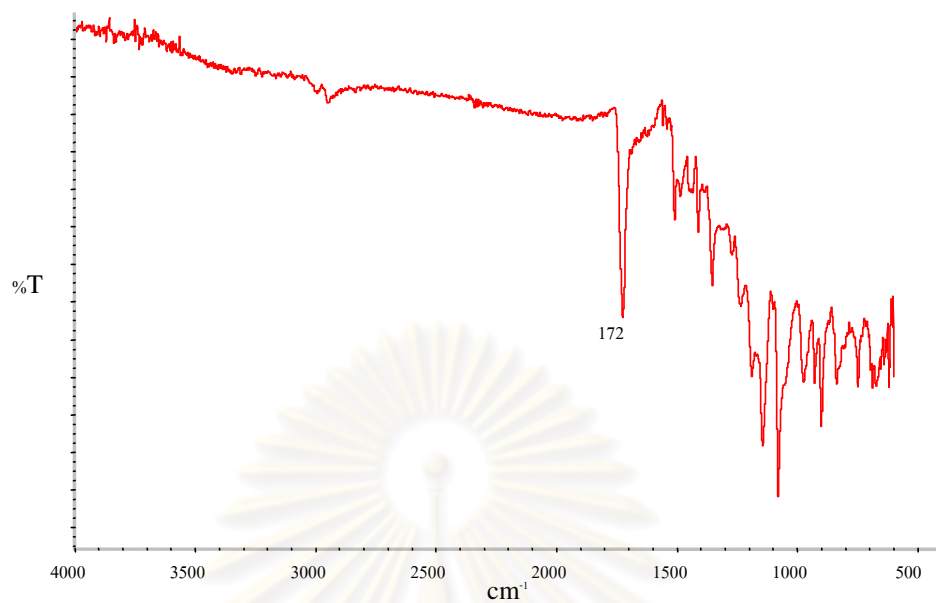


**Figure A-3** FT-IR spectra of 3:1 PEDOT/PMMA composite film without pressing at 70 °C for 48 h.

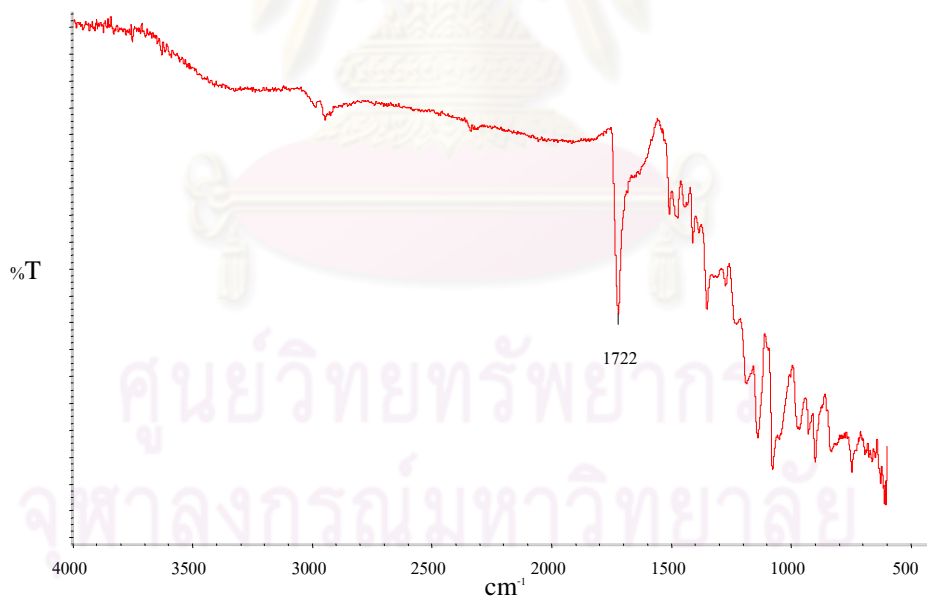


**Figure A-4** FT-IR spectra of 4:1 PEDOT/PMMA composite film without pressing at 70 °C for 48 h.

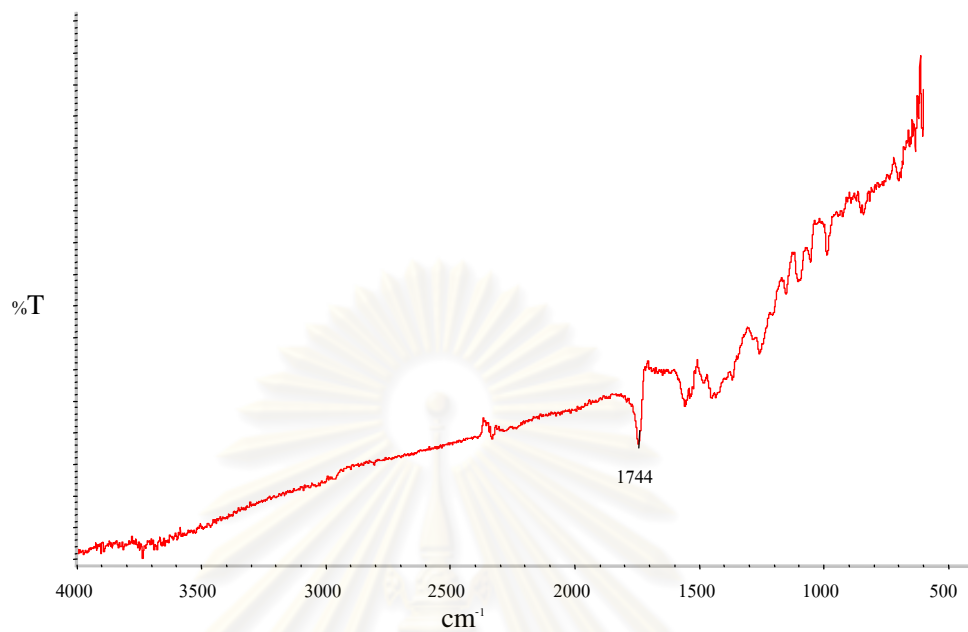


**Figure A-5** FT-IR spectra of 3:1 PEDOT/PMMA composite film pressing at  $70 \text{ }^{\circ}\text{C}$  for 48 h.

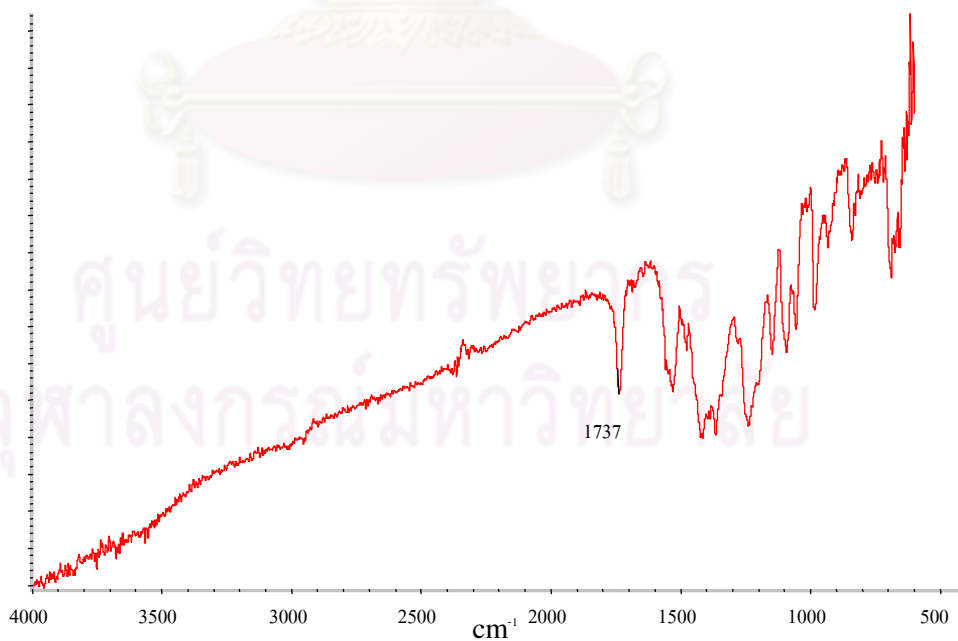


**Figure A-6** FT-IR spectra of 4:1 PEDOT/PMMA composite film pressing at  $70 \text{ }^{\circ}\text{C}$  for 48 h.

### Conductivity measurement by four point probe technique [52]

Four tiny electrodes are arranged in straight line separated at exactly equal distances ( $d_1 = d_2 = d_3$ ) and touch the surface of the sample to be measured. (Figure A-1) The electrodes are further connected with an electrical circuit equipped with an Amp meter (A) and Voltmeter (V). Contacts between the four electrodes and the sample surface must be equal. During the measurement, the current (I) is applied through electrode contact 1 to 4, and difference ( $\Delta V$ ) across electrode contacts 2 and 3 is measured. The resistivity and conductivity of the sample can be calculated from the equation A-1 and A-2, respectively.

Resistivity ( $\Omega \cdot \text{cm}$ );

$$\rho = (\pi \cdot t / \ln 2) (V/I) = 4.53 (R \cdot t) \quad (\text{A-1})$$

Conductivity ( $\text{S} \cdot \text{cm}^{-1}$ );

$$\sigma = 1/\rho \quad (\text{A-2})$$

Where

I is current (A)

V is voltage (Volt)

R is resistant (ohm)

t is film thickness (cm)

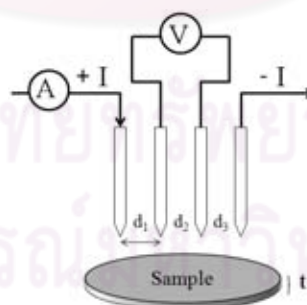


**Figure A-7** Schematic representation of 4-point probe configuration

**Table A-1** Conductivity measured on the top side and the bottom side of the PEDOT/PMMA composite film (thickness of  $55.8513 \pm 13.8211 \mu\text{m}$ ) prepared by SSP of the electrospun 3:1 (w/w) DBEDOT/ PMMA fiber mats by heating  $70^\circ\text{C}$  with pressing as a function of reaction time.

Time (h)	Resistant ( $\Omega$ )	Conductivity (S/cm)
	Top side	
12	45.49	0.869
24	4.18	9.025
36	3.36	11.763
48	1.51	26.175
60	1.98	19.961
72	2.36	16.747
<b>Bottom side</b>		
12	27.74	1.425
24	3.90	10.135
36	2.21	17.884
48	1.33	29.718
60	1.78	22.205
72	1.86	21.250

Example Conductivity calculation of 8 h Sample in table A-1

From Resistivity ( $\Omega \cdot \text{cm}$ );  $\rho = 4.53(R \cdot t)$   
 Conductivity ( $\text{S} \cdot \text{cm}^{-1}$ );  $\sigma = 1/\rho$   
 R is resistant ( $45.49 \Omega$ )  
 t is film thickness ( $5.58513 \times 10^{-3} \text{ cm}$ )  
 $\rho = 4.53 \times (45.49 \Omega \times 5.58513 \times 10^{-3} \text{ cm})$   
 $= 1.151 \Omega \cdot \text{cm}$   
 $\sigma = 1/1.151 \Omega \cdot \text{cm}$   
 Conductivity =  $0.869 \text{ S} \cdot \text{cm}^{-1}$

**Table A-2** Resistance measured on the top side of the PEDOT/PMMA composite film (thickness of  $55.8513 \pm 13.8211 \mu\text{m}$ ) prepared by SSP of the electrospun 3:1 (w/w) DBEDOT/ PMMA fiber mats by heating  $70^\circ \text{C}$  and  $80^\circ \text{C}$  with pressing as a function of reaction time.

Time (h)	Resistant ( $\Omega$ )	
	Heating temperature at $70^\circ \text{C}$	Heating temperature at $80^\circ \text{C}$
4	91.15	159.20
6	66.43	92.86
8	43.69	65.51
10	36.21	46.96



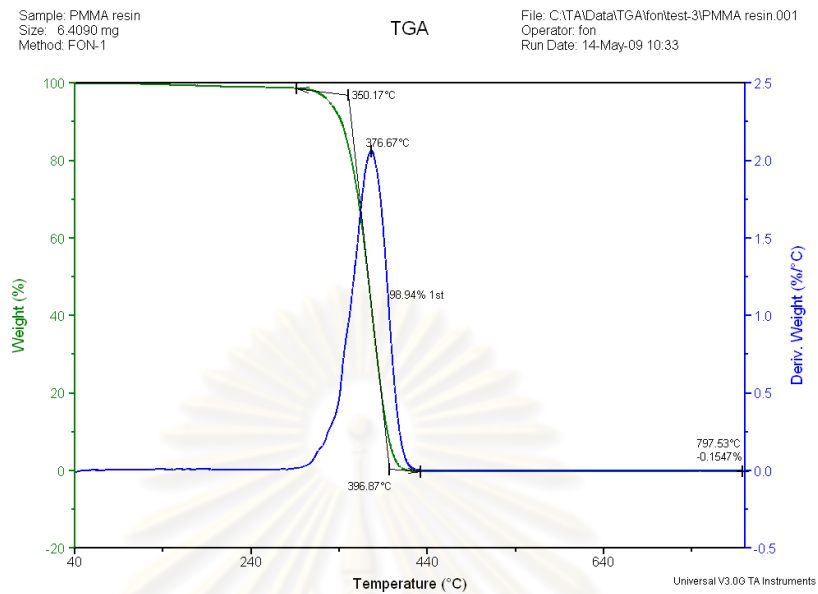


**Figure A-8** TGA thermograms of electrospun PMMA fiber mat

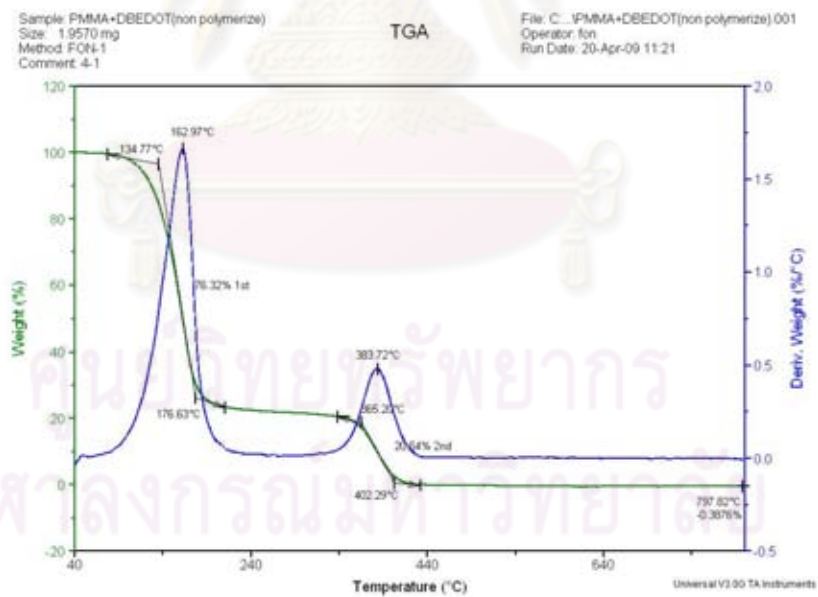


**Figure A-9** TGA thermograms of electrospun DBEDOT/PMMA fiber mat

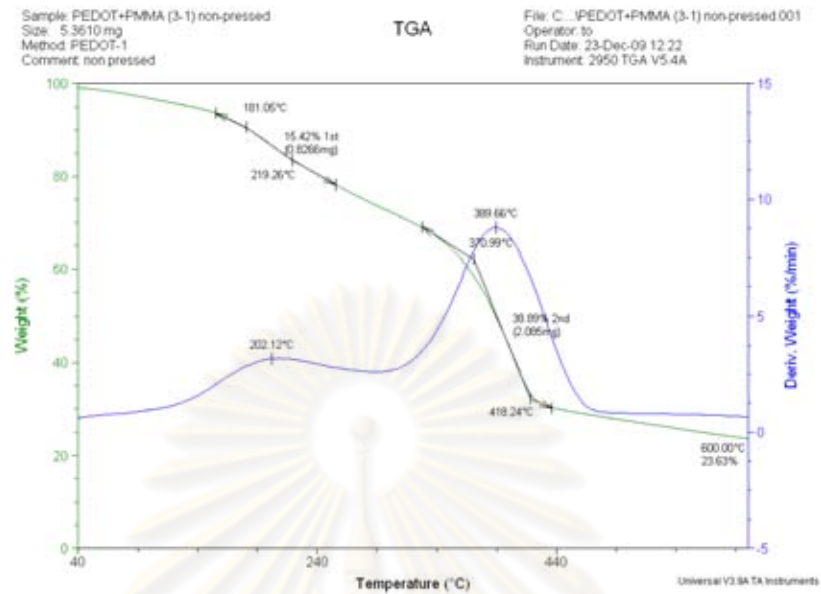


**Figure A-10** TGA thermograms of PEDOT/PMMA (3:1) composite film without pressing

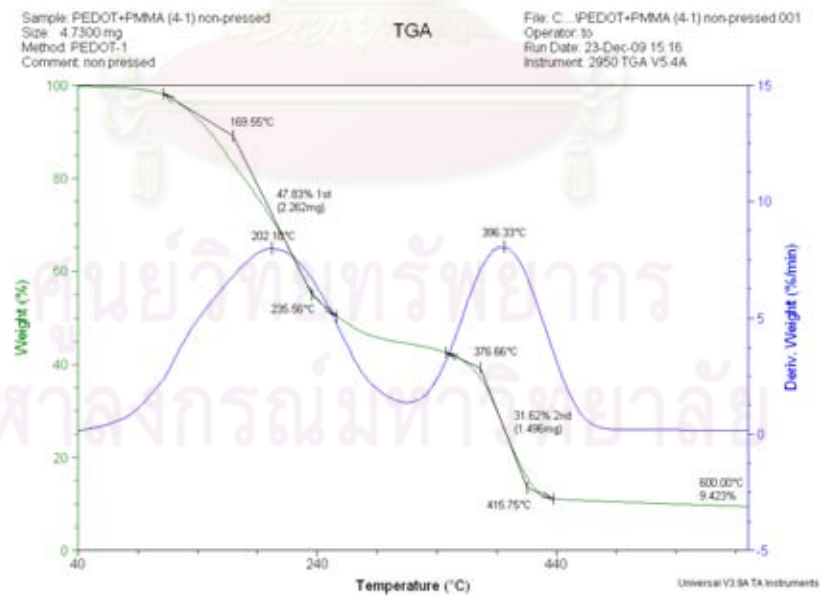


**Figure A-11** TGA thermograms of PEDOT/PMMA (4:1) composite film without pressing

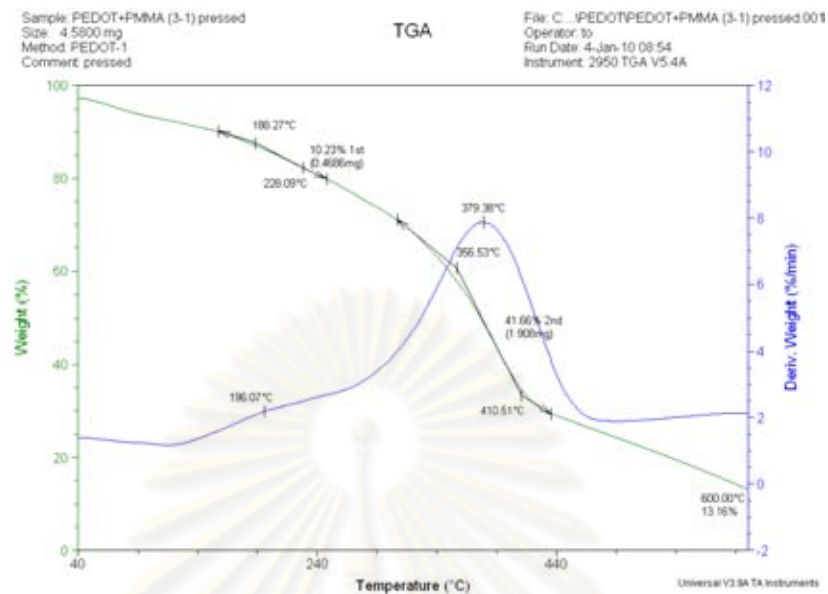


**Figure A-12** TGA thermograms of PEDOT/PMMA (3:1) composite film with pressing

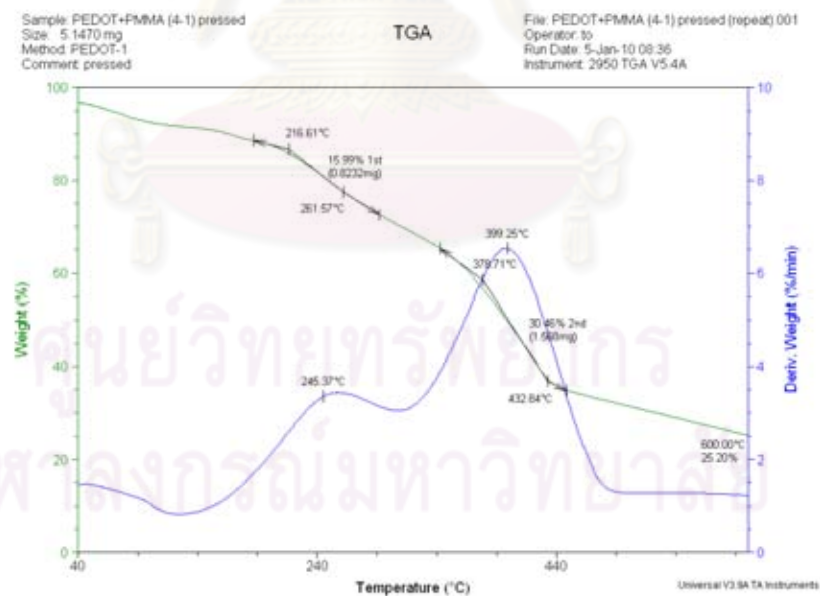


**Figure A-13** TGA thermograms of PEDOT/PMMA (4:1) composite film with pressing

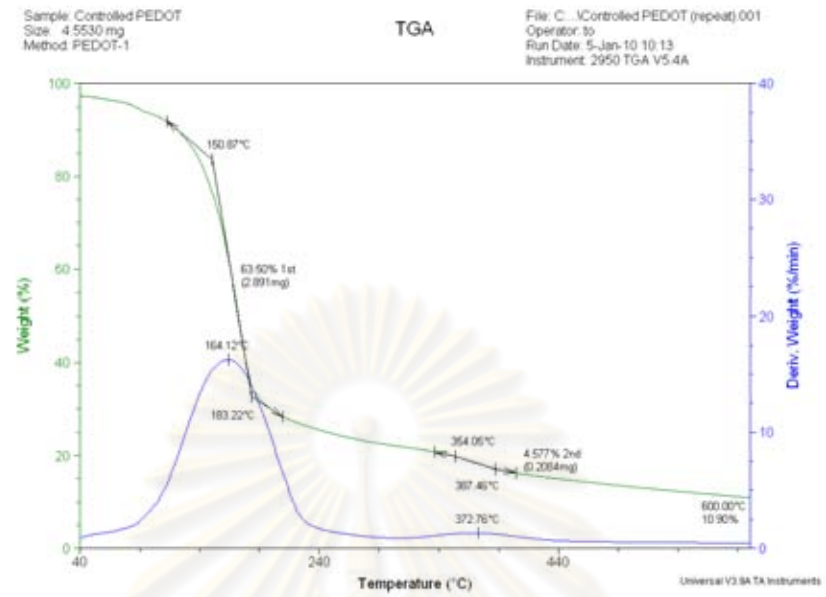


Figure A-14 TGA thermograms of controlled PEDOT

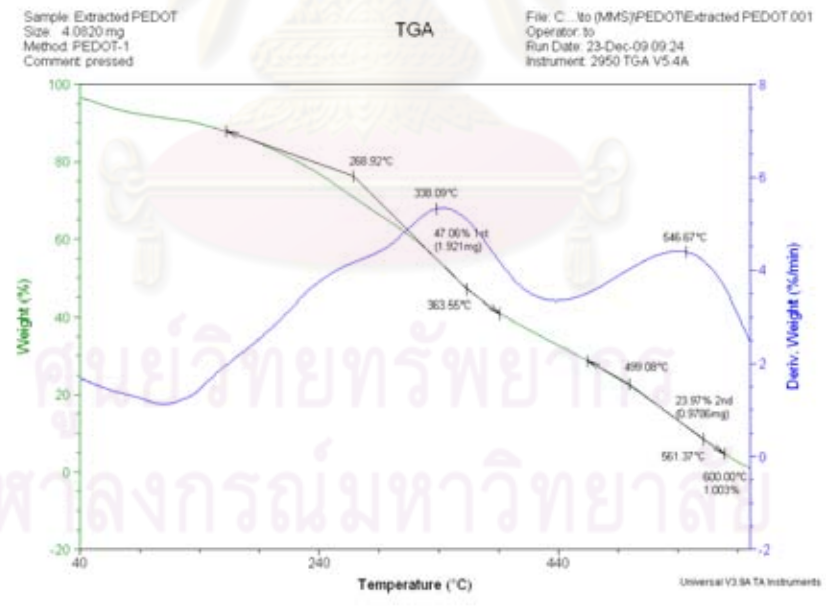
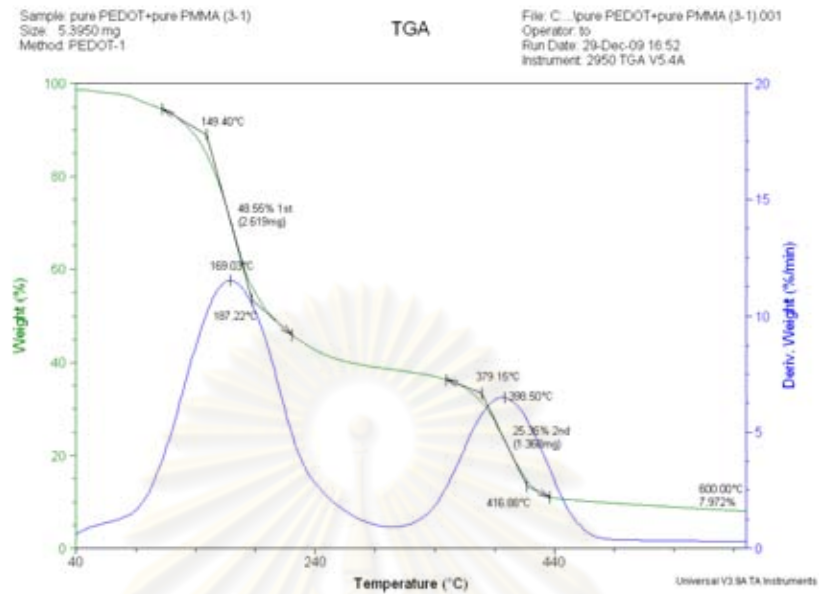


Figure A-15 TGA thermograms of extracted PEDOT



**Figure A-16** TGA thermograms of manually mixed pure PEDOT powder and PMMA fiber mat at 3:1 weight ratio

ศูนย์วิทยทรัพยากร  
จุฬาลงกรณ์มหาวิทยาลัย

## APPENDIX B

B-1 The 13<sup>th</sup> Asian Chemical Congress 2009, Shanghai China.

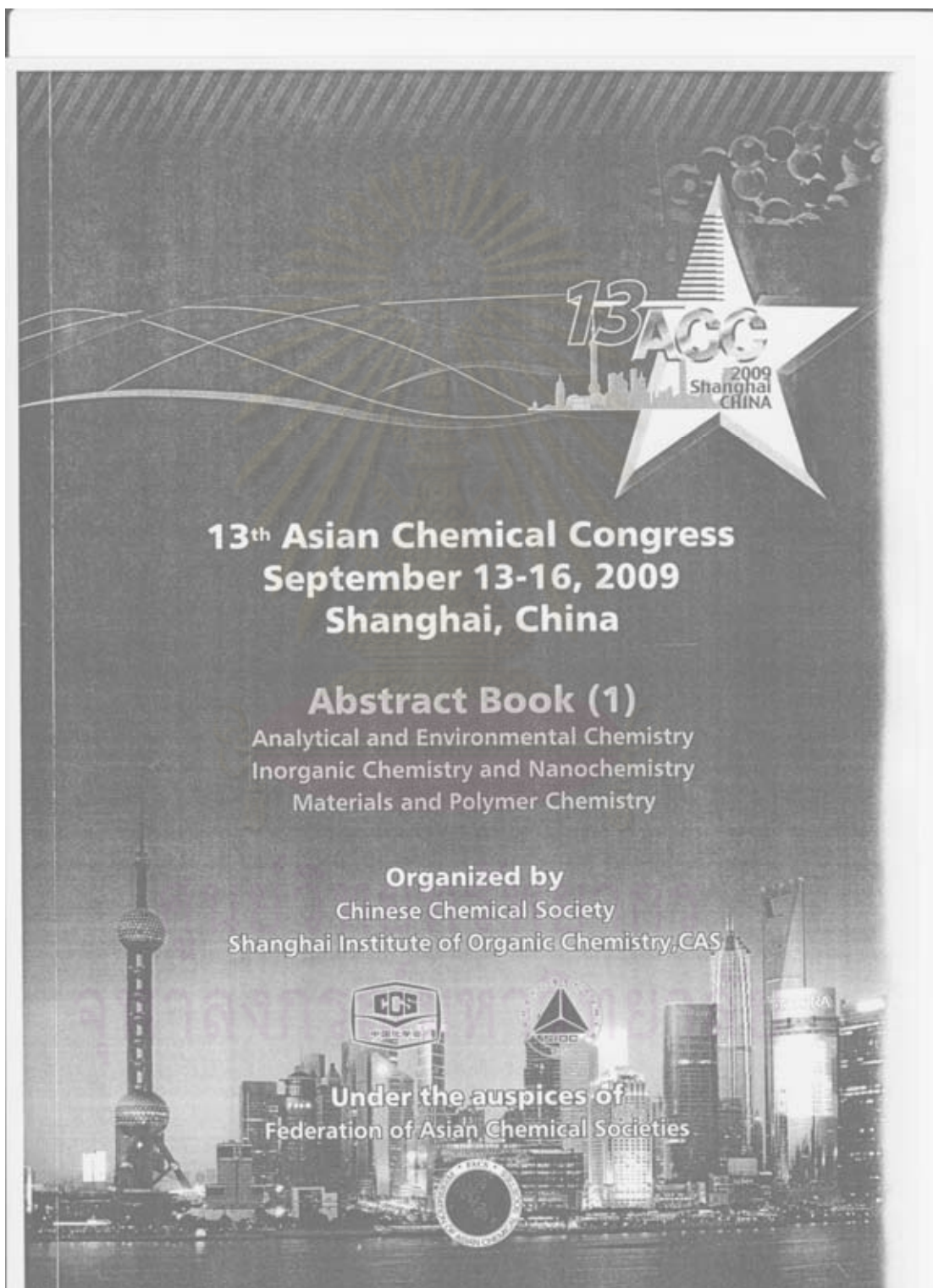
B-2 The 35<sup>th</sup> Congress on Science and Technology of Thailand, Burapha University, Chonburi, Thailand.

B-3 The 6<sup>th</sup> ISAMAP, Chulalongkorn University, Bangkok.



ศูนย์วิทยทรัพยากร  
จุฬาลงกรณ์มหาวิทยาลัย

B-1



PM-PP-33: Thermal polymerization of  
2,5-dibromo-3,4-ethylenedioxythiophene in poly(methyl methacrylate)  
matrix

Kitikulvarakorn K.<sup>a</sup>, Hoven V.P.<sup>a,b</sup>, Sritana-anant Y.<sup>a</sup>

<sup>a</sup>Program of Petrochemistry and Polymer Science, Faculty of Science, Chulalongkorn University, Bangkok, 10330  
Thailand

<sup>b</sup>Organic Synthesis Research Unit, Department of Chemistry, Faculty of Science, Chulalongkorn University,  
Bangkok, 10330 Thailand

\*Tel (+66) 02-218-7632 Fax. (+66) 02-218-7598 E-mail: yongsak.s@chula.ac.th

**Abstract**

The PEDOT composites in PMMA matrix have been prepared by thermal polymerization of 2,5-dibromo-3,4-ethylenedioxythiophene (DBEDOT). The composite film was obtained from electrospinning the solution mixture of 3:1, 4:1, 5:1 weight ratios of DBEDOT:PMMA at the concentration of 0.18 g/mL PMMA. The polymerization of DBEDOT embedded in the PMMA matrix was induced at 80 °C. The result showed that the sample prepared at weight ratio 4:1 of DBEDOT:PMMA incubated for 72 h gave the lowest surface electrical resistance. The values of electrical resistance of the PEDOT composite film were found to decrease upon storage, possibly due to slow polymerization of the remaining monomer or slow reorganization of the polymer structure in doped state. The composite film was stable and remained highly conductive up to at least 2 months.


**Keywords:** PEDOT, PMMA composite, thermal polymerization, conducting polymer

**References**

- [1] Meng, H.; Perepichka, D. F.; Wudl, F. Facial solid-state synthesis of highly conducting poly(ethylenedioxythiophene). *Angew. Chem. Int. Ed.*, 2003, 42, 658.
- [2] Meng, H.; Perepichka, D. F.; Bendikov, M.; Wudl, F.; Pan, G. Z.; Yu, W.; Dong, W.; Brown, S. Solid-state synthesis of conducting polythiophene via an unprecedented heterocyclic coupling reaction. *J. Am. Chem. Soc.*, 2003, 125, 15151.
- [3] Ji, S.; Li, Y.; Yang, M.; Gas sensing properties of a composite composed of electrospun poly(methyl methacrylate) nanofibers and in situ polymerized polyaniline. *Sensor and Actuator B.*, 2008, 133, 644.
- [4] Groenendaal, L.; Jonas, F.; Freitag, D.; Pielartzik, H.; Reynolds, J. Poly(3,4-ethylenedioxythiophene) and its derivatives: Past, Present, and Future. *Adv. Mater.*, 2000, 12, 481.



B-2



  
BURAPHA UNIVERSITY  
STT 35  
FACULTY OF SCIENCE

# Abstracts

THE 35<sup>th</sup> CONGRESS  
on SCIENCE and TECHNOLOGY  
of THAILAND (STT 35)  
การประชุมวิชาการวิทยาศาสตร์และเทคโนโลยีแห่งประเทศไทย  
ครั้งที่ 35 (วทท 35)

*วิทยาศาสตร์และเทคโนโลยีเพื่ออนาคตที่ดีขึ้น*  
*SCIENCE AND TECHNOLOGY FOR A BETTER FUTURE*

*To Celebrate the 35<sup>th</sup> Anniversary of Faculty of Science, Burapha University*  
*To Celebrate the 30<sup>th</sup> Anniversary of Ministry of Science and Technology*

October 15 - 17, 2009  
Venue : The Tide Resort (Bangsaen Beach), Chonburi, Thailand.  
15-17 ตุลาคม 2552 ณ เดอะ ทีด รีสอร์ท (หาดบางแสน) จังหวัดชลบุรี  
[WWW.STT35.SCISOC.OR.TH](http://WWW.STT35.SCISOC.OR.TH)

การเตรียมฟิล์มคอมพอสิตพอลิเมอร์นำไฟฟ้า PEDOT/PMMA โดยวิธี Electrospinning และ ปฏิกิริยา  
พอลิเมอไรเซชันในสถานะของแข็ง

CONDUCTIVE PEDOT/PMMA COMPOSITE FILM PREPARED BY  
ELECTROSPINNING AND SOLID STATE POLYMERIZATION

กชพร กิติกุลวารการ<sup>1</sup>, วรวิทย์ ไสว่วน<sup>1,2</sup> และ ยงศักดิ์ ศรีธนาอนันต์<sup>1,2\*</sup>

Kodchaporn Kitikulvarakorn<sup>1</sup>, Voravee P. Hoven<sup>1,2</sup> and Yongsak Sritana-anant<sup>1,2\*</sup>

<sup>1</sup>Program of Petrochemistry and Polymer Science, Faculty of Science, Chulalongkorn University, Bangkok, 10330 Thailand

<sup>2</sup>Organic Synthesis Research Unit, Department of Chemistry, Faculty of Science, Chulalongkorn University, Bangkok, 10330 Thailand

\*Tel 02-218-7632 Fax: 02-218-7598 E-mail: yongsak.s@chula.ac.th

**บทคัดย่อ:** ฟิล์มคอมพอสิตพอลิเมอร์นำไฟฟ้าเตรียมได้โดยวิธีอิเล็กโทรสปินนิงของสารละลายผสมระหว่าง 2,5-ไดโบรมโอ-3,4-เอทิลีนไดออกซีไทโอฟีน (ดีบีดีไอที) และ พอลิเมอริสเมอ โนอีตราส่วน 3:1, 4:1 ที่ความเข้มข้น 0.18 กรัมต่อมิลลิกรัมของพอลิเมอริสเมอ แต่ความด้วยปฏิกิริยาพอลิเมอไรเซชันในสถานะของแข็งของ 2,5-ไดโบรมโอ-3,4-เอทิลีนไดออกซีไทโอฟีน ที่ถูกเตรียมอยู่ในเมทริกซ์ พอลิเมอริสเมอ โดยการใช้ความร้อนที่อุณหภูมิ 80 องศาเซลเซียส จากผลการทดลองพบว่าแผ่นฟิล์มที่อัตราส่วน 4:1 ของ ดีบีดีไอทีต่อพอลิเมอริสเมอ ที่ใช้ความร้อนเป็นเวลา 72 ชั่วโมง มีค่าความต้านทานทางไฟฟ้าบนพื้นที่ผิวที่น้อยที่สุด และเมื่อวางฟิล์มนี้ทิ้งไว้ที่ความต้านทานจะลดลงอีกอาจจะเนื่องมาจากการเกิดปฏิกิริยาพอลิเมอไรเซชันอย่างช้าๆของมอนอเมอร์ที่ยังหลงเหลืออยู่ หรือ เกิดการจัดเรียงตัวใหม่ของโครงสร้างพอลิเมอร์ในสถานะได้ป

**Abstract:** The conductive polymer composite film was first prepared by electrospinning the solution mixture of 2,5-dibromo-3,4-ethylenedioxythiophene (DBEDOT) and PMMA in 3:1, 4:1 weight ratios at the concentration of 0.18 g/mL PMMA. The solid state polymerization (SSP) of the result DBEDOT embedded in the PMMA matrix was then heated at 80 °C. The result showed that the sample prepared using the 4:1 weight ratio of DBEDOT:PMMA incubated for 72 h gave the lowest surface electrical resistance. The resistivity of this incubated PEDOT/PMMA composite film was found to decrease upon storage, possibly due to slow polymerization of the remaining monomers or reorganization of the polymeric structure in doped state.

**Introduction:** Conducting polymer have been drawing attention due to its many advantageous properties such as low cost, lightweight and mechanical flexibility upon constructing the materials for many applications including light emitting diodes, antistatic coating, gas sensor and molecular actuator [1]. Poly(3,4-ethylenedioxythiophene) (PEDOT) is arguably the most heavily studied and commercialized conjugated polymer in recent years because of its many attractive properties such as high stereo-regularity, high conductivity up to 550 S/cm in the electrochemical doped state, transparency and good stability comparing to other conducting polymers. [2] PEDOT was usually insoluble in solvents and not processible. This shortcoming was later overcome by the incorporation of water soluble counter-anions poly(styrene sulfonate) (PSS) into PEDOT/PSS composites dispersion in water. However

PEDOT:PSS composites still possess quite low conductivity less than 1 S/cm, which is lower than that of some good conducting polymers by one to two orders of magnitude. Also, it is typically laid down in an acidic water-based solution whose corrosive properties cause other problems.[3] The PEDOT synthesis is conventionally confined to chemical or electrochemical oxidation of polymer solution. As a consequence, defect sites and a relatively low degree of intermolecular order limit the number of possible applications. It is generally not possible to obtain a well-defined polymer structure, unless the synthesis of conducting polymers is carried out via pure chemical polymerization routes, without adding any catalysts. A possible solution for this lies in a solid state polymerization of a structurally pre-organized crystalline monomer. The advantages of solid state polymerization include low operating temperatures, which refrain side reactions and thermal degradation of the product, while requiring inexpensive equipment, and uncomplicated and environmentally sound procedures. The process was discovered by chance as a result of prolonged storage of the DBEDOT monomer at room temperature. By this process, the colorless crystalline DBEDOT could be transformed into a blue-black doped PEDOT crystal with varying high range of conductivity (20-80 S/cm).[4-5]

**Methodology:** All the chemicals and reagents used were of analytical grade. PMMA ( $M_w=120000$  Daltons) pellets, 3,4-ethylenedioxythiophene (EDOT) and N-bromosuccinimide (NBS) were purchased from Sigma-Aldrich. 2,5-Dibromo-3,4-ethylenedioxythiophene (DBEDOT) was synthesized by bromination of EDOT using NBS. [6]

**Preparation of PEDOT/PMMA composites film:**

A mixed solution of PMMA and DBEDOT at the concentration 0.18 g/mL of PMMA [7] was prepared by dissolving 0.36 g PMMA in 2 mL dimethylformamide (DMF) followed by an addition of 1.08 g DBEDOT and stirring the mixture for 30 min. The composite film was processed by electrospinning apparatus (Figure 1) operated at the voltage of 20 kV. A blunt 20-gauge stainless steel hypodermic needle (OD= 0.91 mm) used as a nozzle was connected with the positive electrode. A grounded metal screen covered by a glass slide, was used as the counter electrode and was placed 10 cm away from the tip of the needle. After continuous spinning for 4 h, the thin film of monomer composite was obtained on the glass slide with approximately 40  $\mu\text{m}$  thick as determined by a profilometer.

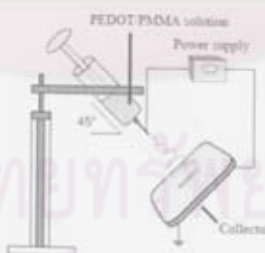
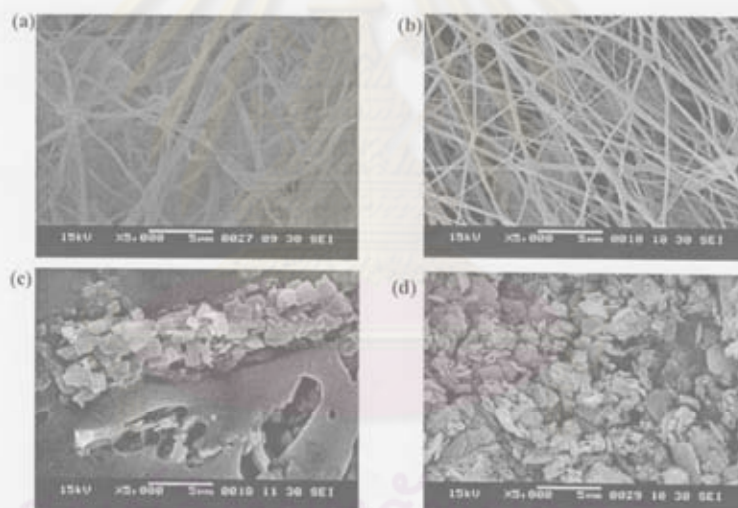


Figure 1 Schematic of electrospinning apparatus set up

#### Solid state polymerization

The thin film of PMMA containing DBEDOT on the glass slide was put in a petri dish and heated at 80 °C in an oven to induce polymerization of DBEDOT. The resulting film of PEDOT/PMMA composite was characterized by scanning electron microscope (SEM), FT-IR spectroscopy and thermogravimetric analysis (TGA). The surface resistance of the PEDOT/PMMA composite film was determined by the four-point-probe Keithley digital multimeter.

**Results, Discussion and Conclusion:** We have found that the lowest concentration of PMMA in the starting solution mixture that can generate bead-free fiber mat by electrospinning was 18 % w/v (Figure 2a). The SEM images showed that the fiber mat of PMMA and DBEDOT mixture before polymerization still maintained its fibrous appearance, quite similar to pure PMMA (Figure 2b) Upon the heat treatment, the mats completely lost the fibrous structure and became crystalline. (Figure 2c) After washing off the PMMA matrix exhaustively from the heated composite mat by chloroform, the remaining insoluble PEDOT appeared to show the crystalline-like structure matching that of the pre-extracted, heated composite. (Figure 2d)



**Figure 2** SEM images of electrospun fiber mat: (a) pure PMMA, (b) PMMA and DBEDOT, (c) PMMA/PEDOT composite after heat treatment at 80 °C, (d) PEDOT after being washed off the PMMA matrix.

FT-IR spectra of PEDOT prepared by SSP of DBEDOT in the polymer matrix were displayed in Figure 3. The FT-IR spectrum of the PEDOT after being washed the PMMA matrix off exhibit the same fingerprint to the controlled PEDOT obtained without the PMMA matrix.[4,5] The peaks at 1510 and 1410  $\text{cm}^{-1}$  originated from the asymmetric and symmetric stretching C=C, respectively, were clearly appeared.

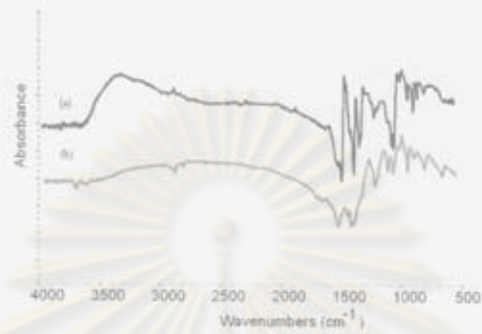


Figure 3 FT-IR spectra of (a) controlled PEDOT and (b) PEDOT from composite film

From the TGA thermograms (Figure 4,5), there are three distinct stages of weight loss in the PEDOT/PMMA composite films. The weight loss at  $\sim 130$  °C corresponds to the removal of bromine gas resulting from the process of SSP of the remaining monomer as it also appears in the controlled experiment (Figure 3b) while those at  $\sim 200$  °C and  $\sim 400$  °C can be assigned to the partial loss of PEDOT and PMMA, respectively. The magnitude of weight loss at  $\sim 200$  °C is proportional to the composition of PEDOT in the composite, meaning the higher the amount of PEDOT in the composite film, the greater the weight loss. From Figure 5c it was found that decomposition between  $\sim 130$  °C to  $\sim 400$  °C of the PEDOT/PMMA composite film at weight ratio 5:1 was the most obvious, showing more phase separation of PEDOT and PMMA in this sample.

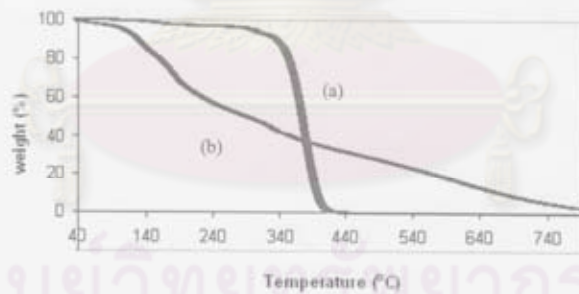


Figure 4 TGA thermograms of (a) PMMA and (b) controlled PEDOT

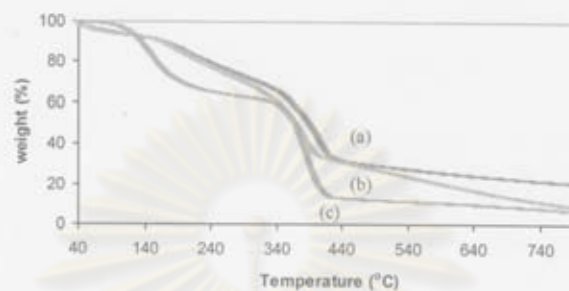


Figure 5 TGA thermograms of PEDOT/PMMA composite film prepared using DBEDOT/PMMA weight ratio of (a) 3:1, (b) 4:1, (c) 5:1

The measured resistance values of the PEDOT/PMMA composites film are shown in Table 1. The result showed that the sample prepared at the 4:1 weight ratio of DBEDOT:PMMA weight ratio 4:1, heated at 80 °C for 72 h, has lowest resistance when immediately measured after the polymerization process. However, after one month storage in ambient condition, all the measured resistance values seemed to further decrease dramatically, with the sample of 4:1 DBEDOT:PMMA heating for 48 h now held the lowest resistance. This continued decreasing of the composite film may be due to slow polymerization of the remaining monomers incompletely polymerized during the heating process, or slow reorganization of the PEDOT polymer structure in the doped state within the PMMA matrix, or both.


Table 1 Resistance of PEDOT/PMMA composite film before and after 1 month storage

DBEDOT:PMMA	Heating time (h)	Resistance ( $\Omega$ )	
		After incubation	After one month storage
3:1	24	$1.4 \times 10^7$	$1.1 \times 10^8$
3:1	48	$5.1 \times 10^6$	$1.3 \times 10^6$
3:1	72	$1.3 \times 10^6$	$2.5 \times 10^4$
4:1	24	$2.2 \times 10^3$	72
4:1	48	$2.1 \times 10^3$	50
4:1	72	$0.7 \times 10^3$	130

**References:**

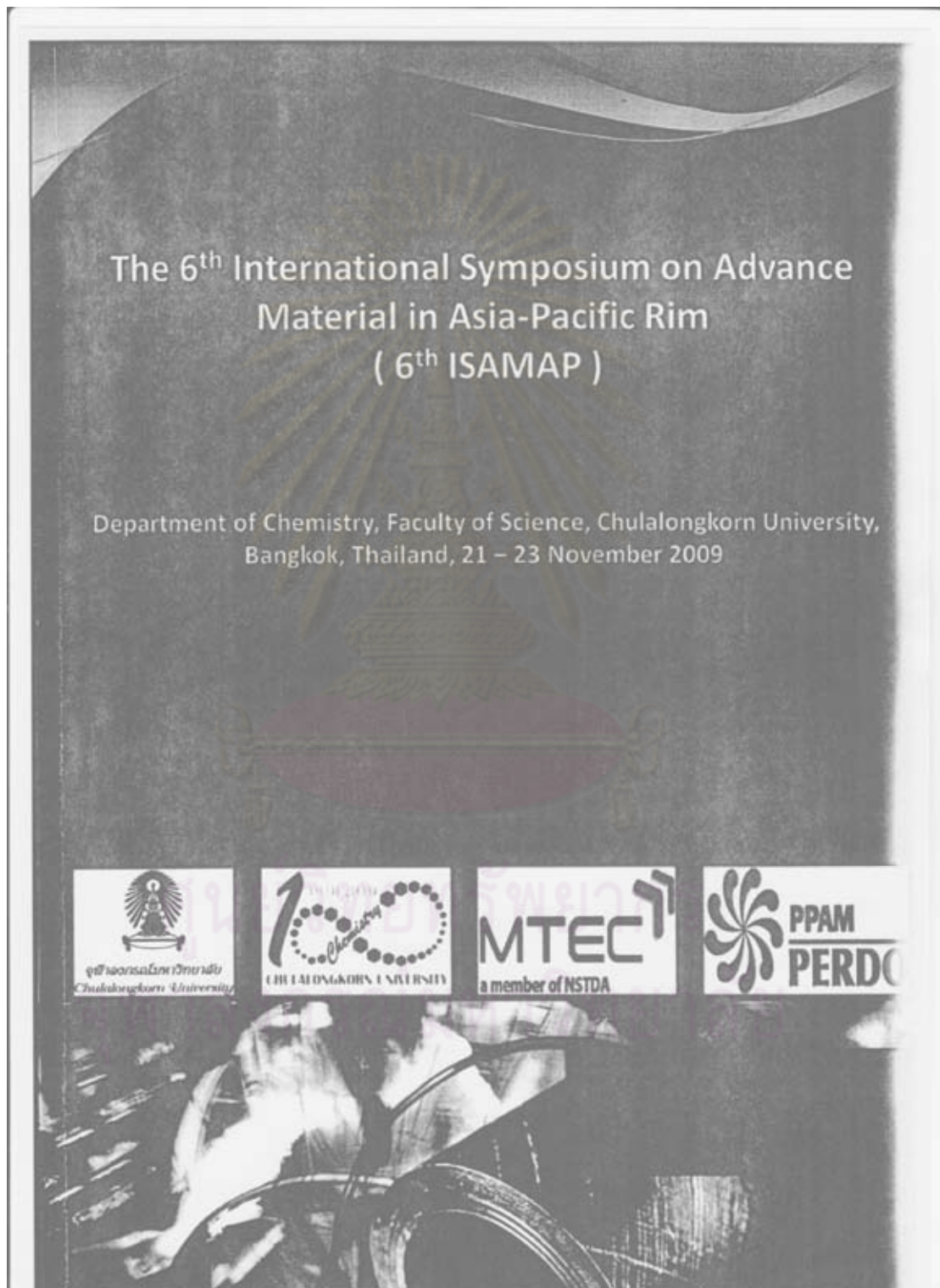
1. Roncali, J. *Chem. Rev.* **1992**, *92*, 711.
2. Pei, Q.; Zuccarello, G.; Ahlsgog, M.; Ingnas, O. *Polymer* **1994**, *35*, 1347.
3. Groenendaal, L.; Jonas, F.; Freitag, D.; Pielartzik, H.; Reynolds, J. *Adv. Mater.* **2000**, *12*, 481.
4. Meng, H.; Perepichka, D. F.; Wudl, F. *Angew. Chem. Int. Ed.* **2003**, *42*, 658.
5. Meng, H.; Perepichka, D. F.; Bendikov, M.; Wudl, F.; Pan, G. Z.; Yu, W.; Dong, W.; Brown, S. *J. Am. Chem. Soc.* **2003**, *125*, 15151.
6. Kellog, R. M.; Schaap, A. P.; Harper, E. T.; Wynberg, H. *J. Org. Chem.* **1968**, *33*, 2902.
7. Ji, S.; Li, Y.; Yang, M. *Sensor and Actuator B* **2008**, *133*, 644.

**Keywords:** PEDOT, PMMA composite, solid state polymerization, conducting polymer



ศูนย์วิทยทรัพยากร  
จุฬาลงกรณ์มหาวิทยาลัย

B-3





Conductive PEDOT/PMMA composite film  
prepared by electrospinning and solid state  
polymerization

*Kodchaporin K.<sup>1</sup>, Voravee P. H.<sup>1,2</sup>, Yongsak S.<sup>1,2\*</sup>*

<sup>1</sup>Program of Petrochemistry and Polymer Science, Faculty of Science, Chulalongkorn  
University, Bangkok, 10330 Thailand

<sup>2</sup>Organic Synthesis Research Unit, Department of Chemistry, Faculty of Science,  
Chulalongkorn University, Bangkok, 10330 Thailand

\*Tel 02-218-7632 Fax. 02-218-7598 E-mail: [yongsak.s@chula.ac.th](mailto:yongsak.s@chula.ac.th)

**Abstract.** The conductive polymer composite film was first prepared by electrospinning the solution mixture of 2,5-dibromo-3,4-ethylenedioxythiophene (DBEDOT) and PMMA in 3:1 and 4:1 weight ratios at the PMMA concentration of 0.18 g/mL. The solid state polymerization (SSP) of the resulted DBEDOT embedded in the PMMA matrix was performed by heating and incubating at 80 °C. The sample prepared using the 4:1 weight ratio of DBEDOT:PMMA incubated for 72 h gave the lowest surface electrical resistance of 50Ω. The resistivity of this incubated PEDOT/PMMA composite film was found to decrease upon storage, possibly due to slow polymerization of the remaining monomers or reorganization of the polymeric structure in the doped state.

**Keywords.** PEDOT, PMMA composite, solid state polymerization, conducting polymer

## VITAE

Ms. Kodchaporn Kitikulvarakorn was born on February 11, 1985 in Trang, Thailand. She received a bachelor degree of Science from Department of Chemistry Industrial, Faculty of Science, King Mongkut's Institute of Technology North bangkok, Bangkok, Thailand in 2006. She was admitted to a Master's Degree Program of Petrochemistry and Polymer Science, Faculty of Science, Chulalongkorn University and completed the program in 2009. Her address is 1008, Sukhumvit 101/1 Road, Bangjak, Phakanong, Bangkok, 10260.



ศูนย์วิทยทรัพยากร  
จุฬาลงกรณ์มหาวิทยาลัย